ELSEVIER

Coordination Chemistry Reviews
176 (1998) 211–322

COORDINATION CHEMISTRY REVIEWS

Chalcogenidometalates of the heavier Group 14 and 15 elements

William S. Sheldrick*, Michael Wachhold

Lehrstuhl für Analytische Chemie, Ruhr-Universität Bochum, D-44780 Bochum, Germany

Received 22 October 1997; accepted 5 January 1998

Contents

* Corresponding author. Tel.: +49 234 7004192; fax: +49 234 7094420; e-mail: shel@anachem.ruhr-uni-bochum.de

PII S0010-8545(98)00120-9

Abstract

The review covers structural aspects of the chemistry of ternary and quaternary chalcogenidometalates of the heavier Group 14 (Ge, Sn, Pb) and 15 (As, Sb, Bi) elements, with particular emphasis being placed on polymeric anionic networks. Technological interest in the design of nanoporous materials with tailor-made properties has stimulated recent research into intermediate-temperature solid-state synthetic methods (e.g. molten flux and solventothermal techniques) for the construction of lamellar and framework anions of this type. Under these relatively mild conditions (T = 100–600°C), intact molecular building blocks such as rings and chains can self-organize to a fascinating variety of polyanions, whose dimensionality and cavity/channel size can be influenced by the choice of suitable structure-directing agents such as alkali metal or alkylammonium cations. Classification of the resultant chalcogenidometalates in this review is therefore performed in terms of both the nuclearity y of the component M_yE_z building units (M = Group 14 or 15 element, E = S, Se or Te) and the dimensionality d of the anion network. Promising novel multifunctional materials, that combine the typical exchange and catalytic features of zeolite-like

phases with the unique optoelectronic properties of Group 14/15 chalcogenides, are presented.

Keywords: Germanium; Tin; Arsenic; Antimony; Chalcogenidometalates; Polyanions

1. Introduction

The recent surge of interest in the preparation of chalcogenidometalates of the heavier Group 14/15 elements has primarily been motivated by the technological potential of solid-state compounds containing regularly spaced pores and cavities. As natural prototypes are provided by the extensive zeolite class of minerals [1–3], with their corner-shared tetrahedral SiO_4 and AlO_4 building blocks, it is not surprising that synthetic strategies for the design of novel nanoporous structures have tended to concentrate either on the structure-direction of channel shape and size in aluminosilicates or on the substitution of the Si and Al atoms in such oxide-based frameworks by Main Group elements and transition metals. Although the suitability of the heavier Group 14 elements Ge(IV) and Sn(IV) for this approach is immediately apparent, it is important to recognize that the construction of open solid-state frameworks is in no way restricted to tetrahedral coordination polyhedra. Both the trigonal bipyramids and octahedra that are commonly found in solid-state Sn(IV) compounds and the ψ-trigonal bipyramids and ψ-octahedra, that are typical for its Group 15 neighbor Sb(III), can connect through shared corners and/or edges into polymeric networks. Despite the importance of chalcogenides in optoelectronic devices, which has led to a growing interest in this class of compounds, until recently relatively few attempts had been undertaken to systematically design potentially multifunctional novel materials by replacing framework O atoms with their heavier congeners S, Se and Te. To a certain extent, previous neglect of the chalcogenidometalates of the heavier Group 14/15 elements was certainly due to the traditional overemphasis on classical ceramic synthetic techniques ($T > 600$°C) in solid-state chemistry. Such experimental conditions generally lead to thermodynamically stable phases with simple lattice structures of high density and often relatively high symmetry. In contrast, milder thermal regimes (100–600°C) can leave characteristic molecular building units such as chains or rings intact to participate in the formation of open often metastable crystalline structures. Exploratory research on the solubilization of Group 14/15 metals and their chalcogenides in strongly polarizing media such as molten salts ($T = 200$–600°C) [4–7] or molecular solvents ($T = 100$–400°C) [8–10] has demonstrated that intermediate temperatures can successfully be employed to afford a potentially vast range of chalcogenidometalates with open cation-directed polymeric structures.

Pioneer work on the preparation of thio- and selenidogermanates and stannates by reaction of alkali metal chalcogenides with ME_2 (M = Ge, Sn; E = S, Se) in aqueous solution was performed by Krebs and co-workers between 1970 and 1987

and summarized in a classical review article on Group 13/14 chalcogenidometalates which appeared in 1983 [11]. The basic structural principles for the analogous Group 15 anions were established in the same period of time by Eisenmann and Schäfer, who exploited both high temperature and mild hydrothermal synthetic methods. Potential technological applications of zeotype Group 14 thio- and selenidometalates appear to have been emphasized in depth for the first time in an article by Bedard et al. in 1989 [12] and have led to a marked increase in activity in this field in the past few years [13]. However, although the chemistry of molecular chalcogen-containing anions of Group 15 elements was reviewed by Drake and Kolis in 1994 [14] and selected aspects of the solid-state structural architecture of the heavier Group 14/15 chalcogenidometalates have been discussed in several review articles [4–7,10,13–15], to our knowledge, no comprehensive and systematic report has recently appeared on this subject.

The present review considers ternary and quaternary chalcogenidometalates $A_mM_yE_z$ and $A_mM'_xM_yE_z$ (E = S, Se, Te) of the heavier Group 14/15 elements (Group 14, M = Ge, Sn, Pb; Group 15, M = As, Sb, Bi) with effective charge separation between cations A(I) and anionic structural units $[M_yE_z]^{m-}$ or $[M'_xM_yE_z]^{m-}$ [charge = $2m$ for divalent cations A(II)]. In accordance with the Zintl–Klemm concept, this state of affairs can reasonably be assumed for alkali and alkaline earth cations and to a lesser extent for Tl(I). Our discussion will therefore be restricted to ternary and quaternary phases containing these or organic cations (e.g. R_4N^+, Ph_4P^+) and will emphasize the structural architecture of polymeric anions. However, a knowledge of possible discrete M_yE_z building blocks is advantageous both in helping our understanding of the principles behind cation-directed self assembly and in the long-range goal of employing such individual units to construct novel materials of designed structure. We have therefore attempted to cover chalcogenidometalates of the heavier Group 14/15 Main Group elements in as comprehensive a manner as possible.

2. General principles

2.1. Synthesis

In the early 1970s, Krebs and co-workers demonstrated that hydrated orthometalates $A_4ME_4 \cdot xH_2O$ (M = Ge, Sn; E = S, Se) can be isolated from aqueous solution at ambient temperature following nucleophilic attack of the relevant chalcogenide anion on a Group 14 dichalcogenide ME_2 [11]. Such tetrahedral anions are stable in strongly alkaline solution but condense to corner- or edge-bridged oligomeric units such as $M_2E_6^{4-}$, $M_2E_7^{6-}$ or $M_4E_{10}^{4-}$ when the pH is lowered. Careful control of both concentration and solution pH is of critical importance for the preparation of pure solid-state phases. Although polymeric anions such as the corner-bridged *zweier* single chains $^1_\infty[SnS_3^{2-}]$ in $K_2SnS_3 \cdot 2H_2O$ [17] or the three-dimensional open framework $^3_\infty[MnGe_4S_{10}^{2-}]$ in $(Me_4N)_2[MnGe_4S_{10}]$ [18] have occasionally been isolated at room temperature,

mild hydro(solvento)thermal conditions (T = 120–200°C) have generally been found to be required for the synthesis of chainlike, layered or framework chalcogenidometalates. This approach was first investigated in a systematic manner for a heavier Group 14/15 element some 20 years ago by Schäfer, whose research team prepared a series of alkali (and alkaline earth) metal thioantimonates(III) by dissolving Sb_2S_3 in aqueous A_2S/ASH solutions at 120–180°C [19]. A variety of synthetic strategies, many of which involve nucleophilic attack of chalcogenide (or polychalcogenide) ions on binary phases M_yE_z in one guise or another, have been developed or (in most cases) improved and extended for Main Group chalcogenidometalates in the past 10–15 years. As detailed review articles have appeared on most of these techniques in recent years, they will only be briefly summarized in this section.

Large counterions such as R_4N^+ (R = Me, Et, Pr^n, Bu^n), Ph_4P^+ or [K(2,2,2-crypt)]$^+$ are generally required for the stabilization of discrete chalcogen-containing anions of higher nuclearity. A range of synthetic methods have been successfully employed for isolated Group 14/15 chalcogenidometalates:

1. nucleophilic attack of chalcogenide (or polychalcogenide) anions on binary compounds (chalcogenides, halides) [14];
2. base-induced disproportionation of binary chalcogenides [14];
3. solvent extraction of Zintl anions from alkali metal/element/chalcogen alloys using large counterions [20];
4. electrochemical synthesis through cathodic dissolution of telluride electrodes [21]; and
5. reduction of binary chalcogenides or alloy phases with elemental potassium in the presence of large counterions [14].

Polymeric anions have been prepared by the following techniques:

1. high temperature fusion (T > 600°C) of the elements or the relevant chalcogenides in the presence of large counterions [14];
2. reactions in molten alkali metal chalcogenide or polychalcogenide fluxes at 200–600°C [4–7,22]; and
3. solventothermal synthesis in superheated polar fluids (e.g. H_2O, CH_3OH, CH_3CN, en) at intermediate temperatures (T = 120–200°C) [10].

Whereas the classic solid-state high temperature fusion reaction clearly provided the preferred route to Main Group chalcogenidometalates in earlier research in this area, interest in the design of porous zeotype phases has led to a very definite shift in emphasis towards the latter milder methods in the past decade.

2.2. Bonding and structural architecture

The structural principles governing the construction of Group 14–15 chalcogenidometalates will be considered in detail in Section 3 and 4. As recent research has often been motivated by potential technological application of such solid state phases it is helpful at this stage to identify a number of underlining trends and to

comment on essential differences between the structural architecture of this class of compounds and the oxide-based silicates and phosphates.

2.2.1. Oxidation states

With few exceptions (see below) extended anionic structures have only been characterized for heavier Group 14 chalcogenidometalate anions with M (Ge, Sn) in its maximum oxidation state (+IV). The absence of both binary chalcogenides PbE_2 (E = S, Se, Te) and chalcogenidoplumbates(IV) is in accordance with the decrease in stability of the +IV state on going down the Group. Isolated ditetrahedral anions $M_2E_6^{6-}$ with a shared M–M bond are known for both Ge(III) (E = S, Se, Te [23–25]) and Sn(III) (E = Te [25]). These building units can connect through joint corners to construct polymeric chains such as $^1_\infty[Ge_2Te_5^{4-}]$ in $Ba_2Ge_2Te_5$ [26] or $^1_\infty[Ge_6Te_{12}^{6-}]$ in $Li_6Ge_6Te_{12}$ [27]. In contrast to the latter polyanion, the $^1_\infty[Ge_2S_4^{2-}]$ chains of $Tl_2Ge_2S_4$ [28] contain both tetrahedrally coordinated Ge(IV) atoms and Ge(II)S_3 pyramids and an analogous valency splitting has also been reported for the tin atoms in the $^3_\infty[Sn_4Se_8^{2-}]$ frameworks of $K_2Sn_4Se_8$ and $Rb_2Sn_4Se_8$ [29,30]. Although discrete face-bridged dipyramidal anions of the type $[M_2E_3]^{2-}$ (E = Se, Te) have been isolated for Sn(II) [31] and Pb(II) [32–34] by employing [K(2,2,2-crypt)]$^+$ as a counterion, and extended thiostannate(II) networks have been found in both $BaSnS_2$ [35] and $BaSn_2S_3$ [36], no examples of alkali metal chalcogenidometalates(II) are known. Indeed, the formation of representatives of this class of compounds would appear relatively improbable, in view of the small +2 formal charge of the metal centers M. A high degree of condensation M:E would be required to provide anions $^n_\infty[M_yE_z^{(2z-2y)-}]$ with an adequate number of chalcogen sites to satisfactorily coordinate the required monovalent alkali metal counterions.

In contrast to Group 14, oligomeric or polymeric chalcogenidometalates with the Group oxidation state (+V) are unknown for the heavier members of Group 15 (As, Sb, Bi). Whereas salts of the discrete tetrahedral anions $[MS_4]^{3-}$ and $[MSe_4]^{3-}$ are readily prepared for As(V) or Sb(V) by reaction of the respective binary chalcogenides M_2E_3 with alkali metal polychalcogenides, no evidence has been presented for the existence of analogous compounds for E = Te or M = Bi. As for their neighbors Ge(IV) and Sn(IV), the ability of the chalcogenidoanions $[AsE_3]^{3-}$ and $[SbE_3]^{3-}$ to condense to units of higher nuclearity is characteristic for As(III) and Sb(III) and leads to a remarkably rich structural chemistry for the chalcogenidometalates(III) of these Group 15 elements. In striking contrast to its neighbor Pb, a similar variety of formula and structure types has also been found for the analogous chalcogen-containing anions of the heavier homolog Bi(III). Only one polyanion with an M–M bond is known for the heavier Group 15 elements, namely $(Me_4N)_2As_2Te_5$ [37], but a relatively large number of binary Zintl anions such as $[As_{10}Te_3]^{2-}$ [38] or $[Sb_9Te_6]^{3-}$ [39] exhibit this structural motif.

Pyramidal thio- and selenidotellurates(IV) $[TeE_3]^{2-}$ are well characterized [40–42] and the thereby documented ability of tellurium to extend its coordination number beyond 2 also leads to a dramatic increase in the number of known

polytellurides [43] in comparison to the analogous compounds of its lighter congeners S and Se. Characteristic building blocks for the extended structures of the tellurium-rich tellurides are provided by T-shaped $TeTe_3$ and square-planar $TeTe_4$ units. Although the bonding in the anionic networks of many of these compounds (e.g. $RbTe_6$ [44], Cs_3Te_{22} [45]) cannot be explained using two-electron single bonds, it is always possible to describe isolated polytelluride anions in a valence precise manner. For instance, the discrete bicyclic $[Te(Te_3)(Te_4)]^{2-}$ anion in $[K([15]\text{-crown})_2]_2Te_8$ [46] can formally be regarded as containing a ψ-octahedral square-planar central Te(II) atom chelated by chainlike Te_3^{2-} and Te_4^{2-} anions. The propensity of Se to exhibit coordination numbers higher than 2 is far less pronounced than for its heavier congener. However, cyclization is also characteristic for polyselenides Se_z^{2-} with $z > 9$, leading, for example, to the presence of two T-shaped $SeSe_3$ units in the fused Se_6 rings of $(Ph_3PNPPh_3)_2Se_{10} \cdot DMF$ [47] or a square-planar central $SeSe_4$ unit in the bicyclic Se_{11}^{2-} anion in $(Ph_4P)_2Se_{11}$ [48–50]. As already discussed for the analogous polytellurides, it is once again possible to treat these anions as chalcogenidometalates. The employment of molten alkali metal polychalcogenide fluxes [4–7] and the use of Se or Te as starting components for reactions carried out under mild solventothermal conditions [10] has led to the recent synthesis of a variety of novel polychalcogenidometalates of the heavier Group 14/15 elements. Many of these contain E_z^{2-} chains as bridging units between metal coordination polyhedra but the $TeTe_4$ unit has also been found in a number of Te-containing polyanions.

2.2.2. Coordination polyhedra

Chalcogenidogermanates(IV) contain exclusively GeE_4 tetrahedra as molecular building blocks. A reluctancy to adopt hypervalent coordination polyhedra is also apparent for trivalent As(III). To our knowledge, relatively undistorted ψ-AsE_4 trigonal bipyramids (Fig. 1) have only been reported for the double chains $^1_\infty[As_6S_{10}^{2-}]$ in $(Me_4N)_2As_6S_{10}$ [51]. However, secondary As···S interactions in the distance range 2.9–3.1 Å (i.e. some 0.75–0.95 Å longer than for typical As–S terminal bonds) are characteristic for polymeric thioarsenates(III) [52,53] and ψ-AsS_3 tetrahedra can therefore be classified as weak, relatively soft electron pair acceptors. The observed restriction of the available building blocks to GeE_4 tetrahedra and (effectively) ψ-AsE_3 tetrahedra leads to a remarkable paucity in the number of structural types exhibited by the chalcogenidogermanates(IV) and -arsenates(III) in comparison to their heavier homologs Sn, Sb and Bi. These elements are able to extend their coordination numbers to 5 and 6 [for Sn(IV)], 4 and 5 for Sb(III) and 4–6 for Bi(III). However, it is important to register an apparent dependency on the electronegativity and size of the chalcogen partner for Sn(IV) in this context. The highest known coordination numbers in structurally characterized chalcogenidostannates(IV) are 6 for E = S (e.g. SnS_6 octahedra in $Cs_4Sn_5S_{12} \cdot 2H_2O$ [54]), 5 for E = Se (e.g. $SnSe_5$ trigonal bipyramids in $Cs_2Sn_3Se_7$ [55]) and only the valency value of 4 for E = Te (e.g. $SnTe_4$ tetrahedra in Cs_2SnTe_4 [56]).

The characteristic ability of Sb(III) to extend its coordination number in chalcogenidometalates beyond three leads to the frequent observation of ψ-SbE_4 trigonal

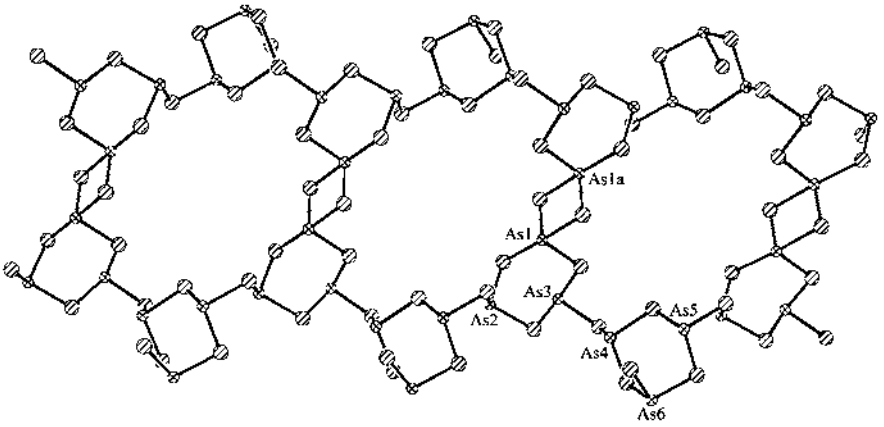

Fig. 1. ψ-AsS_4 trigonal bipyramidal coordination polyhedra in the $^1_\infty[As_6S_{10}^{2-}]$ double chains of $(Me_4N)_2[As_6S_{10}]$ [51].

bipyramids and more rarely ψ-SbE_5 octahedra. In this context, it is important to note that the assignment of a particular coordination polyhedron can often remain a rather arbitrary exercise, owing to the fact that many of the approximately linear E–Sb–E three-center bonds are strongly asymmetric. An instructive example is provided by the structure of $RbSb_3Se_5$ [57], the anionic part of which is depicted in Fig. 2. Three short Sb–Se bonds in the range 2.535(2)–2.729(2) Å are found for each of the crystallographically independent Sb atoms.

When only such contacts are considered, then the structure contains isolated fused tricyclic anions $[Sb_6Se_{10}]^{2-}$, whose basic ψ-tetrahedral $SbSe_3$ building blocks are highlighted in Fig. 2 by the employment of full bonds. However, a significant influence from weaker Sb(2)⋯Se(1) [3.055(2) Å] and Sb(3)⋯Se(1) [3.103(2) Å] interactions to neighboring anionic units is apparent for the *trans* sited bonds Sb(2)–Se(4) [2.756(2) Å] and Sb(3)–Se(5) [2.729(2) Å]. These contacts are depicted as open bonds in Fig. 2 and their inclusion leads to the description of the anionic structure of $RbSb_3Se_5$ as polymeric sheets $^2_\infty[Sb_3Se_5^-]$ constructed from one SbE_3 ψ-tetrahedron and two ψ-SbE_4 trigonal bipyramids. Further Sb⋯Se contacts in the range 3.346(2)–3.488(2) Å are found between such anionic sheets and extend the coordination polyhedra of each of the Sb atoms to ψ-octahedral. As these distances are still significantly shorter than the sum of the van der Waals radii of Sb and Se (3.90 Å [58]), it is also possible to describe $RbSb_3Se_5$ as a framework selenidoantimonate(III).

The responsible characteristic flatness of the energy hypersurfaces for E–Sb–E three-center bonds has led to some confusion in the literature classification of dimensionality for chalcogenidoantimonates(III). However, as exemplified by $RbSb_3Se_5$ it is generally possible to establish three distinct bonding regions between the sums of the covalent (r_c) and van der Waals (r_W) radii for the participating atoms: short (2.535–2.729 Å in $RbSb_3Se_5$), intermediate (3.055–3.103

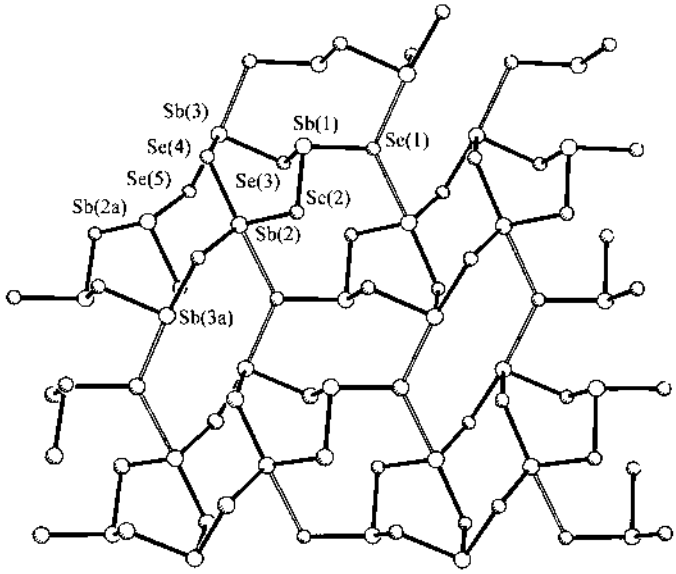

Fig. 2. The anion sheet $^{2}_{\infty}[Sb_3Se_5^-]$ in $RbSb_3Se_5$ [57]. Sb–Se distances shorter than 2.73 Å are depicted as full bonds, the longer Sb(2)–Se(1) and Sb(3)–Se(1) interactions [3.055(2), 3.103(2) Å] as open bonds.

Å in $RbSb_3Se_5$) and long (3.346–3.488 Å in $RbSb_3Se_5$). As will be discussed in more detail in Section 4, we have assigned the dimensionality of chalcogenidoantimonates(III) by including both short and intermediate Sb–E interactions. Similar considerations apply to the heavier homolog Bi(III), whose ability to adopt higher coordination numbers is, as expected, more pronounced than for Sb(III). This is exemplified by the isostructural pair $BaSbTe_3$ and $BaBiSe_3$ [59] which exhibit layered anionic structures. In accordance with the above discussion, distinct bonding regions (three bonds 2.849–2.966 Å, two bonds 3.314–3.365 Å, one bond 3.586 Å) can be identified for the Sb–Te interactions of $BaSbTe_3$, allowing a description of the coordination polyhedron as ψ-octahedral. In contrast, $BaBiSe_3$ exhibits three short (2.735–2.913 Å) and three intermediate (3.095–3.202 Å) Bi–Se bonds, thereby justifying the assignment of the coordination number 6. Indeed, the adoption of such distorted ME_6 octahedra is typical for the heavier Group 15 element.

2.2.3. Connectivity

Linkage patterns for ME_z ($z = 3$–6) coordination polyhedra in Group 14/15 chalcogenidometalates can be classified in the following manner:

I. M–E–M and M–$(\mu E)_2$–M;
II. M–(E_n)–M; and
III. M–M.

In contrast to the oxide-based silicates [60], both corner- and edge-bridging M–E–M connectivities are possible for ME_z polyhedra in the chalcogen-containing anions of the heavier Group 14/15 elements. The ability of Group 14 $M(IV)E_4$ tetrahedra to exhibit edge-bridging reflects the essentially p character of the M–E bonds, that allows the adoption of endocyclic E–M–E angles close to 90° in four-membered $(ME)_2$ rings. Effectively no distortion is required to provide such an angle, when the bridging chalcogen atoms E of the $(ME)_2$ ring are sited axial (ax) to one M atom and equatorial (eq) to the second M atom in an SnE_5 trigonal bipyramid or a ψ-ME_4 trigonal bipyramid (M = Sb, Bi). Not surprisingly, this connectivity pattern is typical for these coordination polyhedra and its adoption by both E_{ax}/E_{eq} pairs in SnE_5 trigonal bipyramids (E = S, Se) leads to the frequent observation of $^1_\infty[SnE_2]$ chains as a structural component of layered or framework thio- and selenidostannates(IV).

The number of characterized polychalcogenidometalates with the second linkage mode M–(E_n)–M has increased rapidly in recent years. Examples are known for both E_n chains (E = S, Se, Te) and square-planar $TeTe_4$ units. Direct M–M bonding has been established for discrete chalcogen-containing anions with both M(IV) tetrahedra (M = Ge, Sn) and M(III) ψ-tetrahedra (M = As). For instance, ditetrahedral Ge_2Te_6 building blocks with a central Ge–Ge bond are connected through common Te atoms in the polymeric anionic chains of both $Ba_2Ge_2Te_5$ [26] and $Li_6Ge_6Te_{12}$ [27].

2.2.4. Cation influence

The counteraction size, shape and charge play a decisive role in the construction of polymeric heavier Group 14/16 chalcogenidometalates. As for the zeolites themselves, alkylammonium and alkali metal cations have often been employed to direct the assembly of structures containing regularly spaced pores and channels. The fact that the size of the cavities can reflect the geometry of the structure-directing cation is suggestive of a templating mechanism. Despite such observations, the organization processes behind the self-assembly of supramolecular frameworks from simple molecular building blocks are still not well understood. For instance, a particular cation can often generate a number of different anionic structures, but alternatively one particular network may often be obtained with different structure-directing agents. Both charge-compensation and space-filling effects appear to play an important role in self-assembly mechanisms.

In accordance with general principles of solid-state structural chemistry, it is possible to identify a number of characteristic parameters, that should reflect the influence of cation size and charge on the topology of chalcogenidometalate networks.

2.2.4.1. Condensation grade (c). Although a relatively wide range of values is possible for individual members, a characteristic trend towards higher coordination numbers can be established for both Group 1 and 2 cations on going from the lighter to the heavier elements [61]. Respective condensation grades c ($c = y/z$) in the ranges $0.25 \leq c < 0.50$ and $0.333 \leq c < 0.667$ are possible for Group 14 and 15

anions $[M_yE_z]^{m-}$ in alkali metal chalcogenidometalates $A_mM_yE_z$. As the number of potentially available chalcogen coordination partners p per unit of anion charge ($p = z/m$) will increase with parameter c in accordance with the following expressions,

Group 14 $p = (2-4c)^{-1}$
Group 15 $p = (2-3c)^{-1}$

higher condensation grades should become increasingly attractive as the size of the alkali metal cation increases. Analogous relationships should be valid for divalent alkaline earth cations.

2.2.4.2. Dimensionality (d). For compounds of a given formula type $A_mM_yE_z$, simple packing considerations would suggest that lowering the dimensionality of an anionic network should, in general, allow the achievement of a higher degree of space-filling for larger cations. Whereas the small alkali metal cation Na^+ should be capable of directing the self-assembly of three-dimensional anionic frameworks, more voluminous cations such as Cs^+ or R_4N^+ (R = Me, Et, Pr^n) would be expected to stabilize anionic sheets and chains with respective dimensionalities of 2 or 1.

2.2.4.3. Average M coordination number (n). Anionic networks containing corner-bridged Group 14 ME_4 coordination tetrahedra will be more flexible than those based on edge-bridged ME_5 trigonal bipyramids or ME_6 octahedra. Similar considerations apply to ψ-ME_3 tetrahedra in comparison to ψ-ME_4 trigonal bipyramids or ψ-ME_5 octahedra of Group 15 elements M. As topologically flexible anionic networks favor higher coordination numbers and more compact structures for voluminous cations, a trend towards lower average M coordination numbers n might be expected as the cation size increases in Group 14/15 chalcogenidometalates of invariable stoichiometry $A_mM_yE_z$.

Kanatzidis has commented on similar correlations between counterion size and the parameters d and n in selected transition metal chalcogenidometalates [6]. For instance, smaller cations such as Me_4N^+ generate compact chain structures with tetrahedral coordination of M (Cu, Ag) in compounds of the type AME_z (E = S, Se; $z = 4-6$). The chains unfold for larger cations (e.g. Ph_4P^+) and the Group 11 metal assumes the lower coordination number of 3. However, it is important to emphasize that such relationships should not be regarded as natural laws. Violations will be encountered and their employment in structure prediction is restricted by the desired metastable nature of many porous chalcogenidometalates prepared under relatively mild thermal conditions.

The differences in the structural architecture of the heavier Group 14/15 chalcogenidometalates and the oxide-based silicates are not restricted to the ME_z coordination polyhedra and their connectivity. Whereas the soft bending potential for Si–O–Si linkages leads to the adoption of angles between 120 and 180° [60], a much narrower typical range (90–115°) is found for M–S–M and M–Se–M units.

However, both S and Se are capable of bridging three different metal centers and this ability is reflected in the presence of broken M_3E_4 cubes in many layered thio- and selenidostannates(IV).

3. Chalcogenidometalates of germanium, tin and lead

3.1. Structural principles and classification

Tetrahedral ortho-anions ME_4^{4-} (E = S, Se) of germanium and tin exhibit a characteristic tendency to condense through corner- or edge-bridging to afford oligomeric entities. The species distribution in solutions used for the preparation of Group 14 chalcogenidometalates under mild solvatothermal conditions will depend strongly on pH and concentration. For instance, Krebs and co-workers have demonstrated that the edge- and corner-bridged ditetrahedral anions $[Ge_2S_6]^{4-}$ and $[Ge_2S_7]^{6-}$ both play an important role in weakly alkaline aqueous solution ($7 \leq pH \leq 11$) [11]. A higher degree of corner condensation leads to the adamantane-like tetranuclear $[Ge_4S_{10}]^{4-}$ anion, whose presence over the wide pH range 3.5–11.0 could be confirmed. As we will discuss in this section, such Ge_4E_{10} molecular building blocks (Fig. 3a) have been found to be endemic for thio- and selenidogermanates(IV) isolated in the temperature range 20–180°C from polar solvents containing large countercations (e.g. Cs^+, alkylammonium cations). They have also recently been successfully employed for the design of porous three-dimensional framework anions such as $^3_\infty[MnGe_4S_{10}^{2-}]$ [12,18], which will be considered in Section 3.6. Although analogous adamantane-like units $[Sn_4E_{10}]^{4-}$ are present as isolated anions in $(Et_4N)_4Sn_4Se_{10}$ [69] and $[K(2,2,2\text{-crypt})]_4Sn_4Se_{10}$ [112] and as building units in the quaternary phases $A_2[MnSnS_4]$ (A = K, Cs) [7,134], the energetic preference of Sn(IV) for higher coordination numbers in its polymeric thio and selenido anions leads to the more frequent observation of Sn_3E_4 building units (Fig. 3b), often described as broken cubes or semi-cubes. These molecular units link through shared trigonal bipyramidal edges to afford chains in $(Et_4N)_2Sn_3Se_7$ [113] or sheets in $Cs_2Sn_3Se_7$ [55], $(Pr^n_4N)_2Sn_4S_9$ [127,128] and $Cs_4Sn_5S_{12} \cdot 2H_2O$ [54]. A consequence of the required connectivity patterns is the presence of edge-bridged $^1_\infty[SnSe_3^{2-}]$ chains as a characteristic motif in the anionic networks of these chalcogenidostannates(IV), a feature also found in the three-dimensional framework anions of $A_2Sn_2S_5$ (A = K [129], Tl [130], $A_2Sn_2Se_5$ (A = K [129], Rb [131]) and $Na_4Sn_3S_8$ [132]. Formula types $A_mM_yE_z$ for thio- and selenidogermanates(IV) and -stannates(IV) with M–E–M linked ME_n polyhedra are listed for monovalent cations in Tables 1 and 2. The analogous classification for divalent cations contains far fewer examples and no new formula or structure types appear for the anions $[M_yE_z]^{m-}$. Relevant compounds will be presented in the appropriate sections of this chapter.

Comparison of Tables 1 and 2 allows the identification of a number of general structural trends:

Table 1
Formula types $A_mGe_yE_z$ (E = S, Se) and their dimensionalities d for thio- and selenidogermanates(IV) with monovalent countercations A[a]

d	E = S	A	E = Se	A
0	A_4GeS_4	Na [62,63], Tl [64]	A_4GeSe_4	Na [65,66]
	$A_4Ge_2S_6$	Na [67], Tl [68]	$A_4Ge_2Se_6$	Na [70], K [71], Tl [72], $(Et_4N)_2(enH)_2$ [69]
	$A_6Ge_2S_7$	Na [73]	$A_6Ge_2Se_7$	Na [74]
	$A_4Ge_4S_{10}$	Na [75,76], Cs [77,78], Tl [79], (Me_4N) [18,80]	$A_4Ge_4Se_{10}$	Na [81], K [82], Rb [83] Cs [84], Tl [85]
	$A_6Ge_8S_{19}$	Cs [11,86]		
1	A_2GeS_3	Na [87]	A_2GeSe_3	Na [88]
	$A_2Ge_4S_9$	$[Pr^n{}_2NH_2][(Pr^n)(Et)NH_2]$ [89]		
2			$A_2Ge_2Se_5$	Na [90]

[a] The following chalcogenidogermanates(IV) contain solvent molecules: $Na_4GeS_4 \cdot 14H_2O$ [62], $Na_4GeSe_4 \cdot 14H_2O$ [65], $Na_4Ge_2S_6 \cdot 14H_2O$ [67], $Na_4Ge_2Se_6 \cdot 16H_2O$ [70], $Cs_4Ge_4S_{10} \cdot xH_2O$ (x = 3,4) [77,78], $Rb_4Ge_4Se_{10} \cdot CH_3OH$ [83], $Cs_4Ge_4Se_{10} \cdot 2CH_3OH$ [84], $Cs_6Ge_8S_{19} \cdot 12H_2O$ [11,86].

1. The incapability of Ge(IV) to extend its coordination number beyond 4 leads to a paucity in the formula and structure types for chainlike and layered chalcogenidogermanates(IV). Ternary phases with framework anions are unknown for Ge(IV).
2. Two families of formula types, namely $A_2Sn_yE_{2y+1}$ (y = 1–4) and $A_4Sn_yE_{2y+2}$ (y = 3,5), have been established for polymeric thio- and selenidostannates(IV).
3. Three-dimensional framework anions have only been constructed for Sn(IV) in the presence of smaller countercations (A = Na, K, Rb, Tl).
4. A trend towards higher condensation grades $c > 0.40$ is apparent for chalcogenidostannates(IV) with larger countercations.

Although isolated anions such as $[SnTe_4]^{4-}$, $[Sn_2Te_6]^{2-}$ and $[Ge_4Te_{10}]^{4-}$ are known for the heavier Group 14 elements, polymeric anionic networks have, to our knowledge, only been characterized for telluridometalates(IV) with polytelluride bridging units such as the Te_2 dumb-bells in Cs_2SnTe_4 [56] or the square-planar $TeTe_4$ building blocks in K_2SnTe_5 [135].

Both M–E–M and M–(E_n)–M bridged ternary chalcogenidogermanates(IV) and stannates(IV) will be discussed in order of increasing dimensionality (d = 0–3) in Section 3.2–3.5. Quaternary phases are considered in Section 3.6 and the lower Group 14 oxidation states III and II in Section 3.7.

3.2. Isolated anions

3.2.1. Mononuclear anions

Compounds of the formula type A_4ME_4 are listed for M = Ge, Sn and E = S, Se in Tables 1 and 2. Discrete tetrahedral $[GeS_4]^{4-}$ and $[SnS_4]^{4-}$ anions have also

Table 2
Formula types $A_mSn_yE_z$ (E = S, Se) and their dimensionalities *d* for thio- and selenidostannates(IV) with monovalent counter cations A[a]

d	E = S	A	E = Se	A
0	A_4SnS_4	Na [91,93], Rb, Cs [94], Tl [95,96]	A_4SnSe_4	Na [97,99], K [99], Rb, Cs [94], Tl [100]
	$A_4Sn_2S_6$	Na [67], $C_{12}H_{25}NH_3$ [442]	$A_4Sn_2Se_6$	Na [98], K [103], Rb [104], Cs [105], Tl [106] $(enH)_2[K(2,2,2\text{-crypt})]_2$, $K(Me_4N)_3$ [101]
	$A_6Sn_2S_7$	Na [107,108]	$A_6Sn_2Se_7$	Na [109], K [110]
			$A_4Sn_3Se_8$	K [111]
			$A_4Sn_4Se_{10}$	Et_4N [69], [K(2,2,2-crypt)] [112]
			$A_6Sn_4Se_{11}$	Rb [113]
1	A_2SnS_3	Na [16], K [17], Tl [115]	A_2SnSe_3	Na [116–118]
			$A_2Sn_2Se_5$	$[MeC(NH_2)_2]$ [10,121]
	$A_2Sn_3S_7$	K [10,121], Rb [104]	$A_2Sn_3Se_7$	Et_4N [113]
2	$A_2Sn_3S_7$	Me_4N [122], Me_3NH [123], Et_4N [124], Cs [125], dabcoH [443]	$A_2Sn_3Se_7$	Cs [55], Me_4N [124], Me_2NH_2 [10,126]
	$A_2Sn_4S_9$	$Pr^n{}_4N$ [127,128], $Bu^n{}_4N$ [127] $(Pr^n{}_4N)(Me_3NH)$ [128]	$A_2Sn_4Se_9$	Rb, Cs [114]
	$A_4Sn_5S_{12}$	Cs [54]	$A_4Sn_4Se_{10}$	K, Rb, Cs [444]
3	$A_2Sn_2S_5$	K [129], Tl [130]	$A_2Sn_2Se_5$	K [129], Rb [131]
	$A_4Sn_3S_8$	Na [132]		
	$A_4Sn_5S_{12}$	Tl [133]		

[a] The following chalcogenidostannates(IV) contain solvent or other neutral molecules: $Na_4SnS_4 \cdot 14H_2O$ [91], $Na_4SnSe_4 \cdot 16H_2O$ [97], $Na_4Sn_2S_6 \cdot 14\,H_2O$ [67], $(C_{12}H_{25}NH_3)_4Sn_2S_6 \cdot 2H_2O$ [442], $Na_4Sn_2Se_6 \cdot 13H_2O$ [98], $K_2[K(18\text{-crown-6})]_2Sn_2Se_6 \cdot 4en$ [102] $K_2SnS_3 \cdot 2H_2O$ [17], $K_2Sn_3S_7 \cdot H_2O$ [10,121], $Rb_2Sn_3S_7 \cdot 2H_2O$ [104], $(Me_4N)_2Sn_3S_7 \cdot H_2O$ [122], $(Me_3NH)_2Sn_3S_7 \cdot 0.72H_2O$ [123], $Cs_2Sn_3S_7 \cdot 0.5S_8$ [125], $(Me_4N)_2Sn_3Se_7 \cdot H_2O$ [124], $Rb_2Sn_4Se_9 \cdot H_2O$, $Cs_2Sn_4Se_9 \cdot H_2O$ [114], $Rb_6Sn_4Se_{11} \cdot xH_2O$ [113], $K_4Sn_4Se_{10} \cdot 4.5H_2O$, $Rb_4Sn_4Se_{10} \cdot 1.5H_2O$, $Cs_4Sn_4Se_{10} \cdot 3.2H_2O$ [444], $Cs_4Sn_5S_{12} \cdot 2H_2O$ [54].

been characterized in their alkaline earth salts $A^{II}_2GeS_4$ (A = Mg [136,137], Ca [136,138], Sr [139], Ba [140]) and $A^{II}_2SnS_4$ (A = Mg [136], Ca [136], α-Ba [93], β-Ba [141]). Although the majority of these compounds were synthesized at high temperature, phases of the type $Na_4ME_4 \cdot xH_2O$ with heavily hydrated Na^+ cations (x = 14 or 16) can, in fact, be isolated at room temperature from aqueous solution at high pH. Whereas the alkali metal compounds A_4SnTe_4 (A = Na [142], K [143], Rb [94]) are known and isolated $[SnTe_4]^{4-}$ tetrahedra are also present in both $K_2BaSnTe_4$ [144] and $Cs_8Sn_2Te_9$ [94], to our knowledge, no report of the structural characterization of a phase containing $[GeTe_4]^{4-}$ anions has appeared. The structures of the chalcogenidogermanates(IV) and -stannates(IV) A_4ME_4 and $A^{II}_2ME_4$ (E = S, Se) were discussed in detail in review articles by Maurin et al.

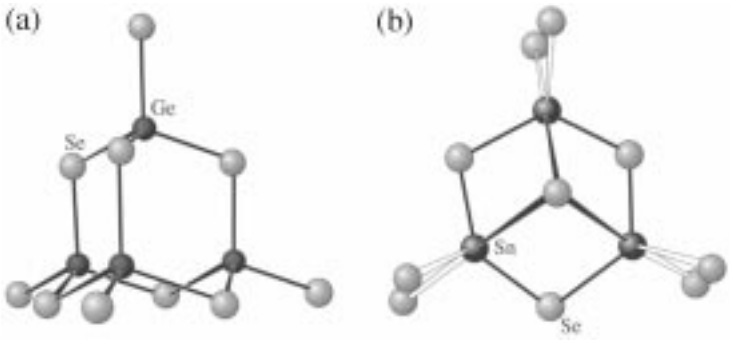

Fig. 3. Characteristic molecular building units (a) M_4E_{10} (M = Ge, Sn) and (b) Sn_3E_4 (E = S, Se) for the heavier Group 14 thio- and selenidometalates(IV). Possible connecting Sn–E bonds for the latter unit are depicted in an open fashion.

[145] and Krebs [11] in 1978 and 1983. Tetrahedral $[GeE_4]^{4-}$ anions exhibit average distances of 2.21 (E = S) and 2.35 Å (E = Se), $[SnE_4]^{4-}$ anions average distances of 2.39 (E = S), 2.52 (E = Se) and 2.75 Å (E = Te) [142].

$Cs_8Sn_2Te_9$ [94] contains two different discrete tetrahedral anions $[SnTe_4]^{4-}$ and $[SnTe_5]^{4-}$, in the latter of which a ditelluride Te_2^{2-} group is coordinated to the central Sn(IV) atom in an *end on* manner (Fig. 4a), Te_2 dumb-bells are also present in the $[GeTe_6]^{4-}$ anions of Cs_4GeTe_6 [146] (Fig. 4b), which was prepared by heating $Cs(CH_3COO)$ with Ge and Te at 900°C. Discrete *tris*-chelated anions $[Sn(E_4)_3]^{2-}$ (E = S, Se) with central octahedral Sn(IV) atoms are accessible as Ph_4P^+ salts at ambient temperature through nucleophilic attack of polychalcogenides on tin(II) chlorides. For instance, $[Sn(S_4)_3]^{2-}$ (Fig. 4c) was prepared by reaction of $(Ph_4P)SnCl_3$ with Na_2S_4 in acetonitrile [147], $[Sn(Se_4)_3]^{2-}$ [148,149] by treatment of a solution of $SnCl_2 \cdot 2H_2O$ in DMF with Na_2Se_6, followed by addition of Ph_4PBr [148]. The Et_4N^+ salt of $[Sn(S_4)_3]^{2-}$ has been reported to cocrystallize together with $[Sn(S_4)_2(S_6)]^{2-}$ at the same crystallographic site [150] and the latter anion (Fig. 4d) has been structurally characterized in Cs_2SnS_{14}, prepared by the molten salt technique using an $Sn/Cs_2S/S$ mixture at 275°C [151]. The Sn–S distances average to 2.578 in $(Ph_4P)_2[Sn(S_4)_3]$ and 2.575 Å in $Cs_2[Sn(S_4)_2(S_6)]$, and the Sn–Se distances average to 2.706 Å in $(Ph_4P)_2[Sn(Se_4)_3]$.

3.2.2. Dinuclear anions

Edge-bridged ditetrahedral anions $[M_2E_6]^{4-}$ (Fig. 5a) are readily formed by condensation of $[ME_4]^{4-}$ ortho-anions (M = Ge, Sn; E = S, Se) in mildly alkaline solution and the hydrated Na^+ salts $Na_4Ge_2S_6 \cdot 14H_2O$ [67], $Na_4Ge_2Se_6 \cdot 16H_2O$ [70], $Na_4Sn_2S_6 \cdot 14H_2O$ [67] and $Na_4Sn_2Se_6 \cdot 13H_2O$ [98] were prepared by Krebs and co-workers at room temperature. Indeed such $[Sn_2E_6]^{4-}$ molecular building blocks have been found to play a central role in the self-assembly of polymeric chalcogenidostannates(IV) under mild solventothermal or molten salt conditions and both $Rb_4Sn_2Se_6$ [104] and $Cs_4Sn_2Se_6$ [105] can been isolated from super-

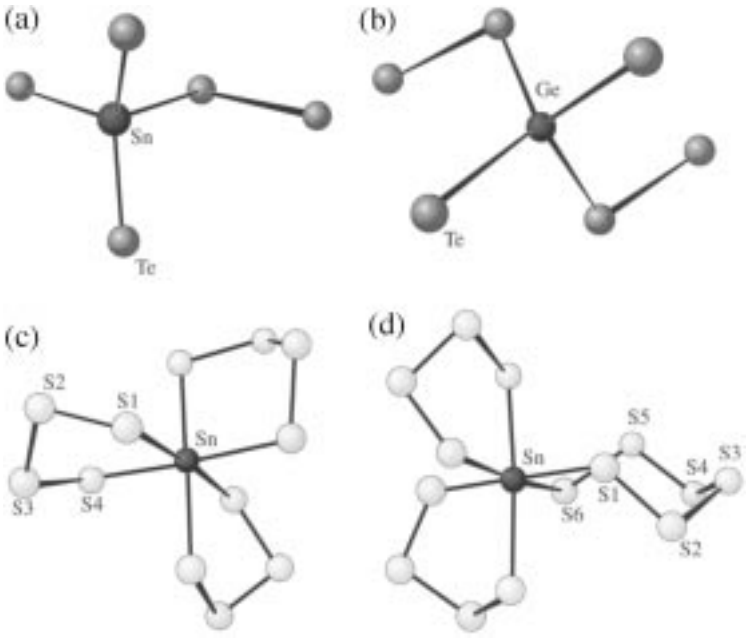

Fig. 4. Mononuclear anions (a) $[SnTe_5]^{4-}$ in $Cs_8Sn_2Te_9$ [94], (b) $[GeTe_6]^{4-}$ in Cs_4GeTe_6 [146], (c) $[Sn(S_4)_3]^{2-}$ in $(Ph_4P)_2[Sn(S_4)_3]$ [147] and (d) $[Sn(S_4)_2(S_6)]^{2-}$ in Cs_2SnS_{14} [151].

heated methanol solutions at intermediate temperature (145 and 160°C, respectively). Despite this facile formation of ditetrahedral Group 14 anions, most of the examples presented in Tables 1 and 2 were, in fact, prepared by high temperature fusion, e.g. $K_4M_2Se_6$ (M = Ge [71], Sn [103]) by heating the elements to 700°C. A totally different approach was recently introduced by Ibers et al., who synthesized $(Et_4N)_2(enH)_2Ge_2Se_6$ [69], in accordance with the elegant technique introduced for Main Group Zintl anions by Haushalter [21], through electrochemical reduction of an alloy of nominal composition Ge_2Se_3 in an electrolyte solution of $(Et_4N)Br$ in ethylenediamine.

Analogous ditetrahedral telluridometalates $[M_2Te_6]^{4-}$ have been reported for both germanium and tin. Whereas $Tl_4Ge_2Te_6$ [152] was prepared by allowing Tl_5Te_3, Ge and Te to react at 750°C, milder solution techniques were applied for $(Me_4N)_4Sn_2Te_6$ [153], $(Et_4N)_4Sn_2Te_6$ [154] and $[Zn(N_2C_2H_8)_3]_2Sn_2Te_6 \cdot en$ [155]. For instance, the Me_4N^+ salt was extracted from a crude K_4SnTe_4 alloy in methanol by layering the solution with excess saturated $(Me_4N)Br$ in the same solvent. $[Sn_2Te_6]^{4-}$ has also been characterized in $Tl_4Sn_2Te_6$ [156], which is isostructural with $Tl_4Ge_2Te_6$ [152] and $Tl_4Sn_2Se_6$ [106].

An analysis of the geometries of $[M_2E_6]^{4-}$ anions has been presented by Eulenberger [72]. In the central planar four-membered rings, the E(b)–M–E(b) angles (b, bridging; t, terminal) are always markedly wider than the M–E(b)–M angles, e.g. respective values of 94.74(5) and 85.26(5)° in $Cs_4Sn_2Se_6$ [105]. Terminal

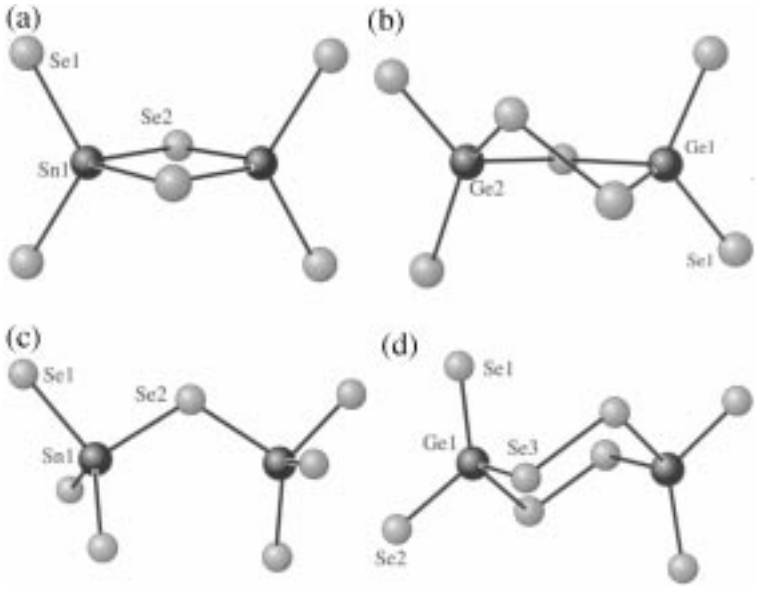

Fig. 5. Dinuclear anions (a) $[Sn_2Se_6]^{4-}$ in $Rb_4Sn_2Se_6$ [104], (b) $[Ge_2Se_7]^{4-}$ in $[Mn(dien)_2]_2[Ge_2Se_7]$ [157], (c) $[Sn_2Se_7]^{6-}$ in $K_6Sn_2Se_7$ [110] and (d) $[Ge_2Se_8]^{4-}$ in $Cs_4Ge_2Se_8$ [84,85].

M–E(t) bonds are significantly shorter than M–E(b) bonds, e.g. 2.447(1) and 2.452(2) Å as opposed to 2.587(1) Å in $Cs_4Sn_2Se_6$.

Two examples of asymmetrically bridged ditetrahedral anions $[M_2E_7]^{4-}$ are known, namely $[Ge_2Se_7]^{4-}$ (Fig. 5b) in $[Mn(dien)_2]_2Ge_2Se_7$ [157] and $[Sn_2Te_7]^{4-}$ in $Cs_4Sn_2Te_7$ [158]. The former anion was isolated under mild solventothermal conditions as was the unique $[Ge_2Se_8]^{4-}$ anion (Fig. 5d) in $Cs_4Ge_2Se_8$ [84], in which two $GeSe_4$ coordination tetrahedra are linked through direct Se–Se bonds to afford a six-membered ring with chair conformation.

In contrast to the other dinuclear anions discussed in this section, corner-bridged species $[M_2E_7]^{6-}$ (Fig. 5c) have only been prepared by high temperature reactions. In addition to $Na_6Sn_2S_7$ [107,108], isolated $[Sn_2S_7]^{6-}$ anions are also present in $Ba_3Sn_2S_7$ [159]. Attempts to isolate a salt of the type $Na_6Sn_2S_7 \cdot xH_2O$ from aqueous solutions of suitable pH proved unsuccessful [107,108], presumably owing to the preferred crystallization of $Na_4SnS_4 \cdot 14H_2O$ [91] or $Na_4Sn_2S_6 \cdot 14H_2O$ [67]. Dinuclear species of the type $[M_2E_8]^{6-}$, with two ME_4 coordination tetrahedra linked through a single E–E bond in a manner analogous to $[Si_2Se_8]^{6-}$ in $Na_6Si_2Se_8$ [160], have not been reported for M = Ge, Sn.

3.2.3. Oligonuclear anions

Characteristic differences between the molecular building units and polyhedron connectivities of polymeric chalcogenidogermanates(IV) and -stannates(IV) are also apparent for discrete anions with nuclearities of three or greater. Anions of

the types $[Sn_3Se_8]^{4-}$ in $K_4Sn_3Se_8$ [111], $[Sn_4Se_{11}]^{6-}$ in $Rb_6Sn_4Se_{11} \cdot xH_2O$ [113] and $[Ge_8S_{19}]^{6-}$ in $Cs_6Ge_8S_{19} \cdot 12H_2O$ [11,86] are all without parallel for the neighboring member of Group 14. Both selenidostannates(IV) were prepared under mild solventothermal conditions and emphasise the importance of edge-bridged ditetrahedral $[Sn_2Se_6]^{4-}$ building units in extended chalcogen-containing Sn(IV) anions. The tritetrahedral $[Sn_3Se_8]^{4-}$ anions (Fig. 6a) of $K_4Sn_3Se_8$ can be regarded as consisting of an Sn_2Se_6 ditetrahedron and an $SnSe_4$ tetrahedron with a shared edge. Condensation of two $[Sn_2Se_6]^{4-}$ anions through a common Se atom affords the novel $[Sn_4Se_{11}]^{4-}$ species (Fig. 6b) of $Rb_4Sn_4Se_{11} \cdot xH_2O$.

In stark contrast to Sn(IV), only tetrahedron corner-sharing has been established for polymeric chalcogenidogermanates(IV) and this connectivity pattern is also adapted in all known isolated anions of higher nuclearity. The endemic formation of adamantane-like species $[Ge_4E_{10}]^{4-}$ (Table 1), which are also present in $Ba_2Ge_4S_{10}$ [76] and $(Et_4N)_4Ge_4Te_{10}$ [161], is a direct consequence of this preference. Both high temperature and mild solution synthetic techniques have been employed to isolate the salts of this anion listed in Table 1. Further condensation through a common edge leads to the formation of the unique $[Ge_8S_{19}]^{6-}$ anions in $Cs_6Ge_8S_{19} \cdot 12H_2O$ [11,86] (Fig. 6d). By lowering the pH value of a thiostannate(IV) solution to 3, Schiwy and Krebs were able to isolate the supertetrahedral anion $[Sn_{10}O_4S_{20}]^{8-}$ in $Cs_8[Sn_{10}O_4S_{20}] \cdot 13H_2O$ [162]. This displays an idealized T_d symmetry with a basic skeleton composed of 10 corner-sharing SnS_4 tetrahedra and may be regarded as being constructed by condensing four adamantane-like $[Sn_4S_{10}]^{4-}$ anions (Fig. 7). Oxygen atoms are encapsulated at the centers of these

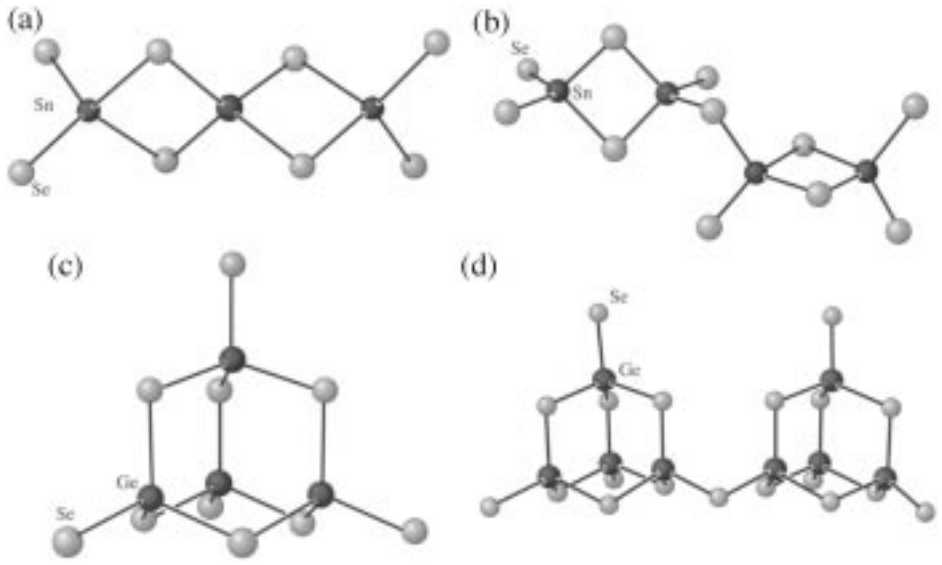

Fig. 6. Oligonuclear anions (a) $[Sn_3Se_8]^{4-}$ in $K_4Sn_3Se_8$ [111], (b) $[Sn_4Se_{11}]^{6-}$ in $Rb_6Sn_4Se_{11} \cdot xH_2O$ [113], (c) $[Ge_4S_{10}]^{4-}$ in $Cs_4Ge_4S_{10} \cdot 3H_2O$ [77,78] and (d) $[Ge_8S_{19}]^{6-}$ in $Cs_6Ge_8S_{19} \cdot 12H_2O$ [11,86].

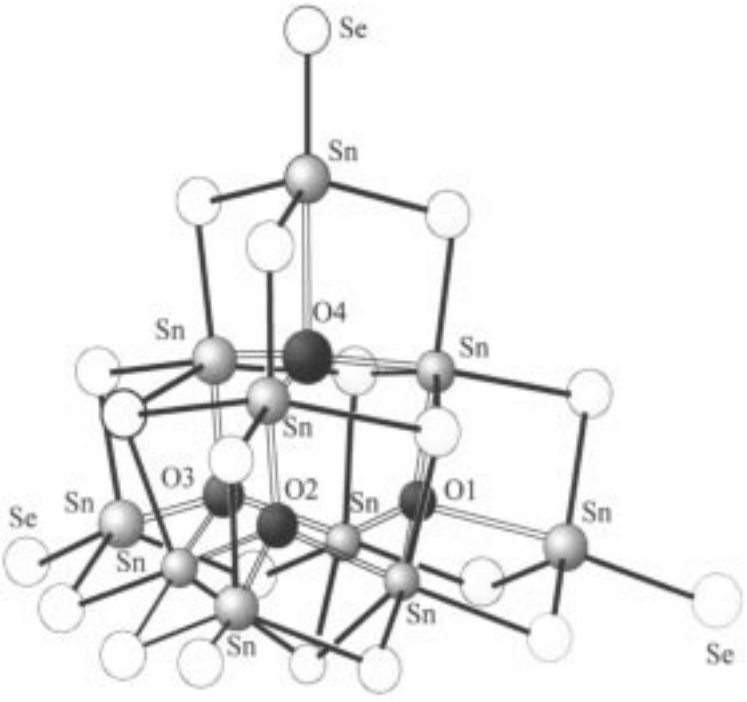

Fig. 7. The supertetrahedral $[Sn_{10}O_4S_{20}]^{4-}$ anion in $Cs_8[Sn_{10}O_4S_{20}] \cdot 13H_2O$ [162] with the encapsulated oxygen atoms depicted as black spheres.

Sn_4S_{10} building units and extend the coordination numbers of the inner six tin atoms to 6. Somewhat surprisingly, in view of the observed dominance of the $[Ge_4S_{10}]^{4-}$ anion over a wide pH range, an analogous Ge(IV) species has not yet been characterized [11].

3.3. Chain polymers

3.3.1. Mononuclear building units

Repeated corner bridging of tetrahedral $[ME_4]^{4-}$ anions (M = Ge, Sn; E = S, Se) leads to the formation of the infinite $^1_\infty[ME_3^{2-}]$ chains that have been found in Na_2GeS_3 [87], Na_2GeSe_3 [88] (Fig. 8a), $K_2SnS_3 \cdot 2H_2O$ [16,17], Tl_2SnS_3 [115], α-/β-Na_2SnSe_3 [116–118], $BaSnS_3$ and $SrSnS_3$ [119,120]. With the exception of $K_2SnS_3 \cdot 2H_2O$, which was isolated from aqueous solution, all these compounds were prepared by the high temperature fusion technique. To the best of our knowledge $^1_\infty[GeTe_3^{2-}]$ chains are unknown, but the analogous telluridostannate(IV) polyanion $^1_\infty[SnTe_3^{2-}]$ has recently been found together with isolated ditelluride ions Te_2^{2-} in Ba_2SnTe_5 obtained from an $A_2Te/BaTe/Te$ (A = Na, K) flux at 450°C [163]. With the exception of β-Na_2SnSe_3 [117,118] with its remarkable *sechser* single chains ($P = 6$ [60]) all known $^1_\infty[ME_3^{2-}]$ anions exhibit a simple *zweier*

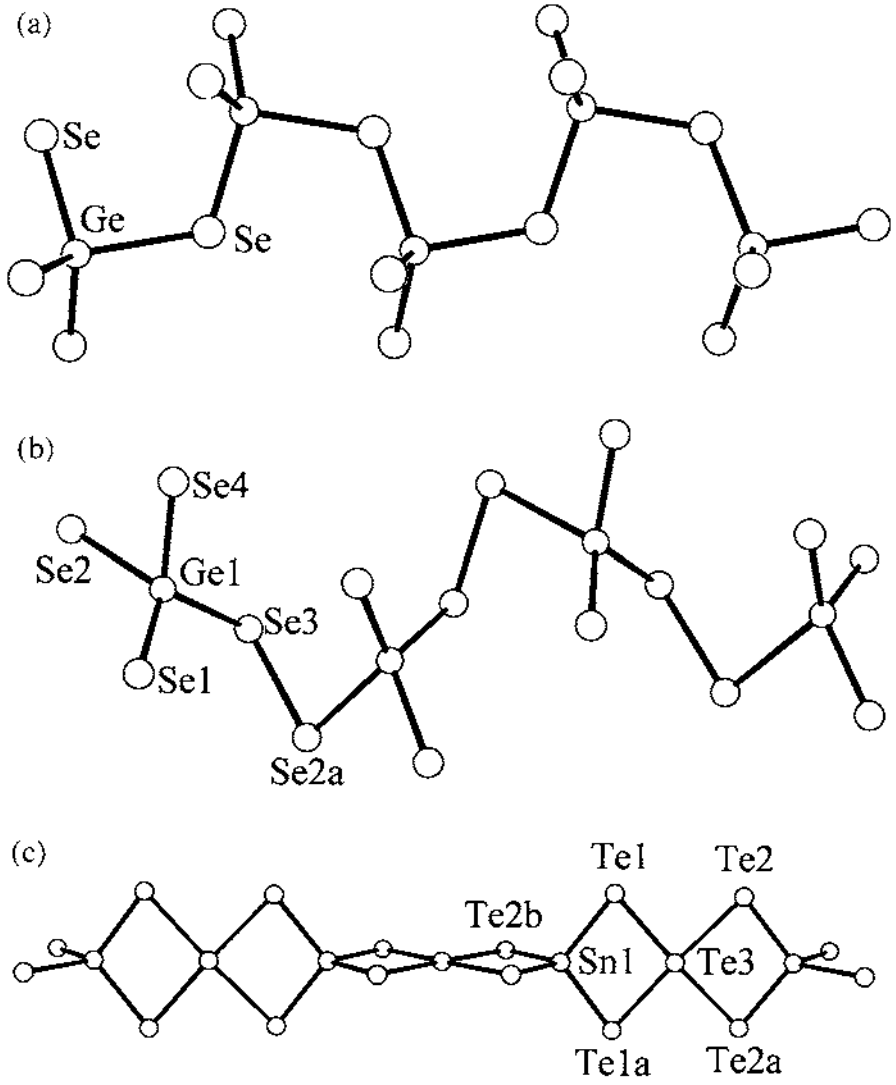

Fig. 8. Polymeric chainlike anions with mononuclear ME_4 (M = Sn, Ge) building units in (a) $^1_\infty[GeSe_3^{2-}]$ in Na_2GeSe_3 [88], (b) $^1_\infty[GeSe_4^{2-}]$ in K_2GeSe_4 [83] and (c) $^1_\infty[SnTe_5^{2-}]$ in K_2SnTe_5 [135].

periodicity ($P = 2$). Chain conformations can be gauged by employing Liebau's stretching factor f_s [$f_s = I_{chain}/(l_T \cdot P)$ with I_{chain} = chain identity period and l_T = tetrahedron edge length [60]], which varies from 0.727 in Ba_2SnTe_5 through 0.818 in α-Na_2SnSe_3 to the high value of 0.995 in β-Na_2SnSe_3.

Connection of ME_4 molecular building blocks through common E–E bonds can afford either oligomeric anions $[(ME_4)_n]^{(2n)-}$ or polymeric anions $^1_\infty[ME_4^{2-}]$. Al-

though cyclic dimeric $[Ge_2Se_8]^{4-}$ anions of the former type have been characterized in $Cs_4Ge_2Se_8$ [84], chain formation is more typical for $GeSe_4$ and $GeTe_4$ tetrahedra. Polymeric $^1_\infty[ME_4^{2-}]$ anions have been found in K_2GeSe_4, Rb_2GeSe_4 [83], A_2GeTe_4 (A = K [164], Rb [83,165], Cs [83]) and Cs_2SnTe_4 [56], all of which can be prepared by methanolothermal reaction of A_2CO_3 with the elements M and E. As may be gauged from their torsion angles of $\pm 167°$ (Te–Te–M–Te, M–Te–Te–M) and 180° (Te–M–Te–Te) the $^1_\infty[MTe_4^{2-}]$ chains of the isotypic compounds Cs_2GeTe_4 and Cs_2SnTe_4 almost achieve a perfectly stretched conformation. In contrast, much smaller torsion angles are found in the likewise isotypic phases K_2GeE_4 (E = Se, torsion angles −75, 87, 138°; E = Te, torsion angles −73, 85, 145°), in which the chains are required to wind round the less voluminous potassium cations to allow the achievement of satisfactory coordination.

The readiness of tellurium to extend its coordination number to 4 is reflected in the incorporation of square planar $TeTe_4$ building units into the $^1_\infty[MTe_5^{2-}]$ chains (Fig. 8c) found in Tl_2GeTe_5 [166], Tl_2SnTe_5 [167], K_2SnTe_5 [135] and Rb_2SnTe_5 [158]. Only modest distortion of the idealized coordination polyhedra is required for the assembly of such polyanions, whose bonding is valence precise [168]. For instance, respective average endo- and exocyclic Te–Sn–Te and Te–Te–Te angles of 103.0/112.8° and 91.8/88.2° are observed in the $^1_\infty[SnTe_5^{2-}]$ chain of K_2SnTe_5. The Te–Te distances of 3.015 and 3.052 Å are typical for $TeTe_4$ units in compounds with metallic character [169].

3.3.2. Building units of higher nuclearity

Synthesis of one-dimensional Group 14 chalcogenidometalates(IV) under mild solventothermal conditions should, in the presence of a suitable larger counterion, allow the incorporation of typical molecular building blocks that are present in polar solvents such as H_2O or CH_3OH. A number of instructive examples have been prepared in recent years (Figs. 9 and 10). For instance, $[(CH_3C(NH_2)_2]Sn_2Se_5$ [10,121] contains corner-bridged ditetrahedral $[Sn_2Se_6]^{4-}$ units, $[Pr^n_2NH_2][(Pr^n)(Et)NH_2]Ge_4S_9$ [89] corner-bridged adamantane-like $[Ge_4S_{10}]^{4-}$ anions. Whereas the molecular units in both these polyanions are constructed through condensation of individual ME_4 coordination tetrahedra, two thirds of the tin atoms in the $^1_\infty[Sn_3Se_7^{2-}]$ chains of $(Et_4N)_2Sn_3Se_7$ [113] participate in $SnSe_5$ trigonal bipyramids. This unique anion displays two of the structural motifs that we will find to be common to many lamellar and framework thio- and selenidostannates(IV), firstly trinuclear Sn_3E_4 semi-cubes and secondly $E_{ax}E_{eq}$ edge-bridged infinite $^1_\infty[SnE_3^{2-}]$ chains with pentacoordinate tin atoms (Fig. 9c). $(Ph_4P)_2Sn_3Se_8$ [7,134], which was prepared at equimolar Se_5^{2-}:Sn ratio in a $(Ph_4P)_2Se_5$ flux at 200°C contains closely related $^1_\infty[Sn_3Se_8^{2-}]$ chains, in which the six-membered Sn_3Se_3 rings are now bridged by a dumb-bell Se_2 unit instead of the typical μ_3-Se atom of a semi-cube. Reaction of a $(Ph_4P)_2Se_5$/Sn/Se mixture in a 1:2:4 molar ratio under similar conditions affords a second compound $(Ph_4P)_4Sn_6Se_{11}$ [7,134], that once again exhibits infinite anion chains with two thirds of the tin atoms in a trigonal bipyramidal environment. However, these pentacoordinate centers are now directly bridged through two Se_3^{2-} chains and an

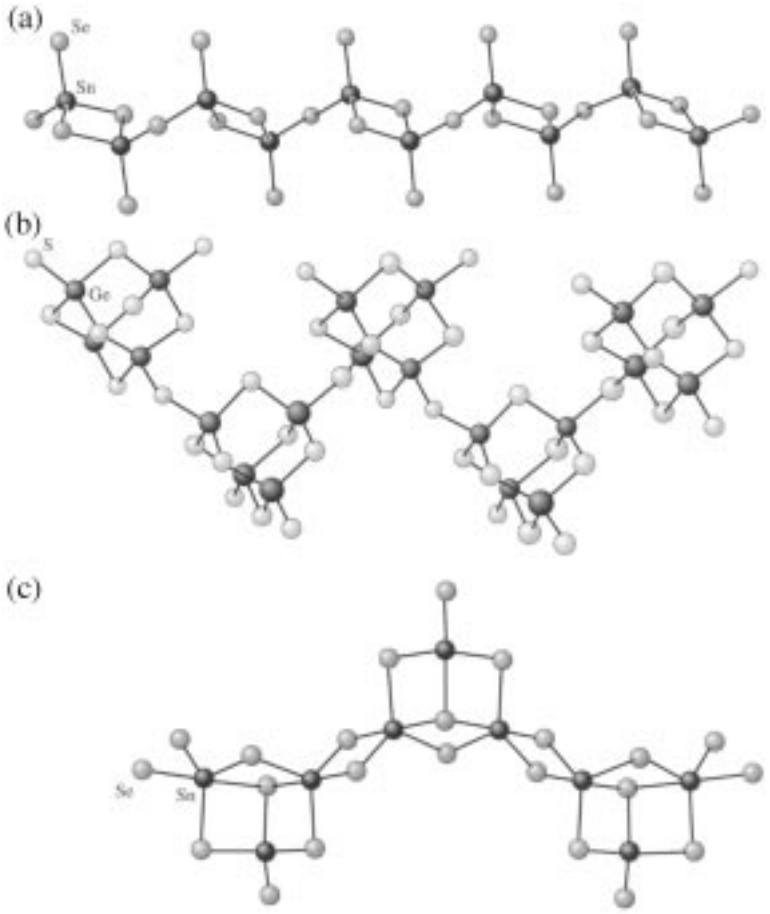

Fig. 9. Chainlike polyanions with M_yE_z building units ($y \geq 2$): (a) $^1_\infty[Sn_2Se_5^{2-}]$ in $[CH_3C(NH_2)_2]Sn_2Se_5$ [10,121], (b) $^1_\infty[Ge_4S_9^{2-}]$ in $[Pr^n_2NH_2][(Pr^n)(Et)NH_2]Ge_4S_9$ [89], (c) $^1_\infty[Sn_3Se_7^{2-}]$ in $(Et_4N)_2Sn_3Se_7$ [113].

axially sited Se atom to provide cyclic $[Sn_2Se_4(\mu\text{-}Se_3)_2(\mu\text{-}Se)]^{6-}$ building blocks, that edge-bridge to linking $SnSe_4$ tetrahedra of the $^1_\infty[Sn_6Se_{11}^{4-}]$ anion.

A totally different construction pattern has been found for the thiostannates(IV) $K_2Sn_3S_7 \cdot H_2O$ [10,121] and $Rb_2Sn_3S_7 \cdot 2H_2O$ [104], which belong to the same formula type as $(Et_4N)_2Sn_3Se_7$ [113]. The less diffuse nature of the sulphur atoms in the former compounds enables two thirds of the tin atoms to achieve octahedral coordination. Such polyhedra edge-bridge to four neighbors to afford an infinite $^1_\infty[SnS_3^{2-}]$ chain, that can be regarded as representing a ribbon section of the dense-packed layers parent tin(IV) disulphide berndtite with it PbI_2 layered structure [170]. Adjacent $^1_\infty[SnS_3^{2-}]$ anions are linked through ditetrahedral Sn_2S_6 building blocks into the $^1_\infty[Sn_3S_7^{2-}]$ double chains depicted in Fig. 10. In fact, the

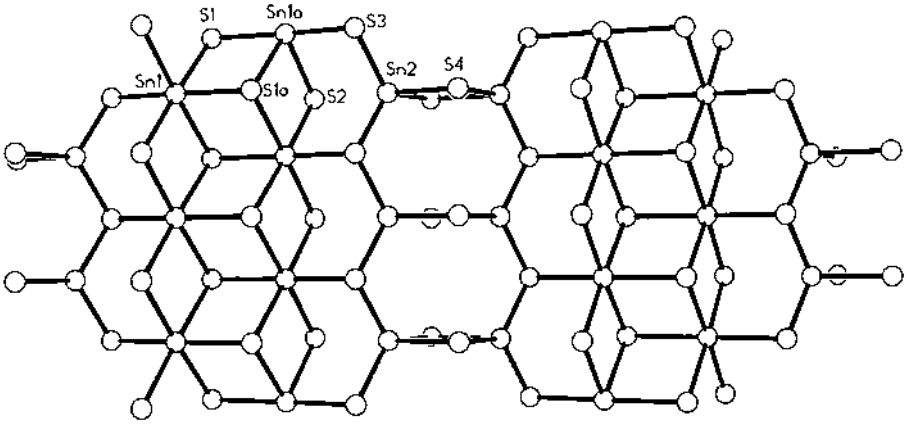

Fig. 10. Structure of the $^{1}_{\infty}[Sn_3S_7^{2-}]$ double chains in $K_2Sn_3S_7 \cdot H_2O$ [10,121] and $Rb_2Sn_3S_7 \cdot 2H_2O$ [104].

$^{1}_{\infty}[SnS_3^{2-}]$ ribbons contain crystallographic centers of symmetry and the central tin and sulphur atoms of the bridging Sn_2S_6 units are disordered with site occupation factors of 0.5. However, an analysis of the likewise disordered cation positions in $K_2Sn_3S_7 \cdot H_2O$ and $Rb_2Sn_3S_7 \cdot 2H_2O$ [104] indicates that neighboring Sn_2S_2 rings must be occupied, thereby giving rise to a ladder structure.

3.4. Layered structures

To our knowledge, only one report of a chalcogenidogermanate(IV) sheet anion has appeared. In $Na_2Ge_2Se_5$ [90], $GeSe_4$ tetrahedra are connected through three shared corners into infinite $^{2}_{\infty}[Ge_2Se_5^{2-}]$ layers (Fig. 11).

The ability of tin(IV) to extend its coordination number to 5 in thio- and selenido-stannates(IV) and 6 in thiostannates(IV) leads to families of 2- and 3-dimensional polyanions not available for germanium(IV). With the exception of $Cs_2Sn_3S_7 \cdot 0.5S_8$ [125], which was prepared by reacting Sn with a Cs_2S_x flux at 400–500°C, all known lamellar chalcogenido-stannates(IV) have been synthesized under mild solventothermal conditions (H_2O, CH_3OH) at temperatures in the range 110–200°C [10]. This technique was also employed for the preparation of the framework anion $^{3}_{\infty}[Sn_2Se_5^{2-}]$ in $Rb_2Sn_2Se_5$ [131]. Whereas structurally analogous $^{2}_{\infty}[Sn_3E_7^{2-}]$ layers and $^{3}_{\infty}[Sn_2E_5^{2-}]$ frameworks have been found in both thio- and selenidostannates(IV), it is apparent that the SnS_6-octahedra containing $^{1}_{\infty}[Sn_3S_7^{2-}]$ chains of $Rb_2Sn_3S_7 \cdot H_2O$ [104] and $^{n}_{\infty}[Sn_5S_{12}^{4-}]$ polyanions of $Cs_4Sn_5S_{12} \cdot 2H_2O$ ($n = 2$) [54] or $Tl_4Sn_5S_{12}$ ($n = 3$) [133] must be without parallel for the heavier Group 16 element. Thus the hydrated rubidium cation directs the assembly of a different formula type $^{2}_{\infty}[Sn_4E_9^{2-}]$ for E = Se [114]. However, it should also be recognized that not only the tin coordination polyhedra but also the subtle interplay between anion geometry, cation size and reaction conditions can lead to

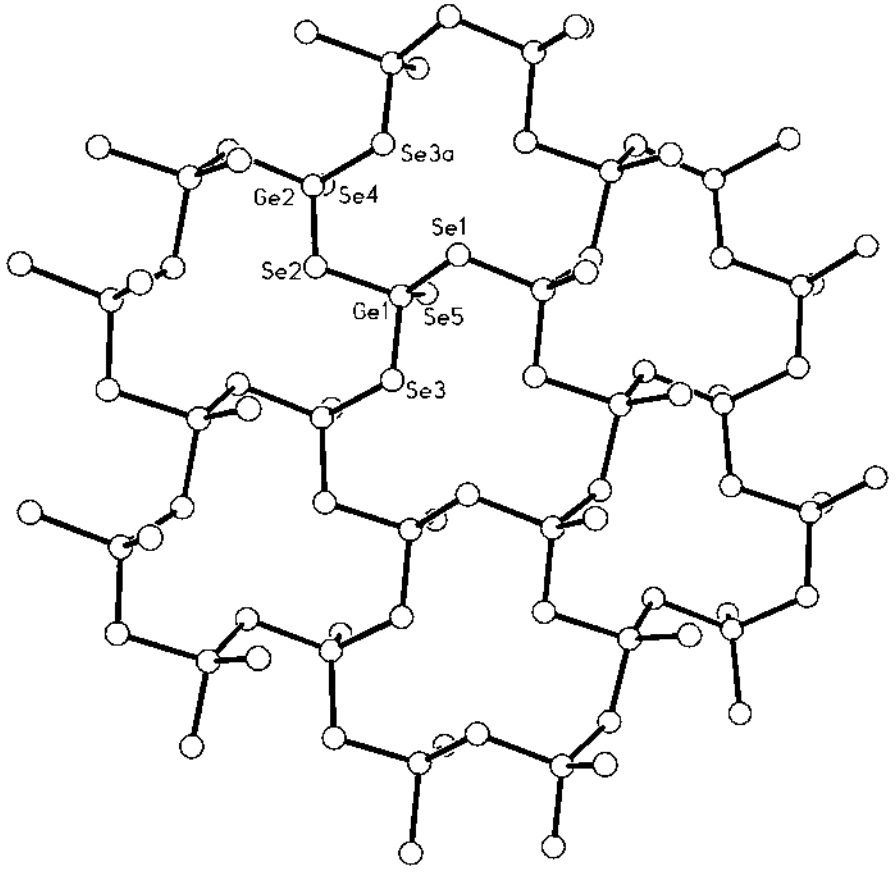

Fig. 11. Lamellar structure of the $^{2}_{\infty}[Ge_2Se_5^{2-}]$ anions in $Na_2Ge_2Se_5$ [90].

the observation of different structure or formula types. For instance, although both $(Et_4N)_2Sn_3S_7$ [124] and $(Et_4N)_2Sn_3Se_7$ [113] contain Sn_3E_4 semi-cubes as molecular building units, these are connected into sheets in the former compound and chains in the latter.

The first structural characterization of a porous lamellar thiostannate(IV), $Cs_4Sn_5S_{12} \cdot 2H_2O$, which was synthesized by W.S. Sheldrick under mild hydrothermal conditions (130°C) from Cs_2CO_3 and SnS_2, appeared in 1988 [54]. Condensation of two trinuclear Sn_3S_4 semicubes leads to formation of Sn_5S_8 units (Fig. 12) with a common central octahedral tin atom. Such building blocks assemble a planar 4^4 net with 20-membered rings by $S_{ax}S_{eq}$ edge-bridging of their remaining four trigonal bipyramidal coordination spheres. The same $^{2}_{\infty}[Sn_5S_{12}^{2-}]$ sheet anion is also present in $(C_4H_{11}N_2)_2(C_{10}H_{24}N_4)Sn_5S_{12}$ [171], whose piperazinium $C_4H_{11}N_2^+$ and 4,4′-ethylene dipiperazinium $C_{10}H_{24}N_4^{2+}$ cations are products of the decomposition of the original structure-directing agent 1,4-diazabicyclo[2,2,2]-octane (dabco).

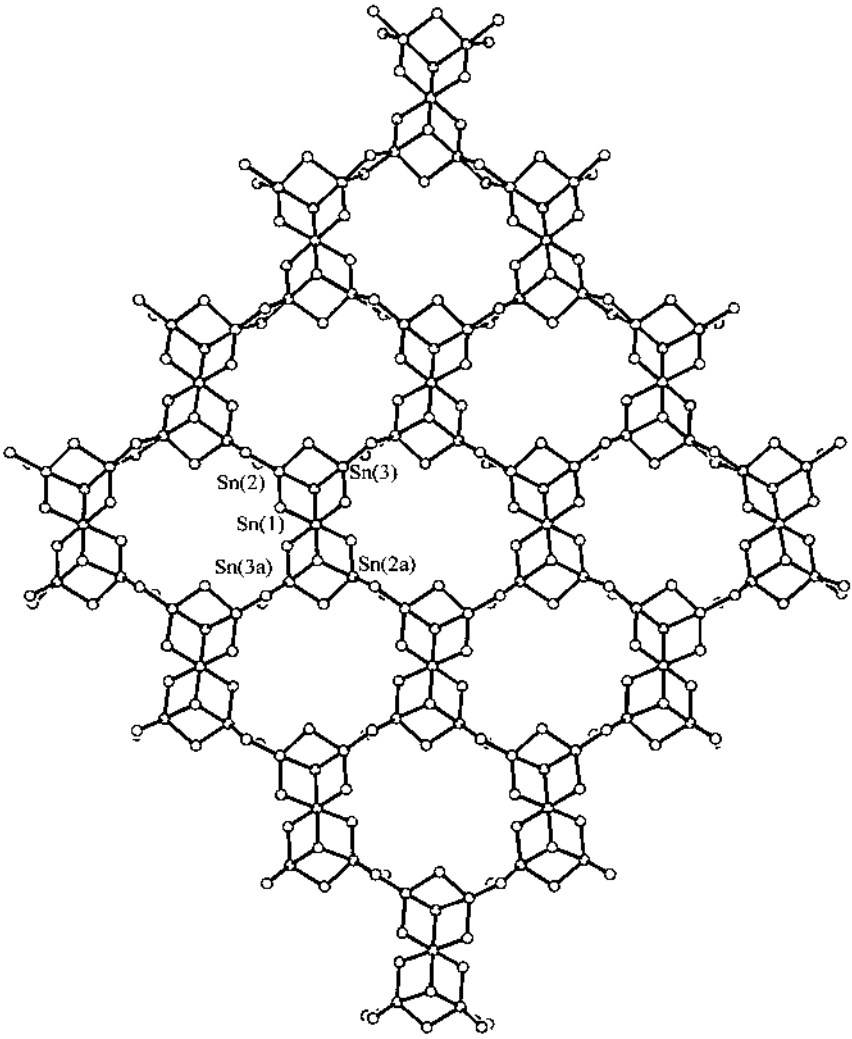

Fig. 12. Lamellar structure of the $^{2}_{\infty}[Sn_5S_{12}^{4-}]$ anion in $Cs_4Sn_5S_{12} \cdot 2H_2O$ [54]. The Sn_3S_4 semicubes are linked through a common octahedrally coordinated Sn atom.

In situ generation of suitable counterions from larger organic amines and tetraalkylammonium cations is frequently observed under mild hydrothermal conditions [10].

Space-filling and charge-compensation effects would therefore appear to be of importance in the cation controlled self-assembly of the highly condensed (c = 0.417) $^{2}_{\infty}[Sn_5S_{12}^{2-}]$ sheets with their molecular-dimension pores. Employment of alkylammonium cations R_4N^+ (R = Me, Et, Pr^n, etc.) to direct the hydrothermal construction of thiostannates(IV) was first reported in 1989 by R.L. Bedard and

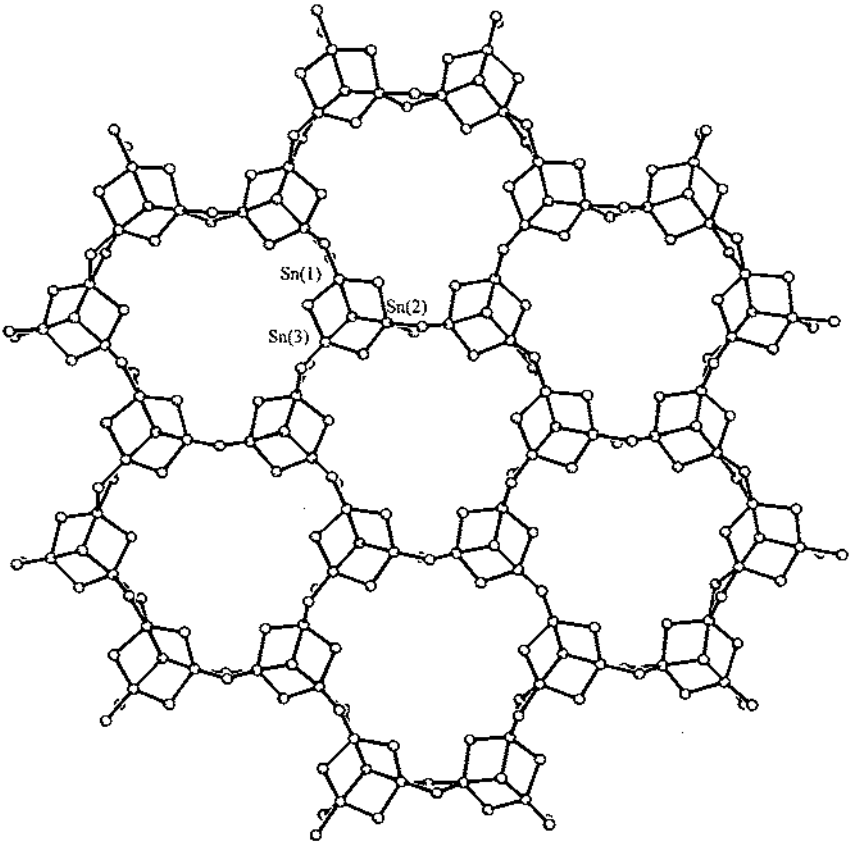

Fig. 13. Lamellar structure of the $^{2}_{\infty}[Sn_3Se_7^{2-}]$ anion in $Cs_2Sn_3Se_7$ [55].

co-workers [172,173], who patented a family of 'tin sulfide sieves' designated in zeolite-type nomenclature as R-SnS-*n* ($n = 1–4$) where *n* represents different structure types. Although these compounds were identified at the time by X-ray powder diffraction, their structures and physical properties were first studied in detail by the research teams of J.B. Parise and G.A. Ozin in the period 1994–1997. R-SnS-1 materials exhibit the formula $A_2Sn_3S_7$ and contain $^{2}_{\infty}[Sn_3S_7^{2-}]$ layers in which SnS_5 trigonal bipyramids participate in Sn_3S_4 semicubes and edge-bridge to afford a 6^3 net (Fig. 13) with 24-membered rings. Single crystal analyses have been reported for $(Me_4N)_2Sn_3S_7 \cdot H_2O$ [122] and $(Me_3NH)_2Sn_3S_7 \cdot 0.72H_2O$ [123] and powder diffraction studies have shown that such $^{2}_{\infty}[Sn_3S_7^{2-}]$ layers can also be assembled under hydrothermal conditions in the presence of NH_4^+, Et_4N^+, $Pr^n_3NH^+$, $Bu^tNH_3^+$, $dabcoH^+$ and the quinuclidinium cation [124]. In fact the prototype selenidostannates(IV), $Cs_2Sn_3Se_7$ [55,126], $(Me_2NH_2)_2Sn_3Se_7$ [126] and $(enH_2)_2Sn_3Se_7 \cdot 0.5en$ [126,174], which contain analogous $^{3}_{\infty}[Sn_3Se_7^{2-}]$ anions were synthesized and structurally characterized several years earlier (1990–1991) by

Sheldrick and Braunbeck. Later examples $(Me_4N)_2Sn_3Se_7$ [124] and $(TETN)Sn_3Se_7$ (TETN = 1,3-diaminoethyl-2-imidazolidone) [175] were denoted as TMA-SnSe-1 and TETN-SnSe-1. It is interesting to register that compounds of the type $A_2Sn_3E_7$ (E = S, Se) exhibit a bewildering range of space groups [e.g. $Cs_2Sn_3Se_7$, $C2/c$; $(Me_2NH_2)_2Sn_3Se_7$, $P2_1/n$; $(enH_2)_2Sn_3Se_7 \cdot 0.5en$, $Fddd$], which result from different stacking arrangements of individual anion layers. This phenomenon is also characteristic of the parent compound SnS_2, for which more than 70 polytype structure have been established.

Materials designated as R-SnS-3 in Bedard's patent exhibit the formula $A_2Sn_4S_9$ and the structure of their $^2_\infty[Sn_4S_9^{2-}]$ anions has been determined for $(Pr^n_4N)_2Sn_4S_9$ [127,128], $(Bu^n_4N)_2Sn_4S_9$ [127] and $(Pr^n_4N)(Me_3NH)Sn_4S_9$ [128]. The presence of very large structure-directing cations now leads to the assembly of 32-membered rings (Fig. 14), in which two edge-bridged Sn_3S_4 semicubes are linked through edge-bridged SnS_4 tetrahedra. This unique family of related layered porous chalcogenidometalates illustrates the interplay between cation volume and anion structure. As the counterion size increases from $[Cs(H_2O)_2]^+$ in $Cs_4Sn_5S_{12} \cdot 2H_2O$, over Et_4N^+ in $(Et_4N)_2Sn_3S_7$ to $Pr^n_4N^+$ in $(Pr^n_4N)_2Sn_4S_9$ so does the ring size of the anion cavities from 20 to 24 and finally 32 members. This change in porosity is accompanied by a continuous increase in the condensation grade c (0.417, 0.429, 0.444) and a concomitant reduction in the average coordination number of the tin atoms (5.33, 5.0, 4.75).

The generation of $A_2Sn_3E_7$ compounds by such a wide variety of cations with different shapes and sizes (e.g. NH_4^+, $Bu^tNH_3^+$, $dabcoH^+$) is a consequence of the remarkable network flexibility and stacking variability of their component $^2_\infty[Sn_3E_7^{2-}]$ sheets. Not surprisingly, this has led to studies ot the ion exchange properties and

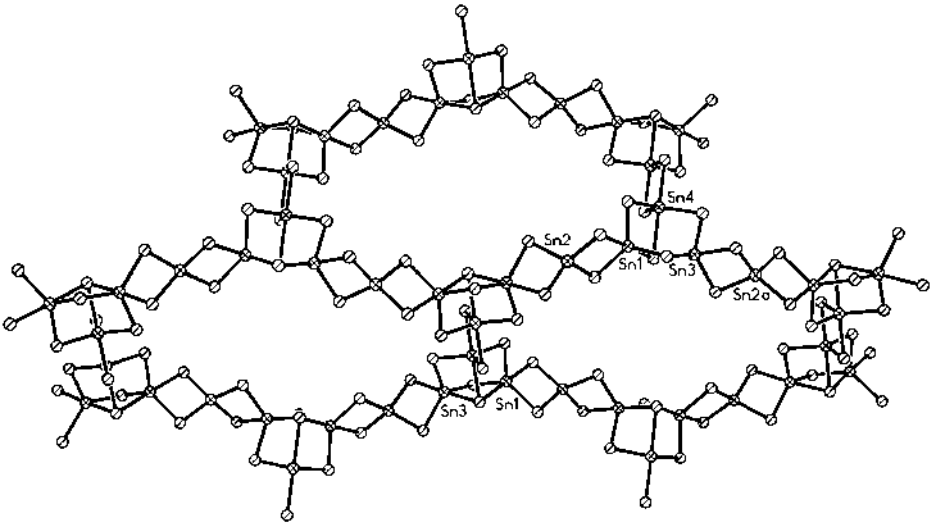

Fig. 14. Lamellar structure of the $^2_\infty[Sn_4S_9^{2-}]$ anion in $(Bu^n_4N)_2Sn_4S_9$ [127].

reversible molecule discriminating optical and electrical responses of these nanoporous semiconductors. Preliminary investigations indicate that alkali and alkaline earth metals as well as some transition metals can indeed replace the Me_4N^+ ions in $(Me_4N)_2Sn_3S_7 \cdot H_2O$ [122]. Upon evacuation, $(Et_4N)(NH_4)Sn_3S_7$ exhibits reversible uptake of water with an accompanying change in the unit cell dimensions and a significant shift of about 20 nm in the optical absorption edge [124]. Ozin et al. have also demonstrated that the absorption edges for the mixed compounds $(Me_4N)_2[Sn_3(S_xSe_{1-x})_7]$ exhibit a monotonous red shift as the selenium content is increased in the range $0 \leq x \leq 1$ [176]. The ability to chemically finely adjust the electronic and optical properties of this class of materials could open exciting perspectives for the development of tuneable semiconductors.

Of course, any envisaged application of these nanoporous chalcogenidostannates(IV) would require the possibility of template removal with retention of framework integrity. Recent thermochemical studies on $(Et_4N)_2Sn_3S_7$ and $(Pr^n_4N)_2Sn_4S_9$ have demonstrated that the thermal stability range (20–200°C) of these materials is more restricted than that of the oxide-based zeolites [177]. At temperatures above 200°C, reaction of chemisorbed water and alkylammonium cations with the anion layers initiates solid-state reconstruction, first to the dense packed layers of SnS_2 then to SnS [178] and Sn_2S_3 [179]. The bulk crystalline nanoporosity of lamellar thiostannates(IV) has been shown to be reflected in their material surfaces as registered by atomic force microscopy [180].

$^2_\infty[Sn_4S_9^{2-}]$ sheets analogous to those of $(Pr^n_4N)_2Sn_4S_9$ and $(Bu^n_4N)_2Sn_4S_9$ [127,128] do not appear to have been reported for selenidostannates(IV). Interestingly, a compound of the same formula type, $Rb_2Sn_4Se_9 \cdot H_2O$, has recently been found to exhibit the novel layered structure depicted in Fig. 15 [114]. The $^2_\infty[Sn_4Se_9^{2-}]$ network contain eight-membered Sn_4Se_4 rings which can formally be regarded as resulting from corner-sharing between Sn_2Se_6 and Sn_2Se_7 ditetrahedral building blocks. These Sn_4Se_{13} units edge-bridge at each of their tin atoms to assemble a 4^4 net with 16-membered rings; as a result, the average coordination number of the tin atoms is now only 4.5 as opposed to 4.75 in $A_2Sn_4S_9$ structures.An alternative way of looking at the anionic sheets of $Rb_2Sn_4Se_9 \cdot H_2O$ is to consider them as being composed of condensed $^1_\infty[Sn_2Se_5^{2-}]$ chains of corner-bridged Sn_2Se_6 units (see Fig. 9a).

Ditetrahedral $[Sn_2E_6]^{4-}$ molecular building blocks are present in all known lamellar chalcogenidostannates(IV) and this would suggest that such anions could provide solution precursors at the solventothermal site of crystallisation. The successful isolation of compounds $A_4Sn_2E_6$ (E = S, A = Me_4N^+, cyclohexylammonium [181]; E = Se, A = Rb [104], Cs [105]) as well as $(enH_2)_2Sn_2Se_6 \cdot en$ [174] from hydro- and methanolothermal reaction mixtures employed for the generation of layered chalcogenidostannates(IV) provides further support for this hypothesis. Using ^{119}Sn NMR and UV–Vis spectroscopy, Ozin et al. [181] have also confirmed that $[Sn_2S_6]^{4-}$ anions are predominant in mother liquors retained from the hydrothermal synthesis of $A_2Sn_3S_7$ and $A_2Sn_4S_9$. However, a degree of caution is necessary in such mechanistic aspects. The evidence for the participation of $[Sn_2E_6]^{4-}$ anions in the self-assembly of chalcogenidostannates(IV) is circumstan-

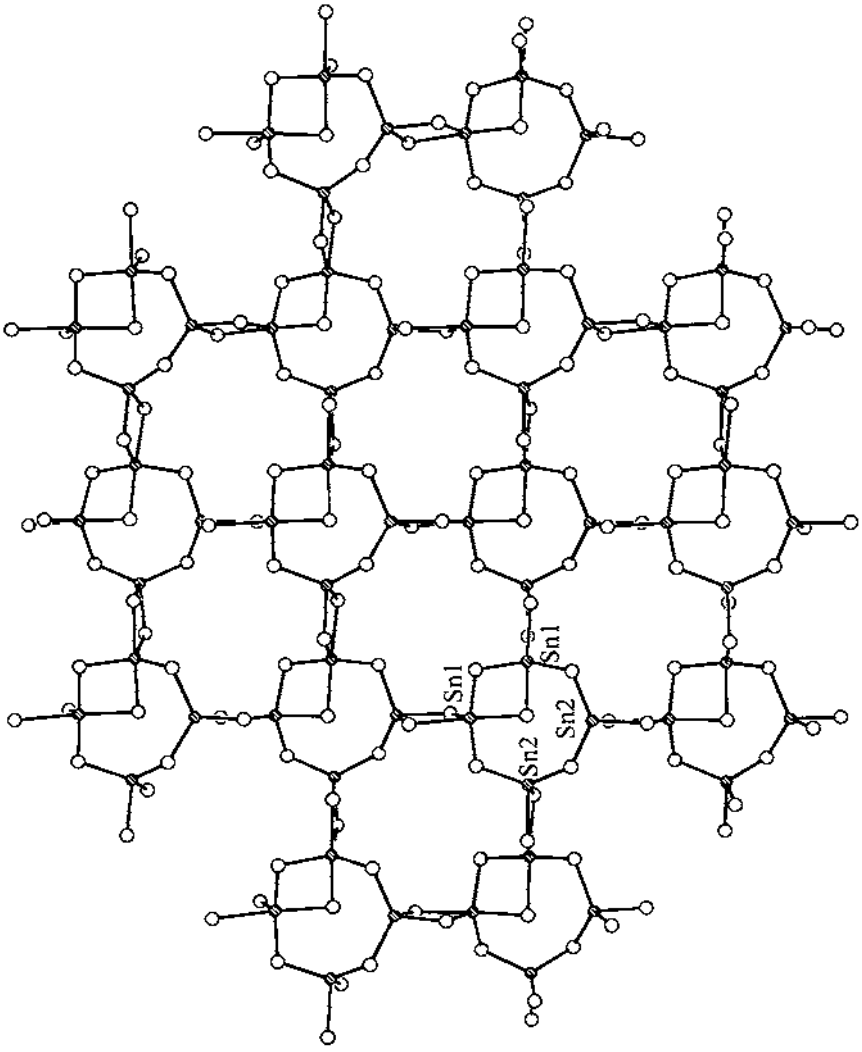

Fig. 15. Lamellar structure of the $^{2}_{\infty}[Sn_4Se_9^{2-}]$ anion in $Rb_2Sn_4Se_9 \cdot H_2O$ [114].

tial and no direct studies of nucleation under solventothermal conditions have been performed. Our preparation of $^{1}_{\infty}[Sn_3Se_7^{2-}]$ chains in $(Et_4N)_2Sn_3Se_7$ [113], which also provide a common structural motif for lamellar thio- and selenidostannates(IV), suggests that such 1-D polyanions could be formed prior to sheet construction. O'Hare and co-workers [182] have studied the synthesis of $(Me_4N)_2Sn_3S_7$ under hydrothermal conditions using real-time in situ energy-dispersive X-ray diffraction. Their results indicate that temperature is the primary factor in determining whether crystalline products are obtained, while pH and

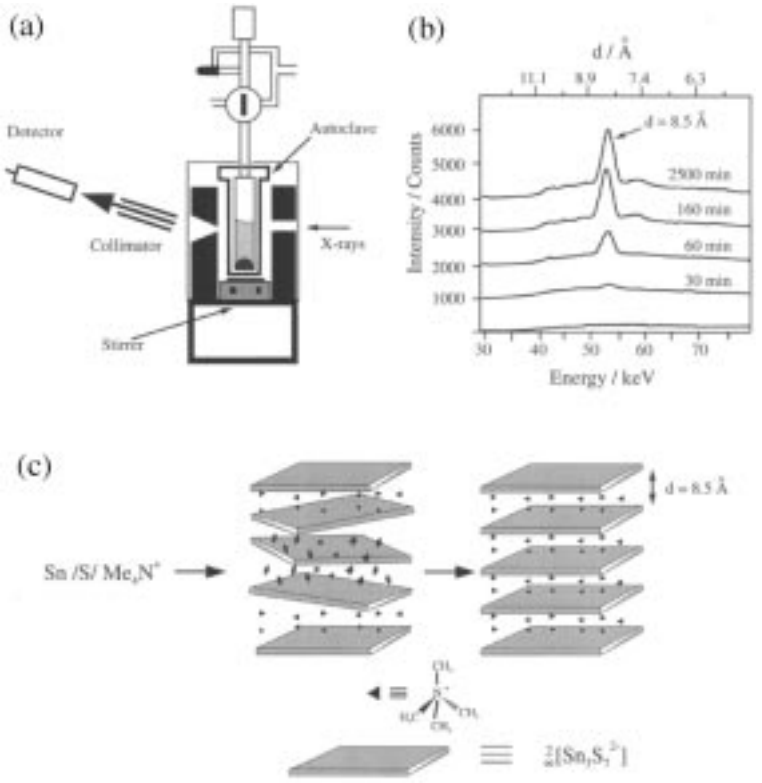

Fig. 16. (a) Experimental apparatus used for in situ diffraction studies of solventothermal reactions; (b) time dependence of the diffraction pattern for the hydrothermal formation of $(Me_4N)_2Sn_3S_7$ at 120°C showing the evolution of the characteristic Bragg reflection at 8.5 Å, corresponding to the interplanar distance between thiostannate(IV) layers; (c) proposed formation of parallel disordered layers followed by slow cation-directed reorganisation to a regular stacking arrangement [182].

starting materials are of importance in controlling the rate of reaction and the polytypic structure formed. Evidence was provided that the construction of $(Me_4N)_2Sn_3S_7$ proceeds via an intermediate phase with disordered $^2_\infty[Sn_3S_7^{2-}]$ sheets (Fig. 16). Crystals of this compound grown in microgravity (on board the Space Shuttle *Endeavor*) show improved crystal habits, less mosaic spread, better optical quality and larger void volumes than materials grown on Earth [183,441].

Kanatzidis and co-workers have prepared a series of polythiostannates(IV) $K_2Sn_2S_8$, α- and β-$Rb_2Sn_2S_8$ and $Cs_2Sn_2S_6$ by the molten salt technique [151]. The basic building units of the isotypic compounds $K_2Sn_2S_8$ and α-$Rb_2Sn_2S_8$ may be described as face-sharing double semicubes (Fig. 17) that are edge-bridged at opposite SnS_4 tetrahedra to create $^1_\infty[Sn_4S_{12}]$ ribbons. These cross link together through tetrasulphide S_4^{2-} ligands to afford a lamellar structure in which the central tin atoms of the double semicubes are octahedrally coordinated. β-

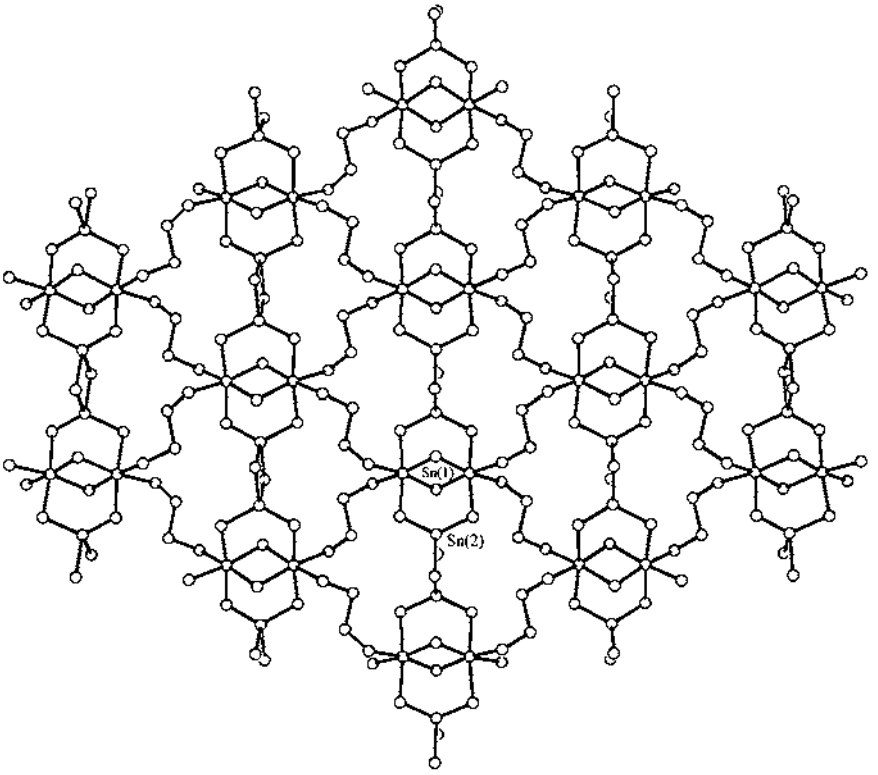

Fig. 17. The sheet structure of the $^{2}_{\infty}[Sn_2S_8^{2-}]$ anion in $K_2Sn_2S_8$ [151].

$Rb_2Sn_2S_8$ (space group *Pbcn*) is a polytype of α-$Rb_2Sn_2S_8$ (space group $P2_1/n$), that can be synthesized at 450°C rather than 330°C. Edge-bridged $^{1}_{\infty}[SnS_3^{2-}]$ chains with trigonal bipyramidal tin centers are connected by S–S bonds in the porous structure of $Cs_2Sn_2S_6$. The isotypic compound $Cs_2Sn_2Se_6$ (Fig. 18a) has recently been prepared by reaction of Cs_2CO_3 with Sn and Se in superheated methanol at 130°C [114].

3.5. Framework structures

The framework anions of both the isotypic compounds $A_2Sn_2E_5$ (E = S, A = K [129], Tl [130]; E = Se, A = K [129], Rb [131]) and the thiostannate(IV) $Na_4Sn_3S_8$ [132] exhibit structures closely related to that of the $^{2}_{\infty}[Sn_2E_6^{2-}]$ sheets in $Cs_2Sn_2E_6$ (E = S, Se). As a common feature, all three structure types contain SnE_5 trigonal bipyramids that are linked through shared edges into $^{1}_{\infty}[SnE_3^{2-}]$ chains. Neighbouring chains at $z = 0$ and $z = 1/2$ in the monoclinic compounds $A_2Sn_2E_5$ (space group $C2/c$) are related by a glide plane and orientated in respective directions and $[1\bar{1}0]$ (Fig. 19a). Cross linking of these ribbons through common equatorial

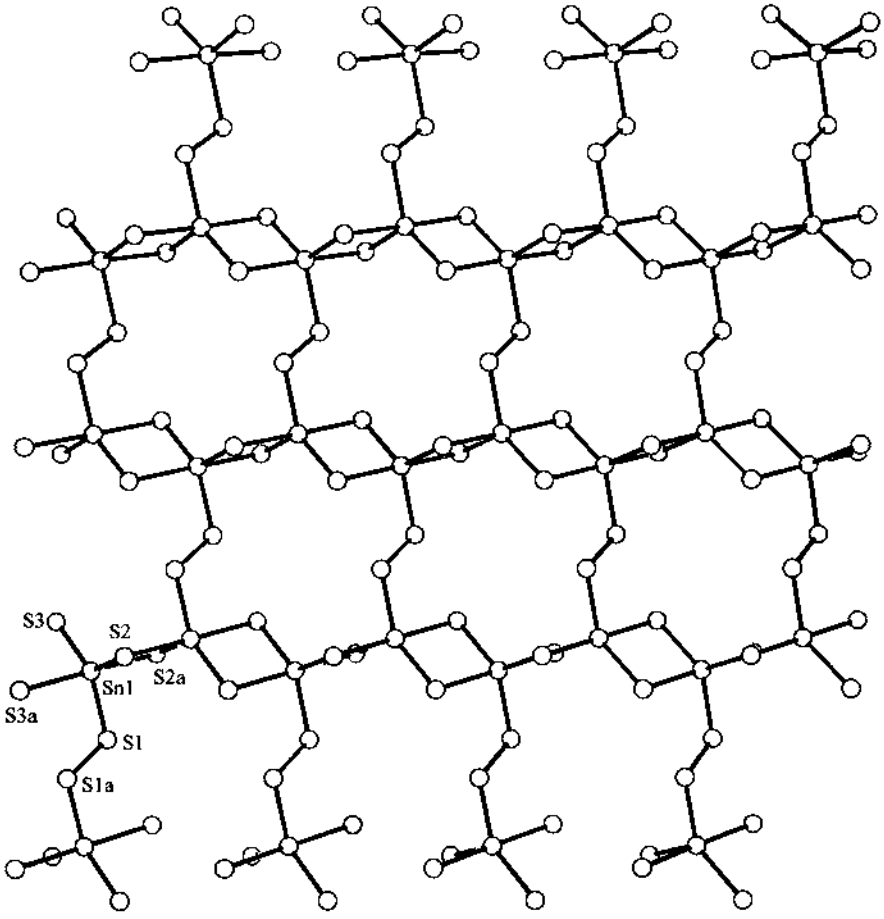

Fig. 18. Fourteen-membered pores and $^{1}_{\infty}[SnS_3^{2-}]$ chains in the $^{1}_{\infty}[Sn_2S_6^{2-}]$ anion of $Cs_2Sn_2S_6$ [151], that is isotypic with $Cs_2Sn_2Se_6$ [114].

chalcogen atoms generates a compact three-dimensional anion network in which the cations fit snugly into channels parallel to direction [010]. With the exception of $Rb_2Sn_2Se_5$ (CH_3OH, 160°C), all $A_2Sn_2E_5$ phases were prepared at temperatures of 300°C ($Tl_2Sn_2S_5$) or higher ($K_2Sn_2E_5$, 900°C). $Na_4Sn_3S_8$ was synthesized by reaction of Na_2S and SnS_2 at 680°C [132] and also crystallizes monoclinic in the space group $C2/c$. Whereas its *a*- and *b*-axes are closely similar to those of $K_2Sn_2S_5$, its *c*-axis is now much longer (17.621 vs. 11.517 Å) owing to the fact that the $^{1}_{\infty}[SnS_3^{2-}]$ ribbons are now cross linked by corner sharing SnS_4 tetrahedra.

It is perhaps somewhat surprising that no examples of framework anions with adamantage-like $[Sn_4S_{10}]^{4-}$ building blocks are known. However, both 2- and 3-D open networks have been constructed with the supertetrahedron $[Sn_{10}O_4S_{20}]^{8-}$,

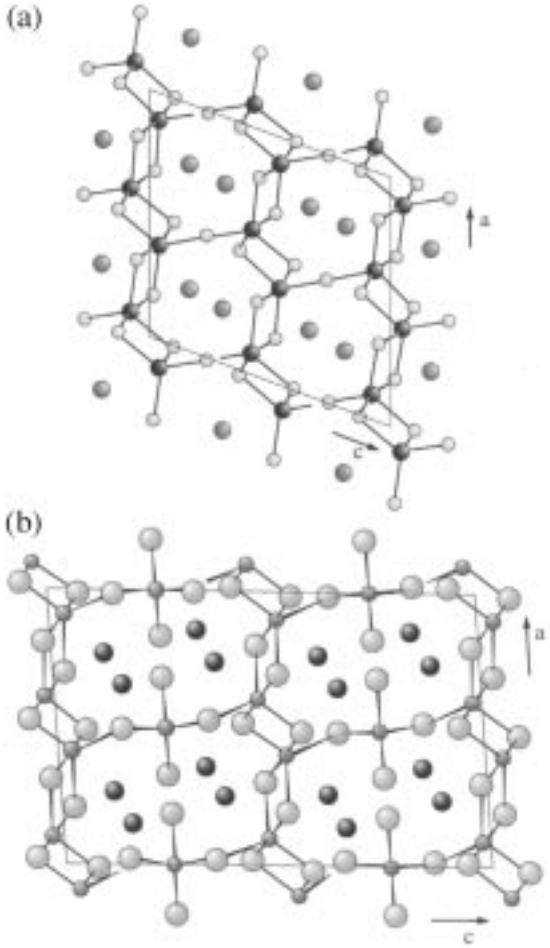

Fig. 19. (a) The porous framework structure of the $^{3}_{\infty}[Sn_2Se_5^{2-}]$ anion in $Rb_2Sn_2Se_5$ [131] with $^{1}_{\infty}[SnSe_3^{2-}]$ chains linked through common corners; (b) the framework structure of the $^{3}_{\infty}[Sn_3S_8^{4-}]$ anion in $Na_4Sn_3S_8$ [132].

that was crystallized as a discrete anion in $Cs_8[Sn_{10}O_4S_{20}]\cdot 13H_2O$ [162]. In $^{2}_{\infty}[S_{20}O_8S_{37}^{10-}]$ (probable counterion $Me_2NH_2^+$) each such building unit corner shares with three neighbors [175], in $(MeNH)_4[Sn_{10}O_4S_{18}]$ all four terminal S atoms are involved to afford two interwoven diamond-like lattices [184].

The recent extension of the soft methanolothermal technique to telluridometalates has enabled the preparation of $Rb_{4+x}Sn_4Te_{17}$ $(0 \leq x \leq 1)$ [185], in the anionic part of which planar thinned 4^4 nets with Te_{12} squares are connected through ditetrahedral Sn_2Te_6 spacers into a unique open framework (Fig. 20). This represents the first example of a nanoporous material to contain a defective square

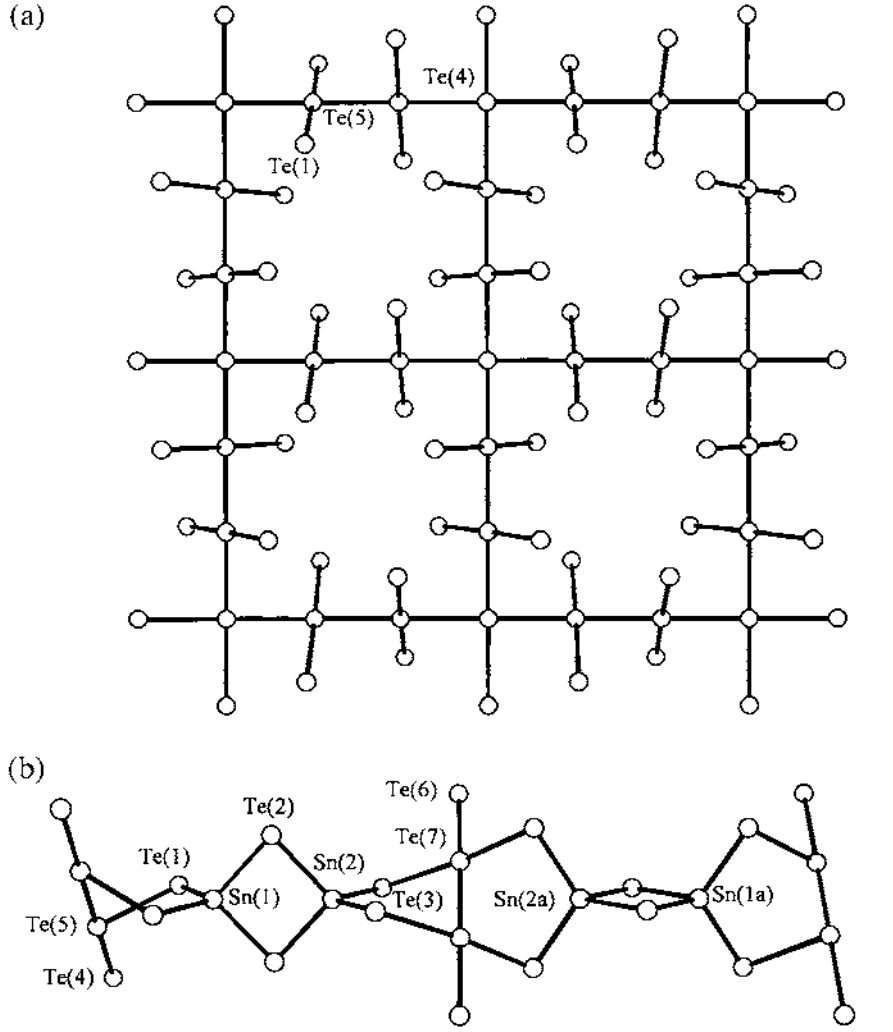

Fig. 20. (a) Planar thinned 4^4 tellurium nets in $Rb_{4+x}Sn_4Te_{17}$ ($0 \leq x \leq 1$) and (b) ditetrahedral Sn_2Te_6 connecting spacers between the layers.

planar tellurium lattice, which on the basis of band structure calculations would be expected to be a new low-dimensional metal. Owing to extreme disordering of the Rb^+ cations in the channel along the [001] direction (Fig. 21), it is not possible to establish their occupation factors with certainty. However, this observation suggests that at least partial ion exchange could be possible.

3.6. Quaternary phases

Quaternary compounds can be formulated generally as $A_mM'_xM_yE_z$, where the

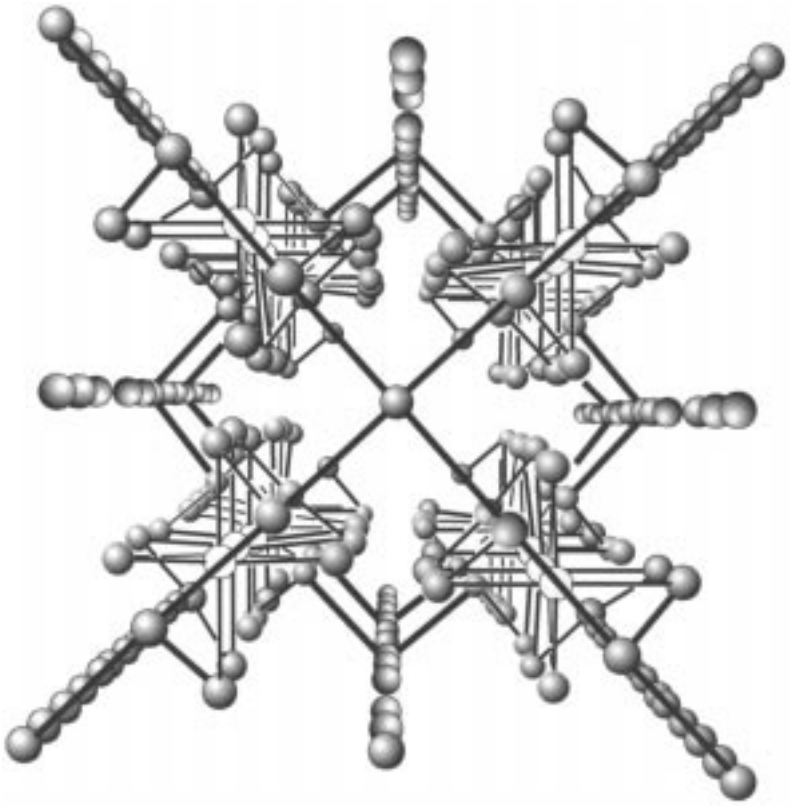

Fig. 21. Crystal structure of the anionic part of $Rb_{4+x}Sn_4Te_{17}$ $(0 \leq x \leq 1)$ [185]. The Rb^+ cations occupy the channels running in the direction [001].

additional M′ atom is either a transition metal or a Main Group metal up to the Zintl border [186]. The fact that the synthesis and characterization of quaternary compounds is still in its infancy is clearly apparent for Group 14 chalcogenidometalates.

As discussed in Section 3.2, the design of ternary chalcogenidometalates(IV) with open 2- and 3-D anion networks is somewhat hampered by the high stability of adamantane-like anions $[M_4E_{10}]^{4-}$. However, an increased degree of connectivity should be favored for isolated anions as the ionic character of E–A bonds to the positive counterion A decreases, and chainlike thiogermanates(IV) are known for A = Sn(II) and Pb(II) [187,188] (e.g. $PbGeS_3$). Such considerations have led to the discovery of a family of quaternary thiogermanates(IV) $(Me_4N)_2[M'Ge_4S_{10}]$ (M′ = Mn, Fe, Cd) first prepared under mild hydrothermal conditions by R.L. Bedard in 1989 [12] and then structurally characterized in the period 1994–1996 by three independent research teams (M′ = Mn [18,189,190], Fe [189,191], Cd [190]). In these isostructural tetragonal compounds (space group $I\bar{4}$), corner linkage of

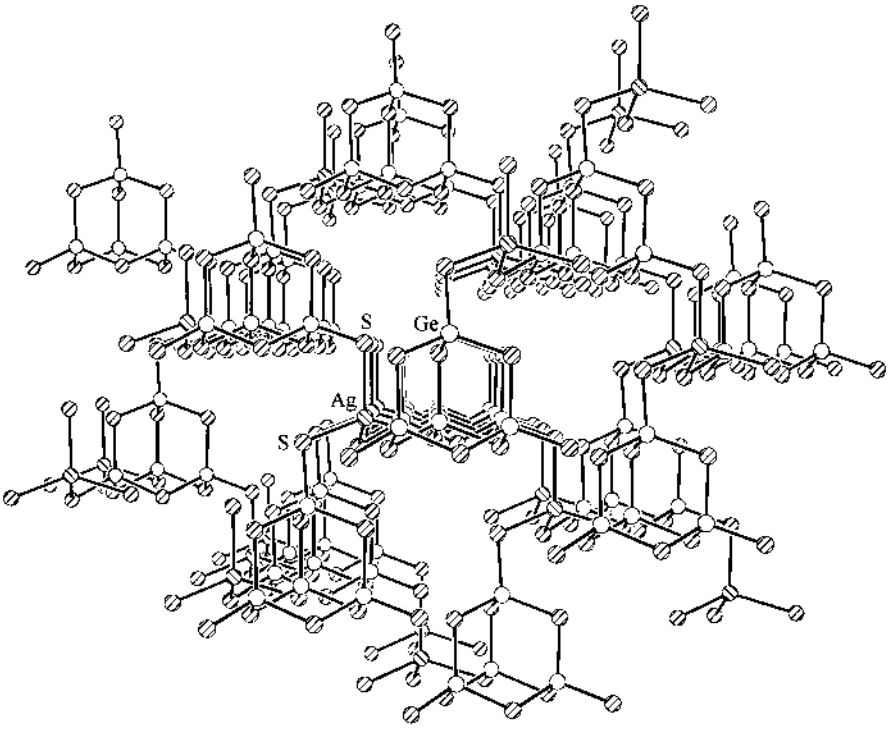

Fig. 22. Open zinc blende-like framework structure of $^{3}_{\infty}[AgGe_4Se^{3-}_{10}]$ in $Rb_3[AgGe_4Se_{10}] \cdot 2H_2O$ [192].

Ge_4S_{10} units and $M'S_4$ tetrahedra generates an open framework structure containing intersecting channels with a diameter of about 0.7 nm. The Cs^+ cation is large enough to support this anionic framework and $Cs_2[FeGe_4S_{10}] \cdot xH_2O$ [191] may be prepared by addition of Fe^{2+} to an aqueous solution of $Cs_4Ge_4S_{10}$. The compound loses physisorbed water at 116°C and chemisorbed water at 188°C, but the framework anion $^{2}_{\infty}[FeGe_4S^{2-}_{10}]$ is stable up to 630°C in vacuum, thereby providing encouragement for the possible technological application of such sulphide-based advanced materials. The analogous selenidogermanates(IV) $A_3[AgGe_4Se_{10}] \cdot 2H_2O$ (A = Rb, Cs) (Fig. 22), $A_2[MnGe_4Se_{10}] \cdot 3H_2O$ (A = Rb, Cs) [192] and $(Me_4N)_2[MnGe_4Se_{10}]$ [113] can also be obtained under hydrothermal conditions. These anionic frameworks exhibit a remarkable capacity to accomodate cations of different sizes. Pronounced changes in the size and shape of the cation channels can be achieved by relatively small modifications of the geometry of the bridging transition metal coordination tetrahedra and their corner linkages to Ge_4E_{10} cages. For instance the volume of the unit cell increases from 1044.0 $Å^3$ in $Cs_2[FeGe_4S_{10}] \cdot xH_2O$ to 1245.5 $Å^3$ in $(Me_4N)[FeGe_4S_{10}]$ [191].

An analogous zinc blende-like architecture, in which Ge_4S_{10} building blocks are linked by dimetal Cu^{2+}_2 or Ag^{2+}_2 units has been reported for the anionic frame-

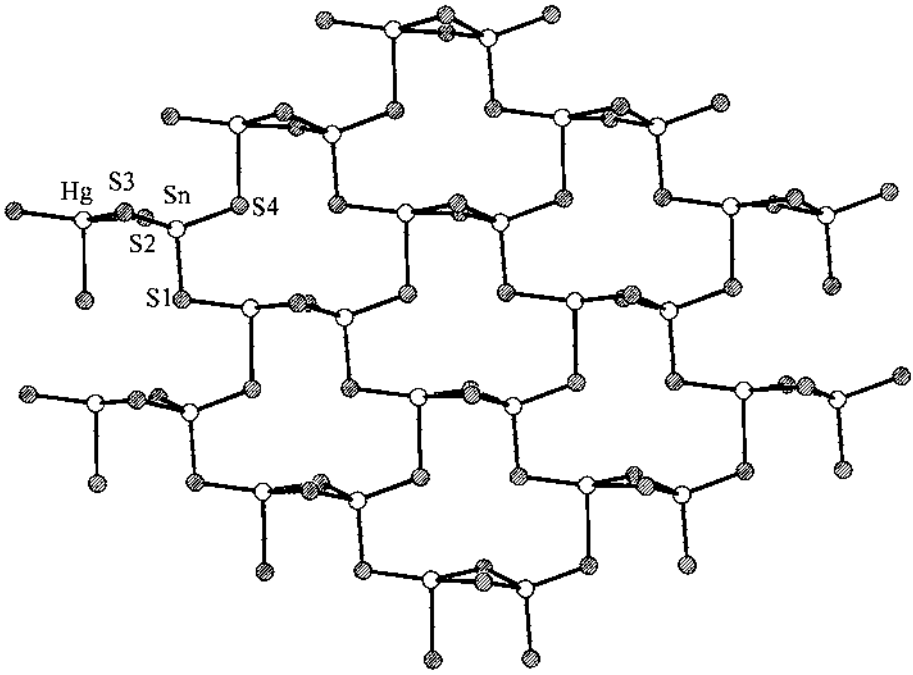

Fig. 23. The sheet structure of $BaHgSnS_4$ [199].

work of $(Me_4N)_2[M'_2Ge_4S_{10}]$ (M′ = Cu, Ag) [193]. Treatment of GeS_2 with an alkylammonium cation in the presence of a bridging coinage metal cation (M′ = Cu, Ag) has also led to the isolation of a number of related Ge_4S_{10}-containing compounds under hydrothermal conditions. Whereas $(Me_4N)[CuGe_2S_5]$ contains a 3-D anionic network with connecting linear CuS_2 units [194], the Cu atoms in the disordered structure of $(Me_4N)_6[(Cu_{0.44}Ge_{0.56}S_{2.23})_4(Ge_4S_8)_3]$ [195] are, in contrast, either 3- or 4-coordinated. In the novel $^1_\infty[AgGe_4S_{10}^{3-}]$ anions of $[(dabcoH)_2(H_3O)][AgGe_4S_{10}] \cdot H_2O$ [196] adamantane-like cages are linked through corner sharing AgS_3 units into double chains. The same structure-directing cation has been employed to construct $(dabcoH_2)[MnGe_4S_{10}] \cdot 3H_2O$ [197], whose framework anion is analogous to zeolite Li–A(BW) [198].

In contrast to such solventothermally prepared materials, most of the known high-temperature quaternary thiogermanates(IV) and -stannates(IV) phases contain only discrete $[ME_4]^{4-}$ tetrahedra, as the smallest possible Group 14/Group 16 building blocks, in their anionic structures. Coordination of the second metal M′ by such ligands generates extended structures with 1-, 2- or 3-D character. The first studies on the high temperature synthesis of quaternary Ge and Sn sulfides were reported between the mid 1970s and 1980s by C.L. Teske, whose Ba compounds $BaHgSnS_4$ [199] (Fig. 23), $BaCdGeS_4$ [200], $BaCdSnS_4$ [201], $BaZnSnS_4$ [202] and $BaMnSnS_4$ [202] all display sheet structures consisting of corner- and edge-sharing

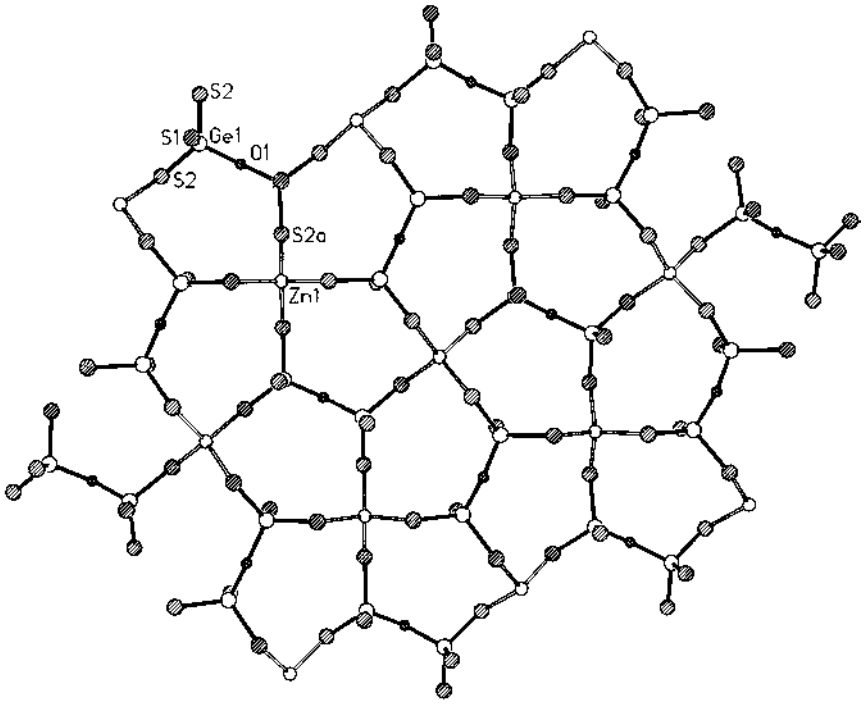

Fig. 24. The sheet structure of $A^{II}_2[ZnGe_2OS_6]$ (A^{II} = Sr, Ba) [211,212], whose $[Ge_2OS_6]^{6-}$ ditetrahedra consist of two $[GeOS_3]^{4-}$ units with a common O atom.

$M'S_4$ and MS_4 tetrahedra. These anionic layers are, in fact, closely related to the $BaIn_2Se_4$ structure [203], which itself is a substitution variant of the TlSe-type [204].

In $BaAg_2GeS_4$ [205], GeS_4 tetrahedra are arranged in a sheet-like manner and connected by distorted tetrahedral AgS_4 units with common S atoms, thereby resulting in a framework that is isostructural to that of KAg_2SbS_4 (Section 4.6). Similar anionic networks hav been found in $SrCu_2GeS_4$, $BaCu_2GeS_4$ [206], $SrCu_2SnS_4$ [207], $BaAg_2SnS_4$ [208], $BaCu_2SnS_4$ [209] and $Ba_3Cd(SnS_4)_2$ [210]. A unique feature is observed in the sheet structures of $Sr_2[ZnGeOS_6]$ and $Ba_2[ZnGeOS_6]$ [211,212], whose two $[GeOS_3]^{4-}$ tetrahedra are linked together through a common O atom into the corner-sharing $[Ge_2OS_6]^{6-}$ anion depicted in Fig. 24.

Some novel quaternary alkali metal Cu(I)-thio- and selenidostannates(IV) were recently prepared by Kanatzidis et al. using the molten flux technique [213]. $Rb_2Cu_2SnS_4$ contains a row of $[SnS_4]^{4-}$ tetrahedra, that are connected by Cu atoms to create a layer structure. Parallel CuS_2 chains, similar to those of SiS_2 [214], result as a characteristic structural motif from this assembly pattern (Fig. 25).

A series of isotypic compounds with the general formula type $ACuSnE_3$ (E = S,

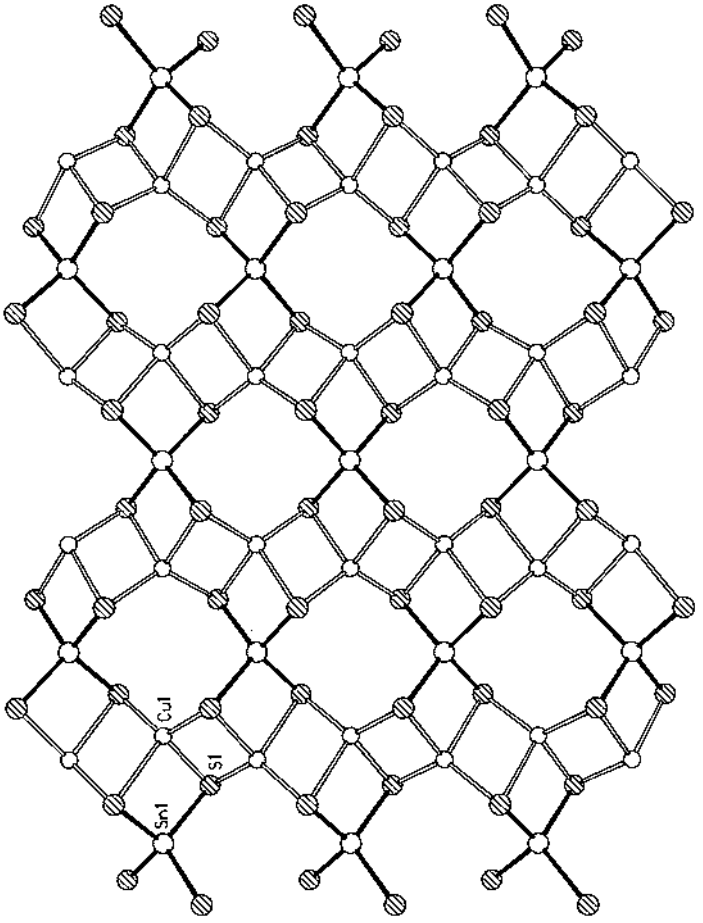

Fig. 25. The $^{2}_{\infty}[Cu_2SnS_4^{2-}]$ layer in $Rb_2Cu_2SnS_4$ [213], with CuS_2 chains highlighted as open bonds.

A = Na, K, Rb, Cs; E = Se; A = K, Rb) [213] display $^{1}_{\infty}[SnE_3^{2-}]$ chains, as also found in a number of ternary compounds (Section 3.3). The two terminal S atoms link neighboring ribbons together through strongly distorted CuS_4 tetrahdra into sheets (Fig. 26a). Although this structure is related to that of Cu_2SnS_3 [216] (ZnS type), replacement of one half of the Cu atoms by an alkali metal cation lowers the anion dimensionality from 3 to 2. The Sn–S bonds within the chain [Sn–S(b)–Sn] are significantly longer than those bridging to the Cu atoms [Sn–S(t)–Cu], although the S–Cu bonds must also be assumed to exhibit pronounced covalent character [e.g. distances of 2.487(4)–2.498(4) Å as compared to 2.334(4)–2.356(4) Å in $RbCuSnS_3$] [213].

Similar structural features are also present in $K_2HgSn_2S_6$ [7,134], but the anionic layers in this material are less voluminous (Fig. 26b). One-dimensional

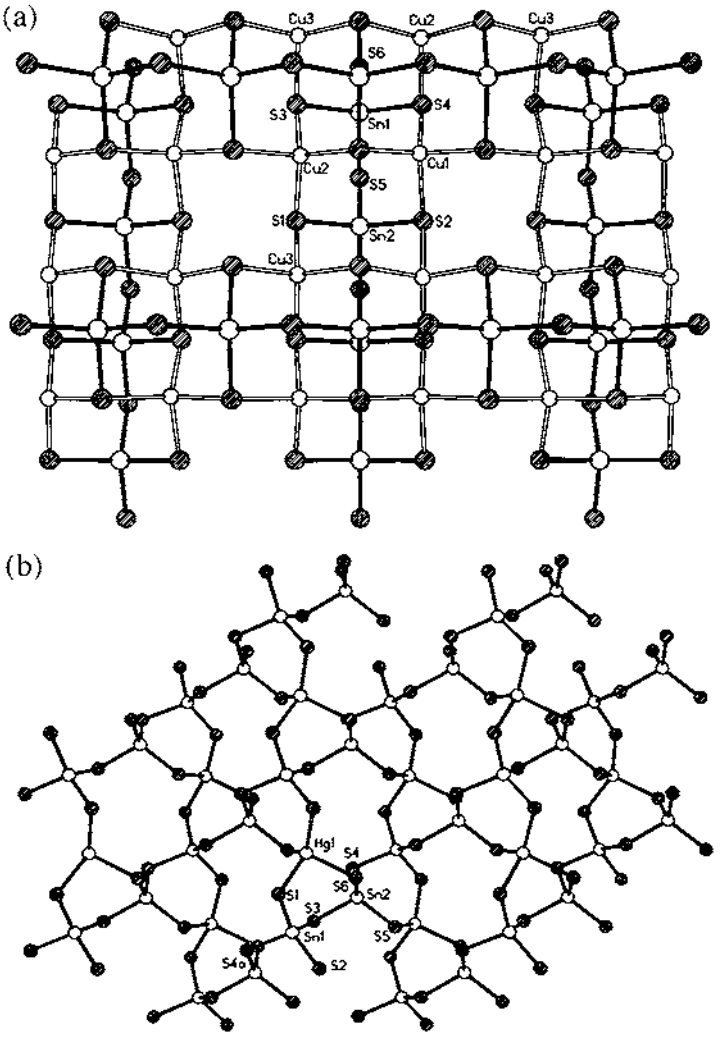

Fig. 26. The sheets (a) of the isostructural compounds $ACuSnE_3$ (A = Na, K, Rb, Cs; E = S: A = K, Rb; E = Se) [213] and (b) of $K_2HgSn_2S_6$ [7,134]. All compounds display $^1_\infty[SnS_3^{2-}]$ chains [16,17,115–120] as structure building components.

$^1_\infty[SnS_3^{2-}]$ ribbons have also been found in the isotypic compounds $K_2MnSn_2S_6$, $CsMnSn_2S_6$ and $Rb_2ZnSn_2S_6$ [7,134], in which *vierer* single chains connect together through tetrahedrally coordinated Mn or Zn atoms to construct a framework structure containing six-membered $[M'Sn_2S_3]$ rings (M′ = Mn, Zn) as an additional motif.

A radically different assembly principle is adopted by K_2MnSnS_4 [7,134]. Half of the tin atoms from an $[Sn_4S_{10}]^{4-}$ adamantane-like cage are statistically replaced by

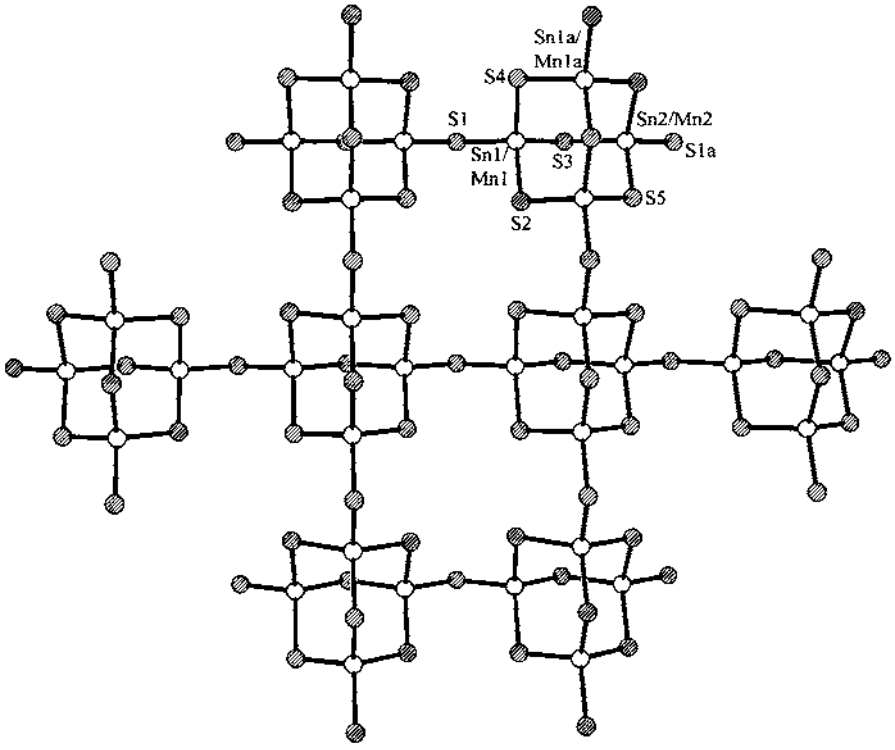

Fig. 27. Structure of K_2MnSnS_4 [7,134] in which the adamantane-like $[Mn_2Sn_2S_{10}]^{8-}$ units are linked into sheets via common terminal S atoms.

Mn atoms and the resulting $[Mn_2Sn_2S_{10}]^{6-}$ anions link together through their four terminal S atoms to construct a sheet of the formula type $^{2}_{\infty}[Mn_2Sn_2S_8^{4-}]$ (Fig. 27).

From a structural point of view the known Au/Sn/S compounds hold a unique status. Presumably the low twofold, linear coordination of Au^{I} is responsible for the fact that the anionic networks of its synthesized quaternary thiostannates(IV) are all restricted to 1-D character. In $K_2Au_2SnS_4$ [213], zigzag-like arranged SnS_4 tetrahedra are linked to four Au atoms, resulting in the assembly of $Au_2Sn_2S_4$ eight-membered rings (Fig. 28a). A similar state of affairs is also found in in $BaAu_2SnS_4$ [214], with the difference that the SnS_4 tetrahedra are now organized in a linear fashion. Although a second potassium compound $K_2Au_2Sn_2S_6$ [213] exhibits a formula type identical to that of the isotypic Cu phases $ACuSnE_3$ mentioned above, it now contains edge-linked ditetrahedral $[Sn_2S_6]^{4-}$ units instead of $^{1}_{\infty}[SnS_3^{2-}]$chains [66,98,101–106]. These building blocks now lie in a row (in a manner similar to $[SnS_4]^{4-}$ in $BaAu_2SnS_4$ [217]) and connect to four Au atoms to build an infinite ribbon (Fig. 28b). Because of the elongated thiostannate(IV) $[Sn_2S_6]^{4-}$ units in this compound, in comparison to the mononuclear $[SnS_4]^{4-}$ building blocks of $BaAu_2SnS_4$, it is now possible to accomodate twice as many

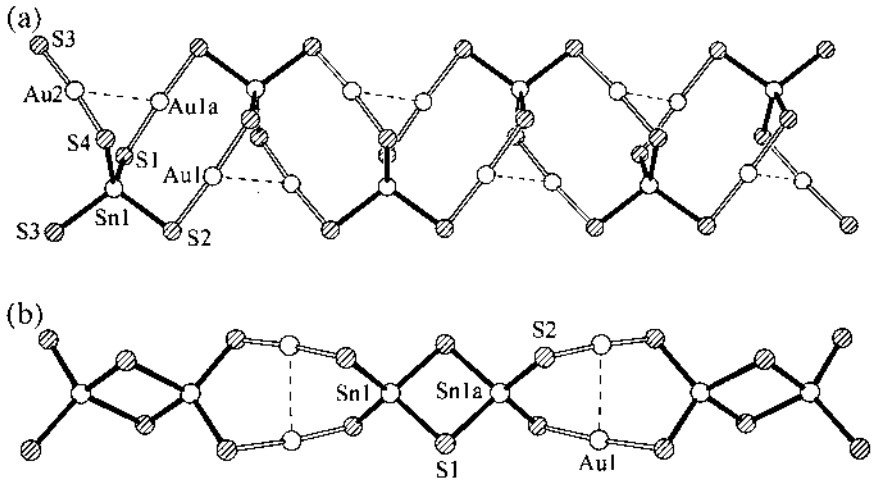

Fig. 28. The chain structures of the potassium phases (a) $K_2Au_2SnS_4$ and (b) $K_2Au_2Sn_2S_6$ [213]. The Au^I atoms in both compounds exhibit linear S–Au–S coordination and short Au ··· Au contacts of 3.363(2) and 3.010(2) Å, respectively.

cations between the chains. $Au_2Sn_2S_4$ rings occur once again, but in this case the presence of short endocyclic Au ··· Au contacts of 3.010(2) Å allow an alternative description as condensed five-membered rings.

Quaternary Group 14/16 compounds are also known with a second Main Group (Group 13; Group 14, Sn or Pb) metal as the M′ component. Whereas the metal M possesses the Group oxidation state, +IV, M′ exhibits a lower number, +III (Group 13) or +II (Sn, Pb), so that additional cations A are required for charge balance. An example of such a mixed Group 14 compound is provided by Tl_2PbGeS_4 with its $^2_\infty[PbGeS_4^{2-}]$ sheet structure. While Pb(II) is surrounded by six S atoms in a distorted octahedral fashion [218], Ge(IV) displays its characteristic tetrahedral coordination sphere. A number of quaternary Group 13/14/16 phases have recently been synthesized by Ibers et al. [219,220]. In $KGaGeS_4$, $KInGeS_4$ and $KGaSnS_4$, the Group 13/14 elements are statistically disordered within the anionic sheets (Fig. 29a,b) and exhibit equivalent connectivities. Their building blocks can be described as edge-linked ditetrahedral units $[(M'M)_2S_6]$, that lie between M′/M–S chains with alternating metal atom positions. The terminal S atoms are connected to the chain M′/M atoms in two different ways; in $KGaSnS_4$, two ditetrahedral units face one another on opposite sides of a given ribbon (Fig. 29a, as in $TlInSiS_4$ [221]), whereas in $KGaGeS_4$ and $KInGeS_4$ these relative positions are shifted by an M′/M–S unit (Fig. 29b). In contrast, the selenidostannate(IV) $AgGaSnSe_4$ shows a completely different structure, consisting of a complex framework involving $GaSe_4$ and $SnSe_4$ tetrahedral units [222].

Activity in this field of solid state research has recently been extended to the corresponding quaternary tellurides. Somewhat surprisingly, in view of the charac-

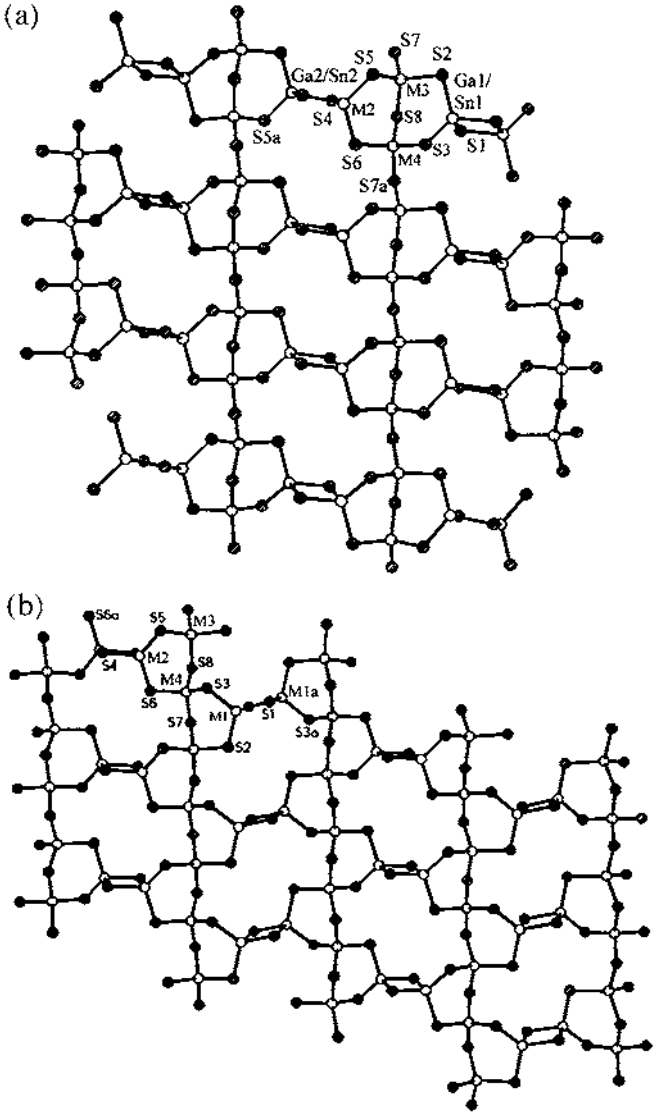

Fig. 29. Sheet structures of the Main Group quaternary compounds (a) $KGaSnS_4$ [219,220] (M = Ga/Sn) and (b) $KInGeS_4$ and $KGaGeS_4$ (M = In/Ge or Ga/Ge) [219,220]. The connectivities pattern in the first compound is similar to that of $TlInSiS_4$ [221].

teristic propensity of Te to extends its coordination sphere beyond two only infinite chains are found in $K_2HgSnTe_4$ [223]. In contrast to the layered anionic structure of K_2MnSnS_4 of the same formula type, the anion assembly principle (Fig. 30) can be compared to that of SiS_2 [214,215], with the Hg(II) and Sn(IV) atoms exhibiting statistical disorder.

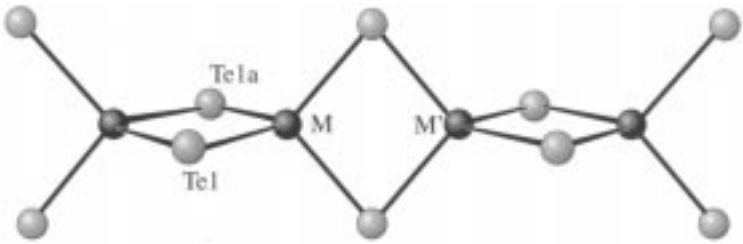

Fig. 30. The anionic chain structures of (a) $K_2HgSnTe_4$, $(Et_4N)[HgSnTe_4]$ or $(Ph_4P)[InGeTe_4]$ [223,224]. Whereas the M and M′ sites in the first two compounds are disordered, the last compound displays ordered In/Ge sites within its chain.

When an alloy of the same stochiometry is treated with $(Et_4N)I$ in ethylenediamine, cation exchange occurs and crystals of $(Et_4N)_2[HgSnTe_4]$ can be obtained [223]. Whereas the potassium phase reveals inter-chain Te ⋯ Te contacts close to the van der Waals distance, similar secondary interactions are not present in the tetraethylammonium compound.

Interestingly, the reaction of $K_4Ge_4Te_{10}$ with $InCl_3$ and $(Ph_4P)Br$ in ethylenediamine at 100°C also leads through decomposition of the adamantane-like framework to an isosteric $^1_\infty[InGeTe_4^-]$ chain anion in $(Ph_4P)[InGeTe_4]$ [223]. In this case, however, the In and Ge atoms occupy crystallographically independent positions within the chain, so that alternating $InTe_4$ and $GeTe_4$ tetrahedra now share common edges (Fig. 30). In contrast, the additional tetrahedral $AgTe_4$ units in $K_2Ag_2SnTe_4$ corner-bridge with $SnTe_4$ tetrahedra to construct a porous framework, whose channels accomodate the K^+ cations.

A striking example for the preparation of a novel polyanion by an uncoventional synthetic approach was recently reported by Haushalter et al. When the pentanary alloy $K_6AuAgSn_2Te_9$ is extracted in ethylenediamine, followed by subsequent treatment of the filtrate with $(Et_4N)I$, a new compound with the composition $(Et_4N)_4[Au(Ag_{1-x}Au_x)_2Sn_2Te_9]$ ($x = 0.32$) can be isolated [225]. The chainlike anion exhibits a structure totally different to those previously discussed in this section. As can be seen in Fig. 31a, it contains both tetrahedral $SnTe_4$ and square planar $AuTe_4$ units.

However, the outstanding structural feature of this compound is provided by an almost linear $^1_\infty[AuTe_3]$ chain, the Te_3 part of which displays a Te–Te–Te angle of 154.7(4)°. Charge compensation analysis for the whole structure indicates that a Te_3^{3-} chain fragment must be present and EHMO calculations predict metallic behavior for the compound. Because its half-occupied one dimensional valence band should be capable of undergoing a Peierls distortion, either a semiconductor or an isolator could also be possible. An experimental study reveals that the compound is, in fact, a semiconductor with a band gap of 0.45(5) eV. The possible distortions (Fig. 31b) cause two successive formula units within a chain to adopt different geometric arrangements, leading to physically unrealistically high temperature factors for the involved Te atoms. Least squares refinement for two indepen-

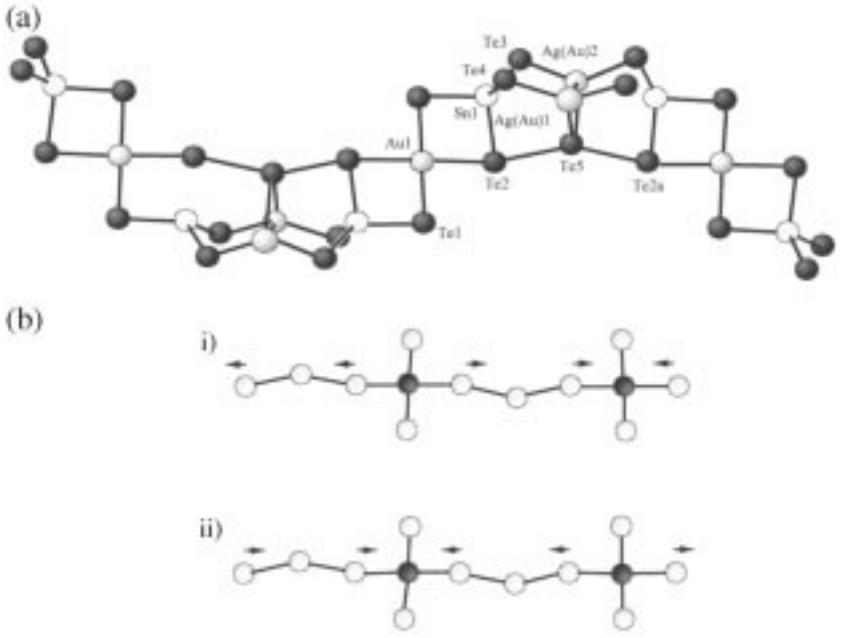

Fig. 31. (a) The anion of the compound $(Et_4N)_4[Au(Ag_{1-x}Au_x)_2Sn_2Te_9]$ ($x = 0.32$) [225]; whose wave-like chain contains square planar $AuTe_4$ and tetrahedral $SnTe_4$ coordination spheres; (b) two possible Peierls distortions, resulting from the presence of Te_3^{3-} units in the polymeric chains.

dent Te positions (the extreme positions suggested by arrows in Fig. 31b) led to a significant reduction in the final reliability index for the X-ray analysis.

Although this section has revealed that the structural diversity of known quaternary transition (Main Group) metal/Group 14/Group 16 chalcogenidometalates is less pronounced than might have been expected, the last example indicates that the potential of this field is certainly greater and the coming years will surely provide further exciting examples of novel non-classical Zintl anions.

3.7. Lower oxidation states +II and +III

A small number of chalcogenidometalates(II) are known for Sn(II) and Pb(II). For instance, ethylenediamine extraction of appropriate alloys $K_mM_yE_z$ in the presence of 2,2,2-crypt affords a series of isolated Sn(II) and Pb(II) anions with the general formula $[M_2E_3]^{2-}$ [31–33] (E = S, Se, Te and mixed chalcogenides) and a shape similar to that of [1,1,1]-bicyclopentane (Fig. 32), with the chalcogen atoms occupying the three bridging positions. Each M(II) atom possesses a non-bonding electron pair and the anions can also be described as trigonal bipyramids with axial Sn/Pb and equatorial E atoms. The homogeneous selenides and tellurides ($[M_2Se_3]^{2-}$, $[M_2Te_3]^{2-}$) have been characterized by X-ray analysis and mixed

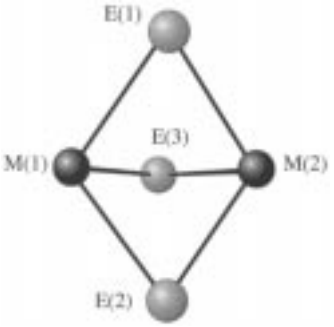

Fig. 32. The structure of the $[M_2E_3]^{2-}$ trigonal bipyramids (M = Sn, Pb; E = Se, Te) [31–33].

chalcogenides of similar structure identified by NMR spectroscopy (^{77}Se, ^{125}Te, ^{117}Sn, ^{119}Sn, ^{207}Pb), e.g. $[Pb_2S_xTe_{3-x}]^{2-}$ ($x = 0$–3) or $[Pb_2SSeTe]^{2-}$.

All known compounds are isotypic and only slight variations in bonding parameters have been established. Table 3 indicates that the bond angle E–M–E always lies close to 90°, whereas the M–E–M angle is significant smaller (65–71°). In the tellurides, the average E–M–E angle is greater than in the corresponding selenides, with an opposite trend apparent for the bridging M–E–M angle. An NMR study of $[Sn_2Se_3]^{2-}$ allowed the measurement of a $^2J(^{119}Sn–^{117}Sn)$ coupling constant for the first time. Its value of 1514 Hz is unusually large for such a two bond parameter and lies in the lower range for a ^1J coupling constant (900–15 000 Hz), but, owing to a lack of comparison data, no conclusion can be drawn as to whether a significant Sn–Sn bonding interaction is present or not. On the other hand the ^1J(M–E) coupling constants are rather small, which could be due to the fact that the participating M–E bonds exhibit almost exclusively *p* character.

A chain anion $^1_\infty[SnS_2^{2-}]$ is present in the high temperature phase $BaSnS_2$ [35], whose anionic structure consists of corner-linked ψ-SnS_3 tetrahedra [distances Sn–S 2.517–2.613(2) Å], similar to those found in the As(III) compounds $AAsSe_2$ (A = K–Cs [262]). When longer Sn ··· S contacts are considered the structure (Fig. 33a) is also related to that of NaCl. Two such chains are connected by common bridged S atoms in $Tl_2Sn_2S_3$ [226], leading to ψ-SSn_4 trigonal bipyramids with equatorial and axial Sn–S bond lengths of, respectively, 2.80(3) Å and 2.931(8) Å (Fig. 33b). A defect NaCl structure results, in which the Tl and Sn atoms occupy the cation positions and 25% of the Cl sites are vacant. In $Tl_2Ge_2S_4$ [28] two Ge–S ribbons with alternating Ge^{II}/Ge^{IV} positions are linked through additional Ge^{II}–S bonds into a double chain with crown-like Ge_4S_4 rings (Fig. 33c).

In $BaSn_2S_3$ [36], chains of four-membered Sn_2S_2-rings are linked together by both direct Sn–S bonds and Sn–S–Sn bridges. The Sn(II) atoms display ψ-SnS_3 tetrahedral coordination spheres and Sn–S distances of 2.754(8) Å or less. On taking longer bonds (3.153, 2 × 3.270 Å, depicted as dashed lines in Fig. 33d into account, these chains are connected into a double sheet with ψ-tetrahedral,

Table 3
Metrical and NMR data for the trigonal bipyramidal anions in $[K(2,2,2\text{-crypt})]_2M_2E_3$ [31–34]

	Sn_2Se_3 [31]	Sn_2Te_3 [31][a]	Pb_2Se_3 [32]	Pb_2Te_3 [32,33]	$Pb_2Te_3 \cdot MeCN$ [34]
M ⋯ M [Å]	3.090(3)	3.270(6)	3.184(3)	3.249(2)	3.232(1)
M–E [Å]	2.637(3)/2.677(3)	2.887(4)	2.726(5)/2.792(8)	2.943(2)	2.954(2)–3.015(1)
E–M–E [°]	87.9–92.1(1)	90.9(1)	87.1–92.4(1)	92.46(4)	92.21–94.33(4)
M–E–M [°]	70.9–71.1(1)	68.7(1)	70.4–70.9(1)	67.01(6)	65.55–66.10
δ(E) [ppm]	12[b]		−99.4[b]	−927.1[c]	−928[c]
^2J(M–M) [Hz]	1514[d]				
^1J(M–E) [Hz]	397[e]		149[f]	1070[g]	1090[g]

[a] Averaged values for X-ray structural analyses at −100°C and 24°C.
[b] Isotopes: ^{77}Se.
[c] ^{125}Te.
[d] ^{117}Sn–^{119}Sn.
[e] ^{77}Se–^{119}Sn.
[f] ^{77}Se–^{207}Pb.
[g] ^{125}Te–^{207}Pb.

ψ-trigonal bipyramidal and ψ-octahedral Sn atoms (Fig. 33d), whose non-bonded electron pairs protrude out of the sheets.

The mixed selenidostannates(II/IV) with the general formula $A_2Sn_4Se_8$ display different structure types for the respective countercations K^+ [29] and Rb^+ or Cs^+ [30]. On the assumption that only Sn–Se bonds are present, every fourth Sn atom must adopt the lower oxidation state +II for charge balance. The framework structure of $K_2Sn_4Se_8$ can be explained in the following way. Edge-linked $[Sn_3Se_{10}]^{8-}$ tritetrahedra may be identified that are linked through four shared terminal Se atoms into a lamellar network $^2_\infty[Sn_3Se_8^{4-}]$ (Fig. 34a). The central $SnSe_4$ tetrahedron has no further contacts within the sheet, but is responsible for the perpendicular linkage of the sheets $^2_\infty[Sn_3Se_8^{4-}]$ through Se–Sn(II)–Se bonds (Fig. 34b). As a result of the stereochemical activity of the metal lone pair, these Sn(II)–Se distances of 2.660(2) and 2.683(2) Å are longer than these involving Sn(IV) atoms [2.461(2)–2.545(2) Å]. Two additional Sn ⋯ Se contacts of 3.132(1) Å to neighboring tetrahedra complete the Sn(II) coordination sphere, which can be described as ψ-SnS_4 trigonal bipyramidal with shorter axial and longer equatorial bonds.

The phases $Rb_2Sn_4Se_8$ and $Cs_2Sn_4Se_8$ [30] are isostructural and display a completely different structure. Their anions contain parallel chains $^1_\infty[SnSe]$ with alternating Sn(II) and Sn(IV) centers (Sn4 and Sn1, respectively), which are connected together by edge-bridged Sn_2Se_6 ditetrahedra (Fig. 35), as found in many ternary selenidostannates(IV) [98,101–106]. The linking Sn–Se bonds are much shorter to Sn(IV) [2.560(2)/2.533(2) Å] than to Sn(II) [2.884(2) Å]. An additional weak Se ⋯ Sn(II) contact of 3.154(2) Å (open bonds in Fig. 35) extends the Sn(II) coordination sphere to a distorted ψ-SnS_4 trigonal bipyramid.

An interesting comparison can be made with the quaternary compound $KGaSnS_4$

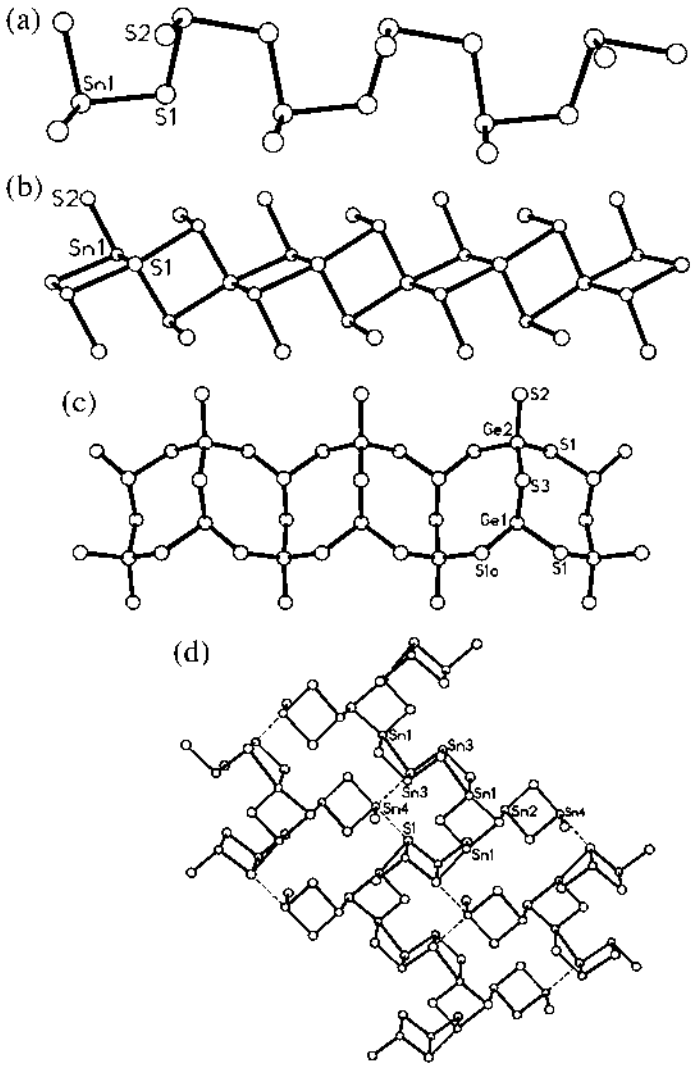

Fig. 33. (a) The chain structure $^{1}_{\infty}[SnS_2^{2-}]$ of $BaSnS_2$ [35], (b) connection of two such chains through common bridging S atoms in $Tl_2Sn_2S_3$ [226], which possess ψ-trigonal bipyramidal environments, (c) two Ge–S ribbons with alternating Ge^{II}/Ge^{IV} positions, that are linked into a double chain by additional Ge^{II}–S bonds in $Tl_2Ge_2S_4$ [28] and (d) the $^{2}_{\infty}[Sn_2S_3^{2-}]$ sheet anion in $BaSn_2S_3$ [36] with Sn4 ··· S1 interactions of 3.269(7) Å depicted as dashed lines.

[221] (Fig. 29a), which has the same connectivity pattern but without the presence of longer bonds, since both Ga and Sn are capable of adopting a near to ideal tetrahedral coordination sphere (Section 3.6). The three phases $A_2Sn_4Se_8$ (A = K, Rb, Cs) provide another good example of the trend to lower anion dimensionality

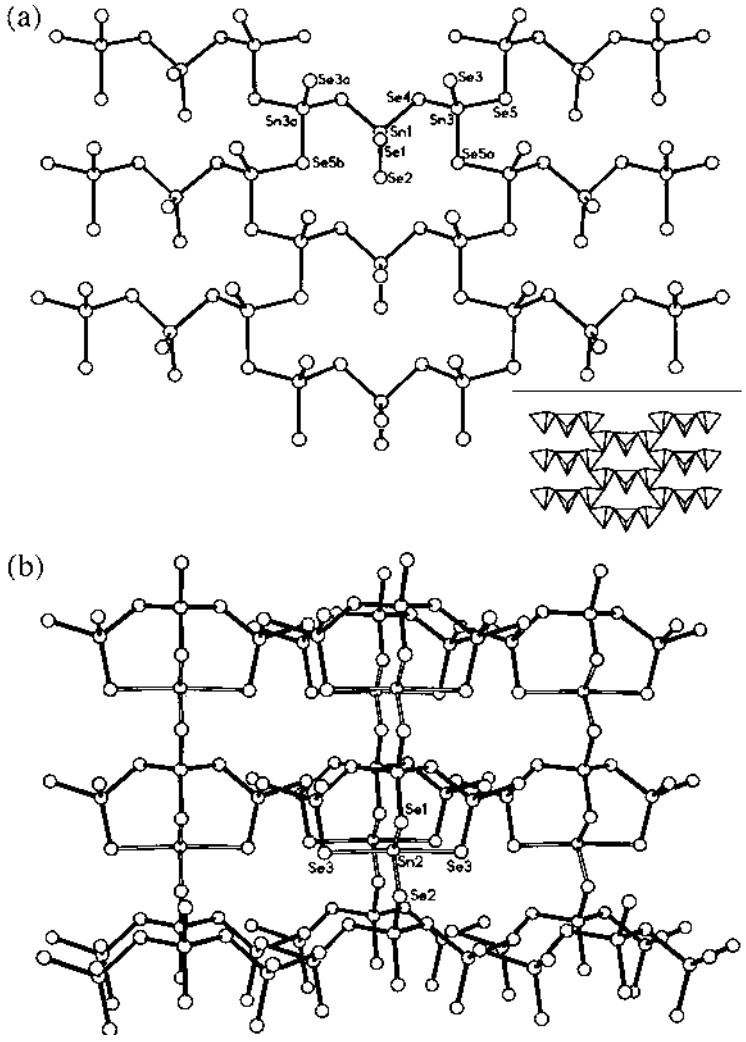

Fig. 34. (a) The sheet anion $^{1}_{\infty}[Sn_3Se_8^{4-}]$ in $K_2Sn_4Se_8$ [29] and (b) linkage of these layers through Sn(II) atoms, whose equatorial Sn–S bonds [2.660(2) and 2.683(2) Å] are significantly shorter than the axial ones [2 × 3.132(1) Å].

on going from a smaller cation (K^+, $d = 3$) to the more voluminous cations Rb^+ and Cs^+ ($d = 2$).

Dinuclear M(III) anions $[M_2E_6]^{6-}$ contain two ME_3 pyramids linked by a common homonuclear M–M bond. This simple structural motif is also found as a building unit in the binary compound Si_2Te_3 [227]. Table 4 lists all known compounds of the type $A_6M_2E_6$ (A = Na, K, Rb, Cs, Tl; M = Si, Ge, Sn; E = S, Se, Te) together with their M–M distances, all of which are in good agreement with

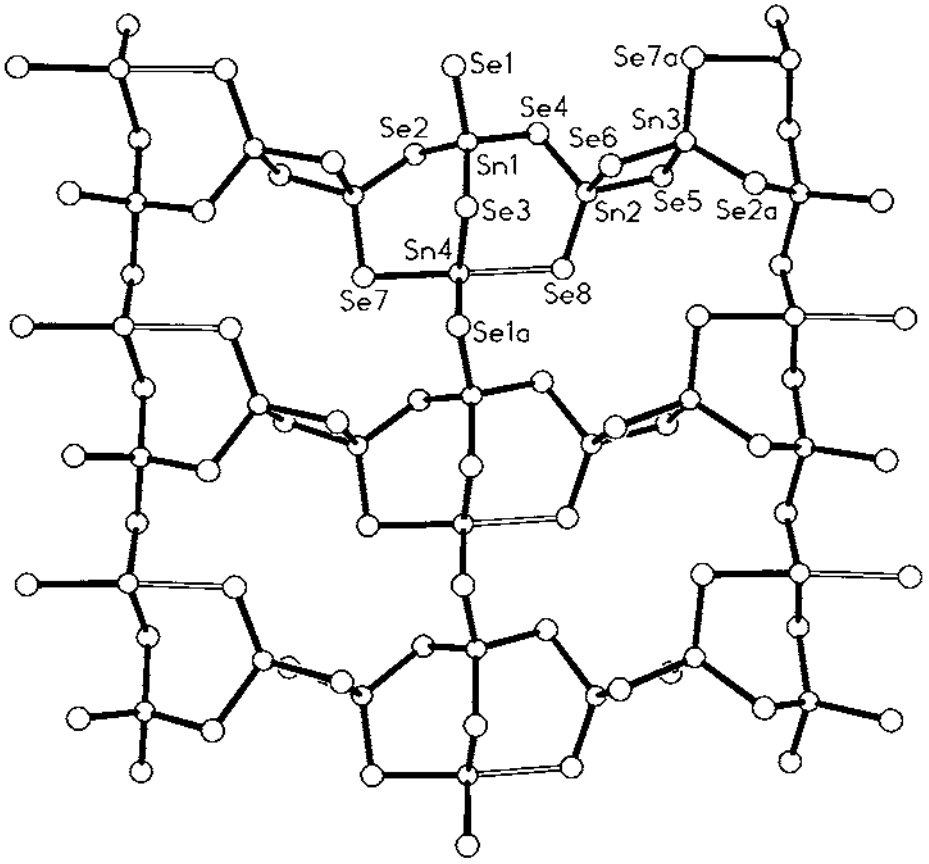

Fig. 35. The structure of $A_2Sn_4Se_8$ (A = Rb, Cs) [30], consisting of Sn–Se chains and Sn_2Se_6 edge-linked ditetrahedra. A long Sn4 ··· Se8 contact of length 3.154(2) Å in $Rb_2Sn_4Se_8$ is shown as an open bond.

the sums of the corresponding covalent radii. With the exception of two phases containing methanol solvate molecules in crystal lattice [233] all compounds were synthesized by high temperature fusion of the elements. A trend to slightly longer M–M distances with increasing chalcogen size can be discerned. In phases of the type $K_6Ge_2E_6$ (E = S, Se [23], Te [25]) the Ge–Ge bond lengthens from 2.454(1) Å in the sulfide over 2.477(1) Å in the selenide to 2.492(8) Å in the corresponding telluride. A dependence on the cation volume is also apparent, as exemplified by the materials $A_6Sn_2Te_6$ (A = K, Rb, Cs) in Table 4. All anions exhibit the more stable staggered conformation for their constituent ME_3 pyramids (Fig. 36a).

A number of interesting Group 14 oligo-chalcogenidometalates(III) have been assembled from this basic building block. In general, synthesis succeeds for element fusion at high temperature, when the quantitiy of alkali metal A and/or

Table 4
M(III) compounds of the formula type $A_6M_2E_6$ with homonuclear M–M bonds

	d(M–M) (Å)	Reference	Σ covalent radii (Å) [335]
$Na_6Si_2Te_6$	2.345(6)	[228]	Si 2.34
$K_6Si_2Te_6$	2.40(1)	[229,230]	
$K_6Ge_2S_6$	2.454(1)	[23]	Ge 2.44
$Na_6Ge_2Se_6$	2.430	[25]	
$K_6Ge_2Se_6$	2.477(1)	[23]	
$Na_6Ge_2Te_6$	2.453(1)	[23]	
$K_6Ge_2Te_6$	2.492(8)	[25]	
$Tl_6Ge_2Te_6$	2.454(6)/2.457(6)	[232]	
$Cs_6Sn_2Se_6$	2.920(3)	[231]	Sn 2.80
$K_6Sn_2Te_6$	2.814(1)	[25]	
$Rb_6Sn_2Te_6$	2.819	[231]	
$Cs_6Sn_2Se_6$	2.852	[231]	

No data are available for $Na_6Ge_2S_6 \cdot 4MeOH$ and $Na_6Ge_2Se_6 \cdot 4MeOH$ [233].

chalcogen E is lowered, since a reduced number alkali metal cations are required for a charge compensation after condensation of the $[M_2E_6]^{6-}$ building blocks.

A variety of condensation patterns are available for such units. A 'head to head and tail' condensation (1:2 center variant) leads to an $[M_4E_{10}]^{8-}$ anion, that is described as modification I in the literature [Fig. 36b, pathway (i)] and found both in $Na_8Si_4Te_{10}$ [234] and $Na_8Ge_4E_{10}$(I) (E = Se, Te) [234,235]. The result is an M_3E_2 five-membered ring, whose directly bonded metal atoms each carry two terminal chalcogens, whereas the remaining M atom (Ge3) is connected to both an ME_3 unit and a further terminal E atom. An alternative condensation mode is provided by the 'head to head–tail to tail' reaction (2:2 variant) outlined as pathway (ii) in Fig. 36b. In this case, the resulting anion contains a six-membered M_4E_2 ring with a typical chair conformation as is present in modification II of both $Na_8Ge_4Se_{10}$(II) [24] and $Na_8Ge_4Te_{10}$(II) [236]. In all examples, bridging M–E bonds are slightly elongated and terminal ones shortened in comparison to the sum of the relevant covalent radii, leading thereby, to bond length differences of between 0.10 and 0.15 Å.

As can be immediately seen by comparison of pathways (i) and (ii) in Fig. 36b, the anions from these two condensation processes display very different structures. However, a comparison of both modifications with the NaCl structure indicates that they are more closely related than might, at first, be expected. The Te atoms occupy the Cl positions in such a lattice to provide a cubic close packing and 20% of Na (alkali) atoms are replaced by Ge_2 dumb-bells, in accordance with a formulation as $Na_8(Ge_2)_2E_{10}$ [= $(NaCl)_{10}$]. The two modifications I and II now only differ in the relative orientation of the Ge_2 dumb-bells to one other. As can be discerned from Fig. 36b, in the first case these are arranged perpendicularly to

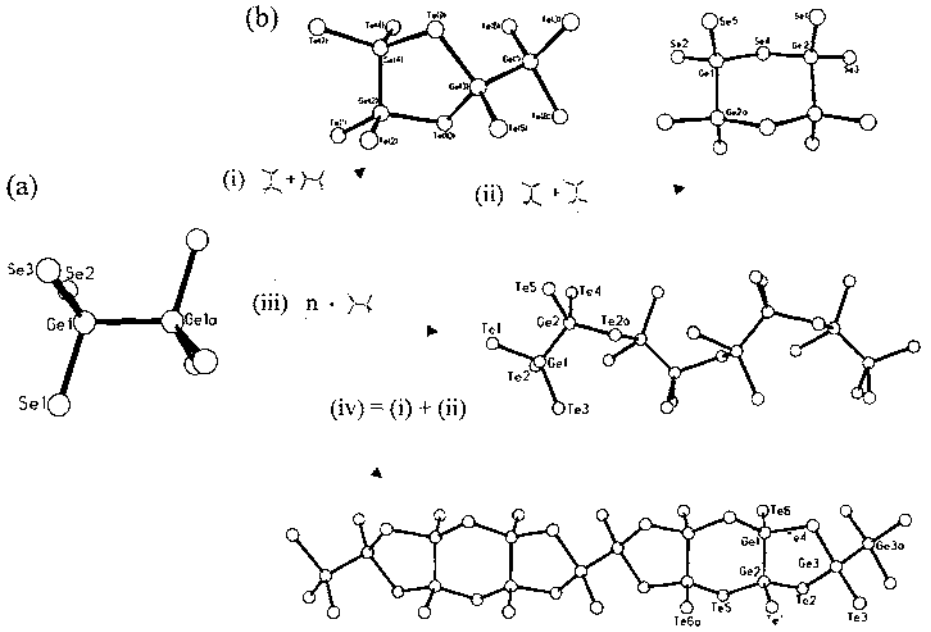

Fig. 36. (a) The dinuclear M(III) anion $[M_2E_6]^{6-}$ in compounds $A_6M_2E_6$ (A = Na, K, Rb, Cs, Tl; M = Si, Ge, Sn; E = S, Se, Te). (b) Condensation pathways to oligo- or chain chalcogenidometalates(III): (i) 'head to head and tail' condensation of two $[M_2E_6]^{6-}$ units leading to the $[M_4E_{10}]^{8-}$ anion (modification I) present in $Na_8Si_4Te_{10}$ [234], $Na_8Ge_4Se_{10}$ (I) [235] and $Na_8Ge_4Te_{10}$ (I) [234]; (ii) the 'head to head/tail to tail' condensation of two $[M_2E_6]^{6-}$ units that generates $[M_4E_{10}]^{8-}$ as modification II in both $Na_8Ge_4Se_{10}$ (II) [24] and $Na_8Ge_4Te_{10}$ (II) [236]; (iii) corner-linking of Ge_2Te_6-octahedra to the $[Ge_2Te_5^{4-}]$ chain of $Ba_2Ge_2Te_5$ [26]; and (iv) combination of pathways (i) and (ii) to afford the $^1_\infty[Ge_6Te_{12}^{6-}]$ anion in $Li_6Ge_6Te_{12}$ [27].

one another in a 1:1 ratio, whereas in modification II all such units adopt parallel positions.

Chainlike anions are present in both $Ba_2Ge_2Te_5$ [26] and $Li_6Ge_6Te_{12}$ [27]. $Ba_2Ge_2Te_5$ contains corner-linked dinuclear $[Ge_2Te_6]^{6-}$ building blocks [Fig. 36b, pathway (iii)] arranged in a corrugated chain $^1_\infty[Ge_2Te_5^{4-}]$, whose doubled formula type corresponds to that of the tetranuclear anions $[M_4E_{10}]^{8-}$ discussed above. Since only half as many alkaline earth cations are now required for charge compensation, chain generation becomes possible.

A very interesting extension of these condensation patterns for $[M_2E_6]^{6-}$ units is provided by the synthesis of the $^1_\infty[Ge_6Te_{12}^{6-}]$ anion in $Li_6Ge_6Te_{12}$ [27]. The rationale behind the construction of such a chain by 'head to head–tail to tail' and 'head to head and tail' condensations in a 1:2 ratio can be sought in the small size of the charge compensating Li^+ cations. The result is a Ge_4Te_2 six-membered ring with five-membered rings fused to opposite Ge–Ge bonds [Fig. 36b, pathway (iv)]. Chain continuation of this tricyclic system is achieved by direct Ge–Ge bonding between endocyclic Ge atoms of the flanking five-membered rings.

A novel anion with a Ge_3 unit has been found in $Cs_6Ge_3Te_7$ [237] and provides the only known example of a mixed M(II)/M(III) compound. A trinuclear anion derived from $[Ge_2Te_6]^{6-}$ by an addition of a third $GeTe_3$ unit would have the formula $[Ge_3Te_8]^{8-}$. Elimination of a tellurium atom through intramolecular ring closure generates a unique Ge_3Te four-membered ring (Fig. 37), whose Ge–Ge [2.523(4)/2.525(4) Å] and Ge–Te [2.663(2)/2.666(2) Å] bonds are significantly lengthened in comparison to the sum of the relevant covalent radii (2.44 and 2.59 Å, respectively).

This suggests the presence of considerable strain in the nearly planar system, with its endocyclic bond angles at Ge lying in the range 91.2–91.6° in contrast to a much smaller Ge–Te–Ge angle of 85.2(1)°. The ring closure forces the six terminal Te atoms into an eclipsed conformation.

4. Chalcogenidometalates of arsenic, antimony and bismuth

4.1. Structural principles and classification

Group 15 element sulfides M_2S_3 (M = As, Sb) dissolve in alkaline aqueous solution to afford ψ-tetrahedral thiometalates(III) of the type $[MS_3]^{3-}$ together with oxothio- and oxoanions. UV–Vis spectroscopic and potentiometric studies have demonstrated that such monomeric $[AsS_3]^{3-}$ ions readily condense to corner-bridged dipyramidal $[As_2S_5]^{4-}$ and cyclic tripyramidal $[As_3S_6]^{3-}$ ions [328], with the latter species predominating in acid and mildly alkaline solution ($pH \leq 11$). Such trinuclear anions can be isolated from an ethylenediamine solution at room temperature in the form of the salts $[enH_2]_3[As_3S_6]_2 \cdot 6en$ [255] and $[Ba(en)_4]_3[As_3S_6]_2$ [256]. In both cases, the As_3S_3 rings exhibit a chair conformation with the terminal S atoms in equatorial sites. A similar structure is also adopted by the analogous $[As_3Se_6]^{3-}$ ion in $[Sr(en)_4]_2[As_3Se_6]Cl$ (Fig. 41d) [257]. Electrospray mass spectrometric measurements on the $K^+/Sb/Se$ system in DMF

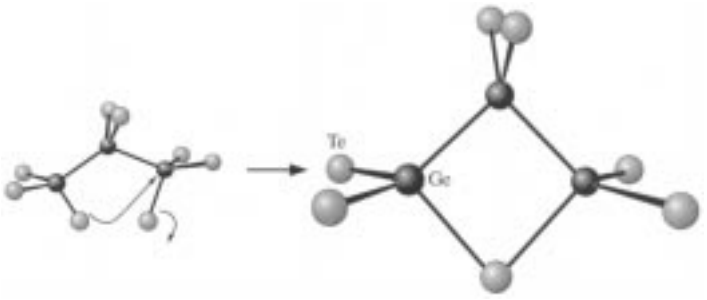

Fig. 37. Ge_3Te four-membered ring in the mixed Ge(II)/Ge(III) compound $Cs_6Ge_3Te_7$ [237] whose possible mode of formation from $[Ge_3Te_8]^{8-}$ is indicated.

Table 5
Anion formula types and dimensionalities *d* for chalcogenido- and polychalcogenidoarsenates(III)

d	E = S	Compounds	E = Se	Compounds
0	$[AsS_3]^{3-}$	A_3AsS_3, A = Na, K [238], Tl [241,242], $Ba_2As_2S_5$ [243]	$[AsSe_3]^{3-}$	Tl_3AsSe_3 [244], $Ba_2As_2Se_5$ [245]
	$[AsS_6]^{-}$	$[Ph_4P][SAsS_5]$ [246]	$[AsSe_6]^{-}$	$[Ph_4P][SAsSe_5]$ [446]
	$[AsS_8]^{-}$	$[Ph_4P][SAsS_7]$ [247]	$[AsSe_8]^{-}$	$[Et_4N][SeAsSe_7]$ [248]
	trans-$[As_2S_4]^{2-}$	$Ba_2As_2S_5$ [243], $[K(2,2,2\text{-crypt})]_2[As_2S_4] \cdot 2CH_3CN$ [249]	*trans*-$[As_2Se_4]^{2-}$	$Ba_2As_2Se_5$ [245]
	$[As_2S_6]^{2-}$	$(Ph_4P)_2As_2S_6$ [251][a]	$[As_2Se_6]^{2-}$	$(Ph_4P)_2As_2Se_6$ [252], $[Na(2,2,2\text{-crypt})]_2[As_2Se_6]$ [253]
	$[As_3S_6]^{3-}$	$(enH_2)_3[As_3S_6] \cdot 6en$ [255], $[Ba(en)_4]_3[As_3S_6]_2$ [256]	$[As_3Se_6]^{3}$	$[Sr(en)_4]_2[As_3Se_6]Cl$ [257]
1	$^1_\infty[AsS_2^-]$	$AAsS_2$, A = Na [258], Rb [260], Tl [241,242]	$^1_\infty[AsSe_2^-]$	$AAsSe_2$, A = Na [261], K, Rb, Cs [262]
			$^1_\infty[AsSe_3^-]$	$KAsSe_3 \cdot H_2O$, $AAsSe_3 \cdot 1/2H_2O$, A = Rb, Cs [263]
	$^1_\infty[As_4S_7^{2-}]$	$(Me_4N)_2[As_4S_7]$ [51]		
	$^1_\infty[As_6S_{10}^{2-}]$	$(Me_4N)_2As_6S_{10}$ [51], $(Et_4N)_2As_6S_{10}$ [248]		
	$^1_\infty[As_8S_{13}^{2-}]$	$A_2As_8S_{13} \cdot H_2O$, A = K, Rb, NH_4 [53]		
2	$^1_\infty[As_8S_{13}^{2-}]$	$Cs_2As_8S_{13}$ [52]		

[a] The As-atoms occupy the 1,3 positions within the six-membered ring in the thioarsenate $[As_2S_6]^{2-}$ and the 1,4 positions in the selenidoarsenates $[As_2Se_6]^{2-}$.

confirm the presence of monomeric $[SbSe_3]^{3-}$ and a series of oligomers $[Sb_2Se_5]^{4-}$, $[Sb_3Se_7]^{5-}$, $[Sb_6Se_{12}]^{6-}$ and $[Sb_8Se_{15}]^{6-}$ [329].

Condensation of $[ME_3]^{3-}$ species (M = As, Sb) under soft solventothermal conditions in the presence of suitable structure-directing cations can lead to a variety of polyanions, as listed in Tables 5–7. Whereas, with the exception of $Cs_2As_8S_{13}$ [52], all known polymeric alkali metal and alkylammonium thio- and selenidoarsenates(III) display chain structures, the ability of the heavier homolog Sb(III) to extend its coordination number beyond 3 allows the self-assembly of a bewildering variety of formula and structure types with dimensionalities of 1–3. As(III) exhibits only a rather weak propensity to extend its species coordination number to 4 (ψ-AsE_4 trigonal bipyramidal) with the consequence that solution species remain recognizable as molecular building blocks in the solid-state structures. For instance, $Rb_2As_8S_{13} \cdot H_2O$ [53] contains cyclic $[As_3S_6]^{3-}$ units, that are linked together by corner-bridging $[As_2S_5]^{4-}$ fragments into a double chain. The energetic advantage of participating in secondary As ⋯ S interactions (2.92–3.03 Å) causes the free terminal S atoms of the As_3S_6 building blocks to adopt unusual

Table 6
Anion formula types with dimensionalities d = 0,1 for chalcogenidoantimonates(III)

d	E = S	Compounds	E = Se	Compounds
0	$[SbS_3]^{3-}$	A_3SbS_3, A = Na, K [238–240], Tl [264]	$[SbSe_3]^{3-}$	Tl_3SbSe_3 [268], $Ba_4Sb_4Se_{11}$ [273]
		$K_3SbS_3 \cdot 3Sb_2O_3$ [265], $Ca_2Sb_2S_5$ [266], $Ba_8Sb_6S_{17}$ [267]		$Na_3SbSe_3 \cdot 3Sb_2O_3 \cdot 1/2Sb(OH)_3$ [272]
	trans-$[Sb_2S_4]^{2-}$	$Ca_2Sb_2S_5$ [266]	*trans*-$[Sb_2Se_4]^{2-}$	$Ba_4Sb_4Se_{11}$ [273]
			cis-$[Sb_2Se_4]^{2-}$	$Ba_4Sb_4Se_{11}$ [273], $[K(2,2,2\text{-crypt})]_2Sb_2Se_4$ [249]
	$[Sb_2S_5]^{4-}$	$Sr_2Sb_2S_5 \cdot 15H_2O$ [274]	$[Sb_2Se_6]^{2-}$	$[K(2,2,2\text{-crypt})]_2Sb_2Se_6$ [250]
	$[Sb_3S_8]^{7-}$	$Ba_8Sb_6S_{17}$ [267]	$[Sb_{12}Se_{20}]^{4-}$	$[Ph_4P]_4Sb_{12}Se_{20}$ [275]
1	$^1_\infty[SbS_2^-]$	ASbS$_2$, A = K [277], Rb [278],	$^1_\infty[SbSe_2^-]$	ASbSe$_2$, A = K [283], Cs [284]
		Cs [279], Tl [280], $[M(en)_3]Sb_2S_4$, M = Co, Ni [445]		$[Ba(en)_4]Sb_2Se_4$ [285], $Ba_2Sb_4Se_8$ [295]
		NH_4SbS_2 [281], $Sr_3Sb_4S_9$ [282], $Ba_2Sb_4S_8$ [294]		
	$^1_\infty[Sb_2S_5^{4-}]$	$Sr_3Sb_4S_9$ [286]		
	$^1_\infty[Sb_3S_5^-]$	$(Pr^n{}_4N)Sb_3S_5$ [286]		
	$^1_\infty[Sb_4S_7^{2-}]$	$(NH_4)_2Sb_4S_7$ [287], $(N_2C_4H_8)Sb_4S_7$ [286]		
		$[M(en)_3]Sb_4S_7$, M = Mn [288], Fe, Ni [445], $Cs_2Sb_4S_7$ [289], $SrSb_4S_7 \cdot 6H_2O$ [290]		
	$^1_\infty[Sb_8S_{13}{}^{2-}]$	$(enH_2)Sb_8S_{13}$ [291], $Na_2[(Sb, As)_8S_{13}] \cdot 2H_2O$ [292]		
			$^1_\infty[Sb_8Se_{18}{}^{12-}]$	$SrSbSe_3$ [366,367]

axial sites above the As_3S_3 six-membered rings. This behavior is observed in many thioarsenates(III) and -antimonates(III) with M_3S_6 units and, when such weak M⋯S contacts are taken into account, it is possible to identify M_3S_4 semicubes analogous to the ubiquitous Sn_3E_4 building blocks of the lamellar chalkogenidostannates(IV).

Four- and six-membered Sb_2E_2 and Sb_3E_3 rings are typical structural motifs in polymeric chalcogenidoantimonates(III). The participating antimony atoms are often ψ-trigonal bipyramidal in the first building unit and repeated extension of such $E_{ax}E_{eq}$ edge-bridging generates infinite $^1_\infty[SbE_2^-]$ chains in $KSbS_2$ [277] (Fig. 38a) or $KSbSe_2$ [283]. In the former compound, Sb atoms are sited on crystallographic C_2 axes and exibit equatorial and axial Sb–S distances of, respectively, 2.41 and 2.76 Å with accompanying S_{eq}–Sb–S_{eq} and S_{ax}–Sb–S_{ax} angles of 102.4 and 173.7°. Despite the fact that a relatively moderately distorted ψ-octahedral geometry is found for one of the two independent antimony centers in the isotypic parent chalcogenides Sb_2S_3 [distances Sb–S_{ax} 2.456, Sb–S_{eq} 2.678(×2), 2.854(×2) Å [330]] and Sb_2Se_3 [distances Sb–Se_{ax} 2.588, Sb–S_{eq} 2.803(×2), 3.007(×2) Å [331]],

Table 7
Anion formula types with dimensionalities d = 2,3 for chalcogenidoantimonates(III)

d	Formula type	Compounds
2	$^{2}_{\infty}[SbE_2^-]$	ß-$NaSbS_2$ [276,293]
	$^{2}_{\infty}[Sb_3E_5^-]$	$RbSb_3S_5 \cdot H_2O$ [296], **$RbSb_3Se_5$** [57]
	$^{2}_{\infty}[Sb_4S_7^{2-}]$	$A_2Sb_4S_7 \cdot H_2O$, A = K [297], Rb [298], $Rb_2Sb_4S_7$ [299], $[C_2H_5NH_3]_2Sb_4S_7$ [300]
	$^{2}_{\infty}[Sb_5E_9^{3-}]$	$Cs_3Sb_5S_9$ [301], $Cs_3Sb_5S_9 \cdot 0.6H_2O$ [302], **$Cs_3Sb_5Se_9$** [301]
	$^{2}_{\infty}[Sb_8S_{13}^{2-}]$	$Cs_2Sb_8S_{13}$ [303], $(C_4H_{10}N)_2Sb_8S_{13} \cdot 0.15H_2O$ [304]
3	$^{3}_{\infty}[Sb_3S_5^-]$	$(Me_4N)Sb_3S_5$ [305]
	$^{3}_{\infty}[Sb_4S_7^{2-}]$	$K_2Sb_4S_7$ [306]
	$^{3}_{\infty}[Sb_8S_{13}^{2-}]$	$(CH_3NH_3)_2Sb_8S_{13}$ [307]
	$^{3}_{\infty}[Sb_{10}S_{16}^{2-}]$	$[H_3N(CH_2)_3NH_3]Sb_{10}S_{16}$ [308]
	$^{3}_{\infty}[Sb_{14}S_{23}^{4-}]$	$Cs_4Sb_{14}S_{23}$ [309]

similar coordination spheres are relatively rare in chalcogenidoantimonates(III). An interesting example is provided by the unique $^{1}_{\infty}[Sb_2S_5^{4-}]$ chain (Fig. 38b) in $Sr_3Sb_4S_9$ [282], whose crystal lattice also contains independent $^{1}_{\infty}[SbS_2^-]$ ribbons with ψ-tetrahedral Sb atoms. Sb–S_{eq} distances in $^{1}_{\infty}[Sb_2S_5^{4-}]$ lie in the range 2.743–2.941 Å for the inner S atoms with their fourfold coordination and 2.666–2.920 Å for the outer μ_2 bridging sulphurs. However, as clearly demonstrated by the structural correlation of *trans*-sited Sb–Se bond lengths in the range 2.53–3.50 Å presented for Sb_2Se_3 [331] and selenidoantimonates(III) in Fig. 39, differences Δ of 0.3 Å or greater are more typical for the inner coordination sphere of the Group 15 element.

According to the widely used bond-valence concept, first introduced by L. Pauling [333–335] and more recently improved and extended by I.D. Brown [336,337] and M. O'Keeffe [338,339], the valency V_i of an atom i in inorganic crystal structures should be equal to the sum of the individual bond valences s_{ij} to atoms in the environment.

$$V_i = \sum_j s_{ij} \tag{1}$$

For distorted coordination polyhedra ME_n, s_{ij} values have often been found to be correlated to distances D_{ij} between atoms i and j by expressions of the type:

$$s_{ij} = \exp\left[(r_0 - D_{ij})/B\right] \tag{2}$$

where B is invariant and approximately 0.37 Å [342] and r_0 represents a bond length of unit valence. However, in their recent analyses of thio- and selenidoantimonates(III), X. Wang and F. Liebau [340,341] have presented a correlation between the average E–Sb–E angle $\bar{\alpha}_i$ in an SbE_n coordination polyhedron and a bond-valence parameter $^{for}_{i}r_0$ calculated using Eq. (2) with B = 0.37 and V_i = 3.

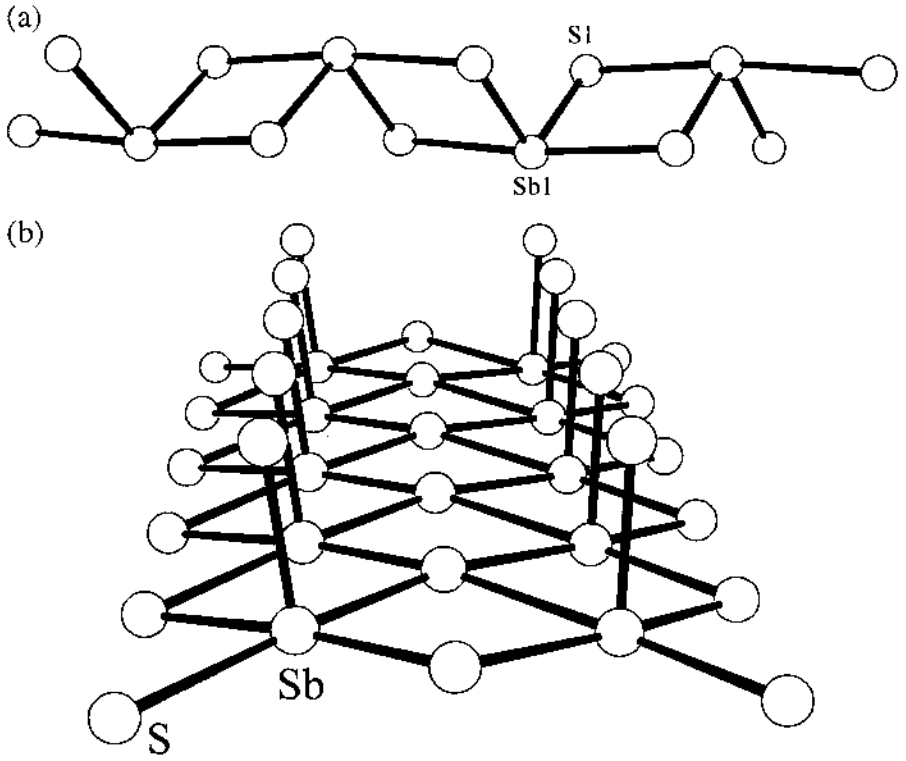

Fig. 38. (a) $^{1}_{\infty}[SbS_2^-]$ chains with ψ-trigonal bipyramidal Sb atoms in $KSbS_2$ [277]. (b) $^{1}_{\infty}[Sb_2S_5^{4-}]$ chains with ψ-octahedral Sb atoms in $Sr_3Sb_4S_9$ [282].

$$^{for}_{i}r_0 = P\cos\bar{\alpha}_i + Q \tag{3}$$

Empirical values of $P = 0.28$ and $Q = 2.455$ Å were obtained by least squares minimization of function (4) for 76 SbS_n polyhedra.

$$\sum_{i=1}^{N}\left(\,^{for}V_{\mathrm{Sb(III)}} - {}^{for}_{cal}V_i\right)^2 \tag{4}$$

$^{for}V_{\mathrm{Sb(III)}}$ was assigned the formal valency 3 for Sb(III) and $^{for}_{\mathrm{cal}}V_i$ calculated by substituting Eq. (3) in Eqs. (1),(2). Analogous bond-valence parameters of 0.30 and 2.593 Å were determined for selenidoantimonates(III) using the metrical data from 14 $SbSe_n$ polyhedra. As both P and Q are positive, the formal unit bond length $^{for}_{i}r_0$ in Eq. (3) will increase as $\bar{\alpha}_i$ decreases, e.g. on going from the isolated pyramidal $[SbS_3]^{3-}$ anions in $Ca_2Sb_2S_5$ (distances 2.443–2.465 Å, angles 94.92–97.77°) [266] to the ψ-SbS_5 octahedra of the $^{1}_{\infty}[Sb_2S_5^{4-}]$ chains in $Sr_3Sb_4S_9$ with S–Sb–S angles in the range 85.93–98.57° for *cis*-sited sulphur atoms [282]. An alternative way of looking at the structural data is to regard the valency V_i of the

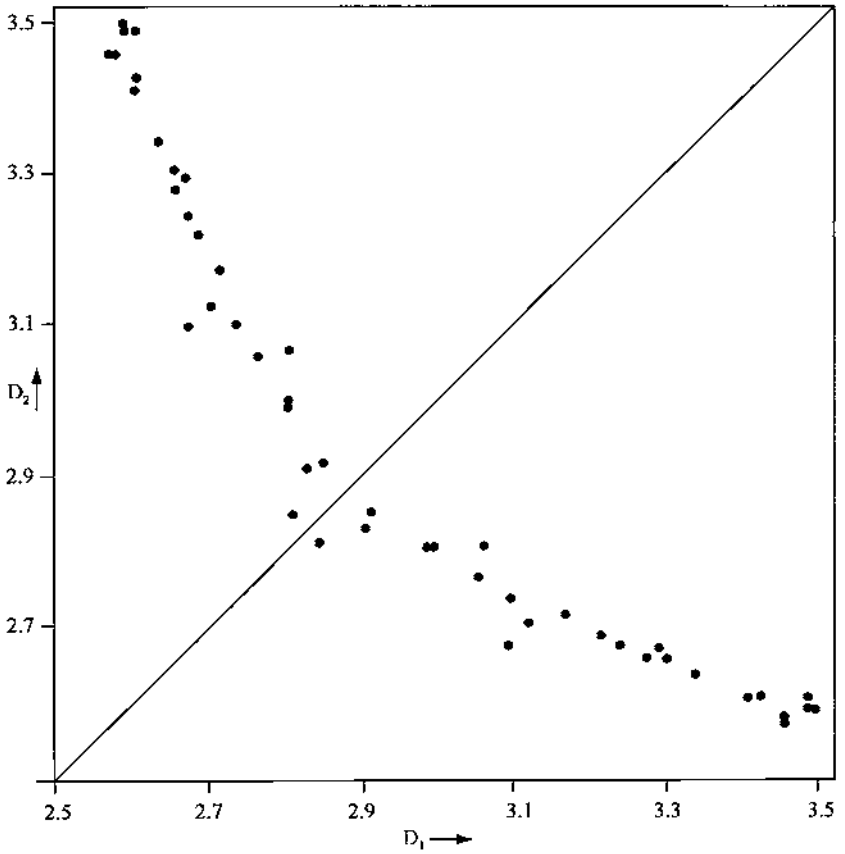

Fig. 39. Structural correlation of *trans*-related Sb–Se distances D_1 and D_2 in Sb_2Se_3 [331] and the selenidoantimonates (III) $KSbSe_2$ [283], $RbSb_3Se_5$ [57], $BaSb_2Se_4$ [295] and $Cs_2Sb_4Se_8$ [232].

central Sb atoms as a variable that will correlate with the average E–Sb–E angle $\overline{\alpha}_i$ Adopting this approach, Wang and Liebau [340,341] calculated effective atomic valences ${}^{eff}V_i$ in chalcogenidoantimonates(III) by assuming that this parameter can be scaled between 3 and 3.75 v.u. in the range $90° \leq \overline{\alpha}_i \leq 109.5°$. They interpreted their observed valence ranges of 2.88–3.80 v.u. for SbS_n polyhedra and 2.98–3.88 v.u. for $SbSe_n$ polyhedra as implying an average transfer of electron density for the non-bonded 5*s* electron pair of Sb(III) to its bonding partners [340,341].

One disadvantage of this approach results from the fact that only average E–Sb–E angles $\overline{\alpha}_i$ are employed. This means, for instance, that the value of ${}^{for}_{i}r_0$ used for the calculation of $Sb–E_{eq}$ bond-valences in a ψ-SbE_4 trigonal bipyramid will be expected to decrease in comparison to that for a ψ-SbE_3 tetrahedron, even though these bonds have no opposite partners. However, it is the correlation between *trans*-sited distances in near linear E–Sb ⋯ E interactions that is charac-

teristic for trivalent antimony. Molecular orbital considerations are also neglected, despite the fact that a significant degree of covalent Sb–E bonding is generally assumed for thio- and selenidoantimonates(III). We therefore prefer the approach that we have previously applied to Group 15 halometalates(III) and their organyls [342–344]. Fig. 40a depicts a qualitative MO diagram for a symmetrical E–M–E three-center bond in which it is assumed that a significant interaction between the 5*s* orbital of M (Sb) and the *p* orbitals of E (S, Se) will lead to a pronounced antibonding character for the $1\sigma_g^+$ orbital. Under such circumstances, the total valence sum for the individual E–Sb–E interaction will now be less than 1, i.e. V_i for a ψ-SbE_4 trigonal bipyramid or a ψ-SbE_5 octahedron with 1 or 2 such three-center bonds will be less than the formal value of 3. As the $1\sigma_u^+$ bonding contribution will clearly be relatively more effective than that of the antibonding $1\sigma_g^+$ orbital at longer range, owing to the more diffuse character of the *p* orbitals involved, asymmetric E–Sb ⋯ E interactions (Fig. 40b) should be energetically favorable in comparison to a symmetric arrangement. For the expected flat minimum, crystal forces will determine the experimental geometry. Structure correlations of opposite Sb–Hal distances in $SbBr_n$ and SbI_n coordination polyhedra have confirmed that V_i reaches a minimum for linear symmetric Br–Sb–Br and I–Sb–I arangements [342,343]. When r_0 and V_i (= 3) are treated as constants in Eq. (2), the scaling constant is found to increase with the Sb–Hal distance D_{ij} according to the expression

$$B = B_0 + A(D_{ij} - r_0) \tag{5}$$

where $B_0 \approx 0.37$ (at $D_{ij} = r_0$) and A is a constant bond-valence parameter. The observed wide spread of opposite Sb–E distances presented in Fig. 39 for solid-state selenidoantimonates(III) and also found for thioantimonates(III) [340,341] indicates that the energy hypersurface for E–Sb ⋯ E interactions is also rather flat. This means that the degree of asymmetry of such three-center bonds will be strongly influenced by anion–cation interactions in a particular structure. In contrast to the findings of Wang and Liebau, who also included metrical data from disordered mixed oxochalcogenidoantimonates(III) of the type $Na_3SbSe_3 \cdot 3Sb_2O_3 \cdot 1/2Sb(OH)_3$ [272], our structural correlations for both SbS_n and $SbSe_n$ polyhedra (Fig. 39) suggest that no significant modification of Eq. (2) is required to calculate s_{ij} values in Group 15 chalcogenidometalates. As a consequence it may be concluded that for most anions participation of the antimony 5*s* orbital in the $1\sigma_g^+$ orbital must be relatively insignificant, i.e. $V_i \approx 3$ for the whole range of E–Sb ⋯ E three-center interactions. Although ionic forces will clearly dominate for longer Sb ⋯ E interactions, we believe that our qualitative MO interpretation provides both a satisfactory explanation of the characteristic distortion of E–Sb–E three-center bonds and a realistic scale ($V_i \leq 3$) for bond-valence analyses.

As discussed in Section 2.2, intermediate Sb ⋯ E distances will be included in assignments of dimensionality (*d*) and Sb coordination numbers in the chalcogenidoantimonates(III). Inspection of Tables 6 and 7 confirms the general structural trends also considered in this previous Section. For instance, condensation

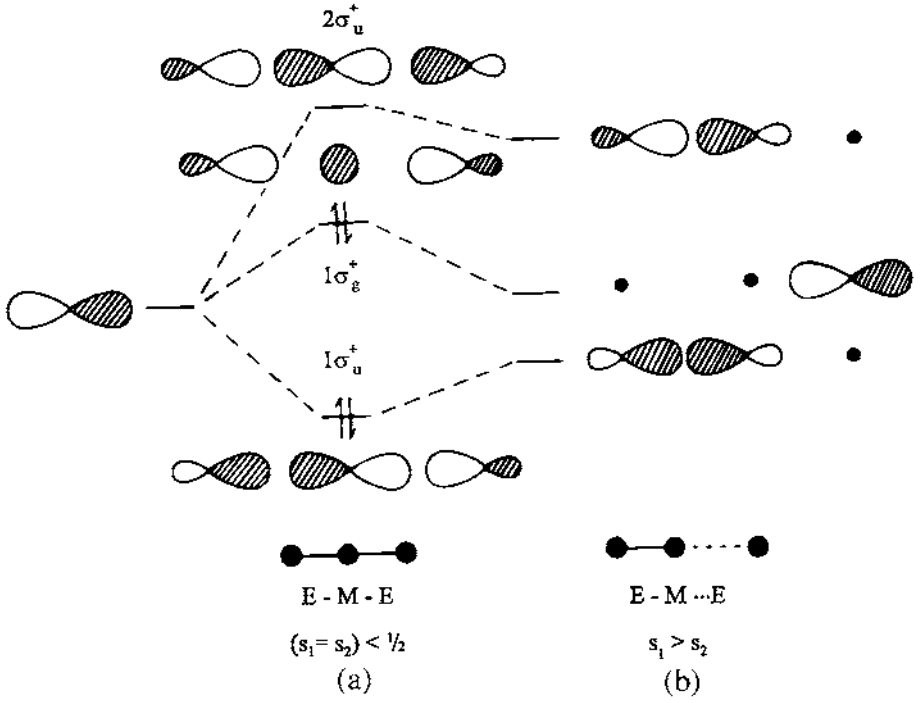

Fig. 40. Qualitative MO diagram for (a) symmetrical and (b) asymmetrical ME_2 three-center bonds.

grades (c) greater than 0.60 have only been found in alkali metal salts with the large Cs^+ countercation, e.g. $Cs_2Sb_8S_{13}$ ($c = 0.615$) [303] and $Cs_4Sb_{14}S_{23}$ ($c = 0.609$) [309]. The highest values of c for the smaller Rb^+ and K^+ cations have been observed in $RbSb_3Se_5$ ($c = 0.600$) [57] and $K_2Sb_4S_7$ ($c = 0.571$) [306], respectively. No less than 10 thioantimonates(III) of the formula type $A_2Sb_4S_7$ have been characterized and as listed in Table 8, both dimensionality and average coordination number (n) of the Sb atoms correlate, in general, with cation size. For instance, a three-dimensional framework anion has only been assembled in the presence of the relatively small K^+ cation. With the exception of the 2-D anionic network of $(C_2H_5NH_3)_2Sb_4S_7$ [300] ($n = 3.33$), n is smaller in chain anions $^1_\infty[Sb_4S_7^{2-}]$ ($n = 3.33$ or 4.0) than in polyanions of higher dimensionality.

The structural chemistry of chalcogenidobismuthates(III) is characterized by the presence of BiE_5 square pyramids and BiE_6 octahedra, in the latter of which the 6s electrons are stereo-chemically inactive. Distorted BiE_7 pentagonal bipyramids are also known. This preference for higher coordination numbers leads to a predominance of 2- and 3-D anion structures. For instance, the bismuth atoms exhibit a perfect octahedral coordination (e.g. Bi–S distances of 3.02 Å in $KBiS_2$) in compounds of the type $ABiS_2$ (A = Li, Na, K) [312–314], which all crystallize in the NaCl-type. Layers of such BiE_6 octahedra are found in many of the

Table 8
Dimensionality (d) and coordination numbers (CN) of the Sb and S atoms in polyanions $^{n}_{\infty}[Sb_4S_7^{2-}]$

Compound	d	ΣSb		ΣS		
		CN = 3	CN = 4	CN = 1	CN = 2	CN = 4
$(NH_4)_2Sb_4S_7$ [287]	1	4	0	2	5	0
$(pipH_2)Sb_4S_7$ [288]	1	4	0	2	5	0
$[Mn(en)_3]Sb_4S_7$ [289]	1	4	0	2	5	0
$Cs_2Sb_4S_7$ [289]	1	3	1	1	6	0
$SrSb_4S_7 \cdot 6H_2O$ [290]	1	3	1	1	6	0
$(C_2H_5NH_3)_2Sb_4S_7$ [300]	2	3	1	1	6	0
$K_2Sb_4S_7 \cdot H_2O$ [297]	2	2	2	0	7	0
$Rb_2Sb_4S_7 \cdot H_2O$ [298]	2	2	2	0	7	0
$Rb_2Sb_4S_7$ [299]	2	0	4	0	6	1
$K_2Sb_4S_7$ [306]	3	2	2	0	7	0

chalcogenobismuthates(III) listed in Table 9. Although a few isotypic Sb(III) phases are known, the coordination sphere of the Group 15 metal is strongly distorted in such cases and best described as ψ-octahedral rather than octahedral as for Bi(III), e.g. $BaSbTe_3$ and $BaBiSe_3$ [59] which were discussed in Section 2.2. As the similarities between the chalcogenidometalates(III) of these Group 15 metals are otherwise rather limited, anions of Bi(III) will be discussed on their own at the end of each of the following sections (Section 4.2–4.4).

4.2. Isolated anions

4.2.1. Mononuclear anions

Compounds of the formula type A_3ME_3 (E = S, Se) with pyramidal $[ME_3]^{3-}$ anions are listed for As and Sb in Tables 5 and 6; additionally Na_3SbTe_3 [269] and K_3SbTe_3 [270,271] are also known.

Isolated ψ-ME_3 tetrahedra have also been found together with other anions in $Ba_2As_2S_5$ [243], $Ba_2As_2Se_5$ [245], $Ca_2Sb_2S_5$ [266], $Ba_8Sb_6S_{17}$ [267] and $Ba_4Sb_4Se_{11}$ [273]. Many mixed oxothio- and oxoselenidoantimonates(III) containing discrete $[SbS_3]^{3-}$ or $[SbSe_3]^{3-}$ anions have been prepared under mild hydrothermal reaction conditions and $K_3SbS_3 \cdot 3Sb_2O_3$ [265] and $Na_3SbSe_3 \cdot 3Sb_2O_3 \cdot 1/2Sb(OH)_3$ [272] provide representative examples of this class of compounds, that will not be discussed in further detail. K_3AsS_3 and A_3SbS_3 (A = Na, K) are isotypic with Na_3AsS_3 [238–240], whose crystal structure can be regarded as being derived from the Th_3P_4-type. The selenidobismuthates A_3BiSe_3 [310], which were recently prepared by heating Bi_2O_3 and the respective alkali carbonate at 850°C in a stream of hydrogen saturated by selenium, also crystallize in the Na_3AsS_3 type. In contrast to Bi_2Se_3 itself with its regular octahedral Bi coordination spheres (distances Bi–Se, 3.006 Å) [345,346], clearly recognizable isolated pyramidal $[BiSe_3]^{3-}$ anions

Table 9
Anion formula types for chalcogenidobismuthates (all dimensionalities $d = 0–3$)

d	Formula type/formula	Compounds [reference]
0	A_3BiE_3	E = Se, A = K, Rb, Cs [310] E = Te, A = K [311]
	$(Ph_4As)[Bi_2S_{34}]$	[362]
1	$Tl_4Bi_2S_5$	[320]
	$A^{II}BiE_3$	A = Sr, E = Se [365]; A = Ba, E = Se, Te [59]
	$Sr_4Bi_6Se_{13}$	[324]
2	ß-$CsBiS_2$	[317]
	$Cs_3Bi_7Se_{12}$	[327]
	$Sr_4Bi_6Se_{13}$	[324]
	$SrBiTe_3$	[366,367]
	$BaBiE_3$	E = Se [366,367], Te [366–368]
3	$A^{II}Bi_2S_4$	A = Ba-modifications I + II [319]
	ABi_3S_5	A = K [321], Rb [322], Cs [323]
	$KBi_{6.33}S_{10}$	[325,326]
	$K_2Bi_8E_{13}$	E = S [325,326], Se [317]
	Tl_9BiTe_6	[375]

NaCl structures: $LiBiS_2$ [312,313], $NaBiS_2$, $KBiS_2$ [312,314], $RbBiS_2$ [265], (α-/γ-)$CsBiS_2$ [266,267], $NaBiSe_2$, $KBiSe_2$ [313], $RbBiSe_2$ [315], $TlBiTe_2$ [318].

are present in these compounds. For instance, K_3BiSe_3 exhibits three short Bi–Se distances (2.658 Å with Se–Bi–Se angles of 100.29°) sited opposite to three very long Bi ⋯ Se contacts (4.196 Å). Application of a current of 1mA between an $NiSb_2Te_6$ cathode and a nickel plate anode in an ethylenediamine solution of $(Bu^n_4N)I$ generates black crystals of $(Bu^n_4N)_3SbTe_4$ [224]. In the discrete $[SbTe_2(Te_2)]^{3-}$ anions a fourth tellurium is attached to one of the terminal Te atoms of an $SbTe_3$ pyramid.

Mononuclear polythio- and polyselenidoarsenates(III) of the type $[SAsS_5]^-$ [246], $[SAsS_7]^-$ [247] and $[SeAsSe_7]^-$ [248] (Fig. 41a) have been isolated from acetonitrile solution by employment of the large countercations Ph_4P^+ (E = S) and Et_4N^+ (E = Se). These cyclic anions contain chelating S_5^{2-} or E_7^{2-} (E = S, Se) chains and may be regarded as substitution derivatives of S_6 or E_8 with their respective chair and crown conformations.

Numerous salts of the tetrahedral ortho-anions $[ME_4]^{3-}$ [M = As(V), Sb(V); E = S, Se] have been structurally characterized. These include the hydrates $Na_3AsS_4 \cdot 8H_2O$ [347], $Ba_3(AsS_4)_2 \cdot 7H_2O$ [348], $Ba_3AsSe_4(OH) \cdot 2H_2O$ [349], the isotypic compounds $Na_3AsSe_4 \cdot 9H_2O$ [350] and $Na_3SbS_4 \cdot 9H_2O$ (Schlippe's salt) [351] and $K_3SbS_4 \cdot 4\frac{1}{2}H_2O$ [352]. All known water-free alkali thio- and selenidoarsenates(V) of the type A_3AsE_4 (E = S, A = K [353]; E = Se, A = Rb, Cs [354]) crystallize in the $(NH_4)_3AsS_4$-type (space group *Pnma*) [355,356]. As–S distances in the slightly disorted tetrahedral anions lie in the range 2.16–2.18 Å,

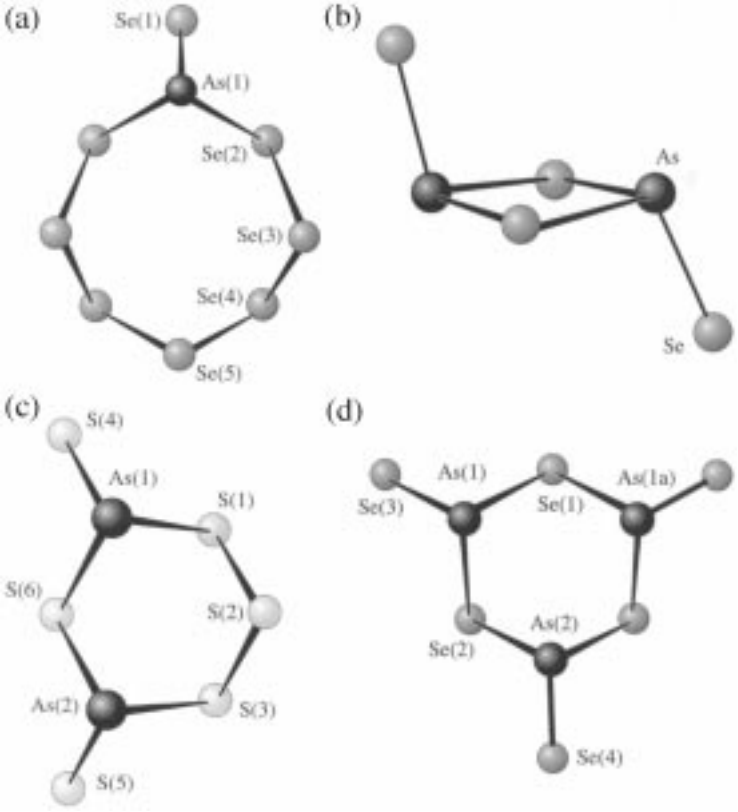

Fig. 41. Discrete anions (a) $[AsSe_8]^-$ in $(Et_4N)[AsSe_8]$ [248], (b) *trans*-$[As_2Se_4]^{2-}$ in $Ba_2As_2Se_5$ [245], (c) $[As_2S_6]^{2-}$ in $(Ph_4P)_2[As_2S_6]$ [251] and (d) $[As_3Se_6]^{3-}$ in $[Sr(en)_4]_2[As_3Se_6]Cl$ [257].

As–Se distances between 2.31 and 2.34 Å. Tl_3AsS_4 has also been structurally characterized [357], as have the water-free alkali thio- and selenidoantimonates(V) A_3SbE_4 (E = S, A = Na [355,356], α-K [355,356], β-K [358], Rb [359]; E = Se, A = Na, K [360], Rb, Cs [354]). Whereas Rb_3SbS_4, Rb_3SbSe_4 and Cs_3SbSe_4 crystallize in the $(NH_4)_3AsS_4$-type, the compounds Na_3SbE_4 (E = S, Se) and α-K_3SbS_4 are all isotypic with $(NH_4)_3SbS_4$ structure (space group $I\bar{4}3m$); β-K_3SbS_4 and K_3SbSe_4 exhibit their own structure types. Typical Sb–S and Sb–Se distances in these chalcogenidoantimonates(V) lie in the ranges 2.32–2.35 and 2.46–2.49 Å.

4.2.2. Dinuclear anions

Edge-bridging of ψ-ME_3 tetrahedra leads to dipyramidal anions $[M_2E_4]^{2-}$. A *trans*-configuration of the terminal chalcogens has been found in the isolated $[As_2S_4]^{2-}$ anions of $Ba_2As_2S_5$ [243], $[K(2,2,2\text{-crypt})]_2[As_2S_4] \cdot 2CH_3CN$ [249] and $[As_2Se_4]^{2-}$ (Fig. 41b] in $Ba_2As_2Se_5$ [245]. The barium salts were prepared at high temperature (650–700°C) and also display discrete $[AsE_3]^{3-}$ anions. $Ca_2Sb_2S_5$

[266] was synthesized by fusion of Sb_2S_3, S and Ca at 900°C and contains the analogous thioantimonates(III) *trans*-$[Sb_2S_4]^{2-}$ and $[SbS_3]^{3-}$. In contrast both *cis*- and *trans*-$[Sb_2Se_4]^{2-}$ anions are present in the crystal structure of $Ba_4Sb_4Se_{11}$ [273], together with $[SbSe_3]^{3-}$ pyramids and Se_2^{2-} dumb-bells. *cis*-$[Sb_2Se_4]^{2-}$ has also been recently prepared by alloy extraction with $[K(2,2,2\text{-crypt})]^+$ as countercation [249].

Two examples of exclusive corner-sharing in a dinuclear M(III) anion appear to be known. Whereas $Sr_2Sb_2S_5 \cdot 15H_2O$ [274] was prepared under mild hydrothermal conditions and exhibits discrete $[Sb_2S_5]^{4-}$ anions with a bridging Sb–S–Sb angle of 92.9°, the tellurium analog $(Me_4N)_4Sb_2Te_5$ [428] is an electrochemical product resulting from the application of a 100-μA current on a 0.15 M ethylenediamine solution of $(Me_4N)I$ between a Sb_2Te_3 cathode and a Ni plate anode.

Both symmetrically and asymmetrically bridged cyclic anions of the type $[As_2E_6]^{2-}$ have been characterized. Alloy extraction was employed to isolate $[Na(2,2,2\text{-crypt})]_2As_2Se_6$, in which pyramidal $AsSe_3$ units are connected through two Se–Se bonds into a six-membered As_2Se_4 ring with chair conformation [253]. A similar anion with 1,4 occupation of the ring positions by As atoms is also found in $(Ph_4P)_2As_2Se_6$ [252] and the tellurium containing phases $[K(2,2,2\text{-crypt})]_2As_2Te_6$ [254] and $(Ph_4P)_2As_2Te_6$ [394]. In contrast, reaction of Na_3AsS_4 with $(Ph_4P)Cl$ in ethanol affords $(Ph_4P)_2As_2S_6$ [251], whose anion structure with μ-S and μ-S_3 bridging of the participating As(III) atoms is depicted in Fig. 41c. A seven-membered ring with similar S^{2-} and S_4^{2-} bridging ligands has been found in $[Mg(N\text{-MeIm})_6]Sb_2S_{15}$ (*N*-MeIm = *N*-methyl-imidazole) [361]. However, in this case the Sb(III) atoms are also chelated by S_5^{2-} chains, one of whose coordinating atoms adopts an axial site *trans* to a μ-S_4 sulphur in a ψ-SbS_4 trigonal bipyramid. An even sulphur-richer anion $[Bi_2S_{34}]^{4-}$ has been isolated with Ph_4As^+ as counter-cation by reaction of $BiCl_3$ with an acetonitrile ammonium polysulphide solution in the presence of $(Ph_4As)Cl$ [362]. Both Bi atoms display ψ-octahedral coordination spheres, whose equatorial S atoms belong to chelating S_7^{2-} ligands with the remaining axial sites being occupied by the terminal atoms of a connecting S_6 chain.

4.2.3. Oligonuclear anions

The cyclic anions $[As_3S_6]^{3-}$ and $[As_3Se_6]^{3-}$ have been isolated from ethylenediamine solution as $(enH_2)_3[As_3S_6]_2 \cdot 6en$ [255], $[Ba(en)_4]_3[As_3S_6]_2$ [256] and $[Sr(en)_4]_2[As_3Se_6]Cl$ [257]. As illustrated in Fig. 41d for $[As_3Se_6]^{3-}$, the six-membered As_3E_3 rings display chair conformations with equatorially sited terminal chalcogen atoms. $Ba_8Sb_6S_{17}$ was prepared by fusion of the constituent binary sulphides at 1120 K and contains, by contrast, linear trinuclear anions $[Sb_3S_8]^{7-}$ in addition to $[SbS_3]^{3-}$ pyramids [273]. The $[Sb_3S_8]^{7-}$ anions display a central ψ-SbS_4 trigonal bipyramid, that is corner-linked to two ψ-SbS_3 tetrahedra through its axial sulphur atoms.

The largest known molecular Zintl anion $[Sb_{12}Se_{20}]^{4-}$ (Fig. 42) was synthesized by reduction of an alloy of nominal composition Sb_4Se_4 with potassium in DMF and isolated as $(Ph_4P)_4Sb_{12}Se_{20}$ by precipitation [275]. This remarkable species

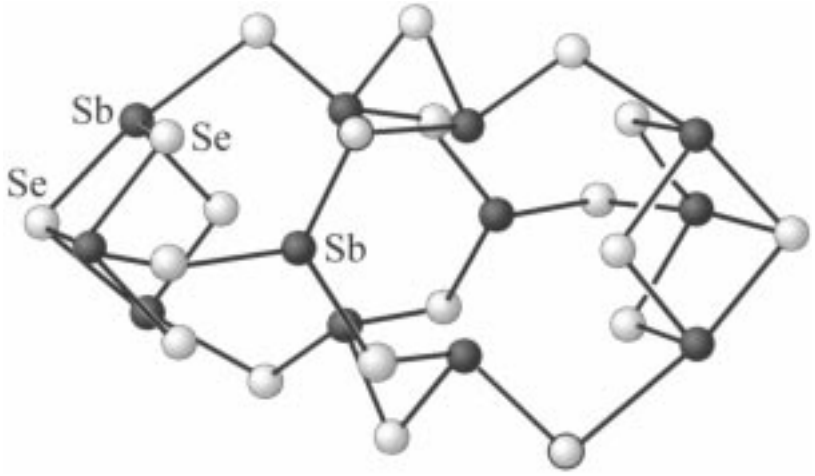

Fig. 42. The largest known molecular Zintl anion $[Sb_{12}Se_{20}]^{4-}$ in $[Ph_4P]_4[Sb_{12}Se_{20}]$ [275].

exhibits both ψ-$SbSe_3$ tetrahedra and ψ-$SbSe_4$ trigonal bipyramids. Two Sb_3Se_4 semicubes are connected to a central Sb_6Se_6 ring by bridging selenium atoms.

4.3. Chain polymers

Chain and sheet chalcogenidoarsenates(III) and -antimonates(III) (E = S, Se) can be assembled by cation-directed corner condensation of cyclic $[M_3E_6]^{3-}$ anions and linear $[M_yE_{2y+1}]^{(2+y)-}$ chains. The compact nature of the required cation coordination spheres often allows trivalent antimony to extend its coordination number to 4 or occasionally 5 in the presence of small structure-directing agents (e.g. NH_4^+, K^+). This leads to the frequent observation of $[Sb_2E_6]^{6-}$ building blocks comprising of two edge-bridged ψ-SbE_4 trigonal bipyramids instead of the corner-bridged ψ-SbE_3 tetrahedra of an $[Sb_2E_5]^{4-}$ unit. In contrast, large cations generally direct the assembly of topologically flexible anion networks, that can adjust to satisfy the charge and size compensation demands of the counterion by providing higher coordination numbers. This can lead to the exclusive presence of ψ-SbE_3 tetrahedra and the adoption of anionic chain structures similar to those found in chalcogenidoarsenates(III) of the same formula type, e.g. $^1_\infty[SbSe_2^-]$ in $[Ba(en)_4]Sb_2Se_4$ [285] or $^2_\infty[Sb_8S_{13}^{2-}]$ in $(enH_2)Sb_8S_{13}$ [291]. Modes of assembly found in Group 15 chain polymers will be considered in the following sections.

4.3.1. Mononuclear building units

Corner-bridging of ψ-ME_3 tetrahedra through two chalcogen atoms can lead either to the formation of cyclic anions such as *trans*-$[Sb_2S_4]^{2-}$ [266] and $[As_3S_6]^{3-}$ or the assembly of infinite $^1_\infty[ME_2^-]$ chains, an example of which ($NaAsSe_2$ [261]) is illustrated in Fig. 43a. Such polymeric anions have also been found in $AAsS_2$

(A = Na [258,259], Rb [260], Tl [241,242]) and $AAsSe_2$ (A = Na [261], K, Rb, Cs [262]). $NaAsS_2$ was prepared by heating As_2S_3 in a Na_2S flux at 220°C, $NaAsSe_2$ by high temperature fusion of the elements at 700°C. In contrast, $RbAsS_2$ and the heavier alkali metal selenidoarsenates(III) $AAsSe_2$ (A = K, Rb, Cs) can be isolated under mild methanolothermal conditions at 130°C. $KAsSe_2$ and $RbAsSe_2$ exhibit *vierer* and $CsAsSe_2$ *zweier* single chains. As Nowacki recognized for $NaAsS_2$ [259], both this structure and that of $NaAsSe_2$ [261] are related to the NaCl-type. In addition to the three short covalent As–E bonds of the $^1_\infty[AsE_2^-]$ chains (e.g. 2.309, 2.454, 2.470 Å in $NaAsSe_2$) these compounds also exhibit three longer As ⋯ E interactions (e.g. 3.423, 3.550, 3.812 Å in $NaAsSe_2$), one within the chain and two between neighbouring chains. When these contacts are taken into account, strongly distorted octahedral coordination spheres can be assigned to the As(III) atoms. A less distorted or even regular polyhedron would, of course, be expected for compounds of the same formula type $NaME_2$ for the heavier elements M = Sb, Bi and this is indeed found to be the case. $NaSbSe_2$ and $NaSbTe_2$ [261] both adopt the NaCl-structure as do the phases $NaBiE_2$ (E = S [217,314], Se [313], Te [261]). This structure type is also found for $LiSbTe_2$ [363], $LiBiS_2$ [312,314], $KBiS_2$ [312,314], $RbBiS_2$ [315], α-$CsBiS_2$ [316], $KBiSe_2$ [313] and $RbBiSe_2$ [315]. The $^2_\infty[SbS_2^-]$ sheets of β-$NaSbS_2$ [276,293] with their edge-bridged ψ-SbS_5 octahedra exhibit a further longer Sb ⋯ S contact to the next anionic layer and both this structure and that of $NaAsSe_2$ can be converted to the NaCl-type at high pressure (37 kbar, 600°C) [261].

ψ-SbE_3 tetrahedra provide the molecular building units in the $^1_\infty[SbE_2^-]$ chains of $RbSbS_2$ [278], $CsSbE_2$ (E = S [279], Se [284]) and $[Ba(en)_4]Sb_2Se_4$ [285]. Analogous $^1_\infty[SbS_2^-]$ anions are also present as *einer* single chains, together with likewise 1-D $^1_\infty[Sb_2S_5^{4-}]$ anions, with their edge-bridged ψ-SbS_5 octahedra (Fig. 38b), in the crystal lattice of $Sr_3Sb_4S_9$ [282]. In contrast, the trivalent antimony atoms extend their coordination number to 4 in the presence of the smaller NH_4^+ and K^+ cations of NH_4SbS_2 [281] and $KSbE_2$ [E = S [277], Se [283]). The characteristic four-membered Sb_2E_2 rings of the $^1_\infty[SbE_2^-]$ chains, depicted for $KSbSe_2$ in Fig. 43b, now contain two shorter equatorial bonds (e.g. 2.531–2.561 Å in $KSbSe_2$) and two markedly longer axial bonds (e.g. 2.804–3.072 Å in $KSbSe_2$).

Hydrothermal reaction of A_2CO_3 with As_2Se_3 at 130°C yields the compounds $KAsSe_3 \cdot H_2O$ and $AAsSe_3 \cdot 1/2H_2O$ (A = Rb, Cs) [263], in which ψ-$AsSe_3$ tetrahedra are linked through Se–Se bonds into $^1_\infty[AsSe_3^-]$ chains (Fig. 43c). This connectivity mode has yet to be established for 1-D Sb(III) polyanions.

4.3.2. Building units of higher nuclearity

Single and double chain polymers based on linear $[M_yE_{2y+1}]^{(2+y)-}$ building blocks will be discussed initially in this section, followed by a description of the connectivity patterns of these units with cyclic $[M_3E_6]^{3-}$ anions. The ability of Sb(III) to extend its coordination number to 4 leads to the assembly of a variety of structure types not found for its lighter congener As(III).

The $^1_\infty[Sb_3S_5^-]$ anions of $(Pr^n_4N)Sb_3S_5$ [286] can be regarded as being composed of two parallel $^1_\infty[SbS_2^-]$ single chains, that are alternatively cross-linked at every

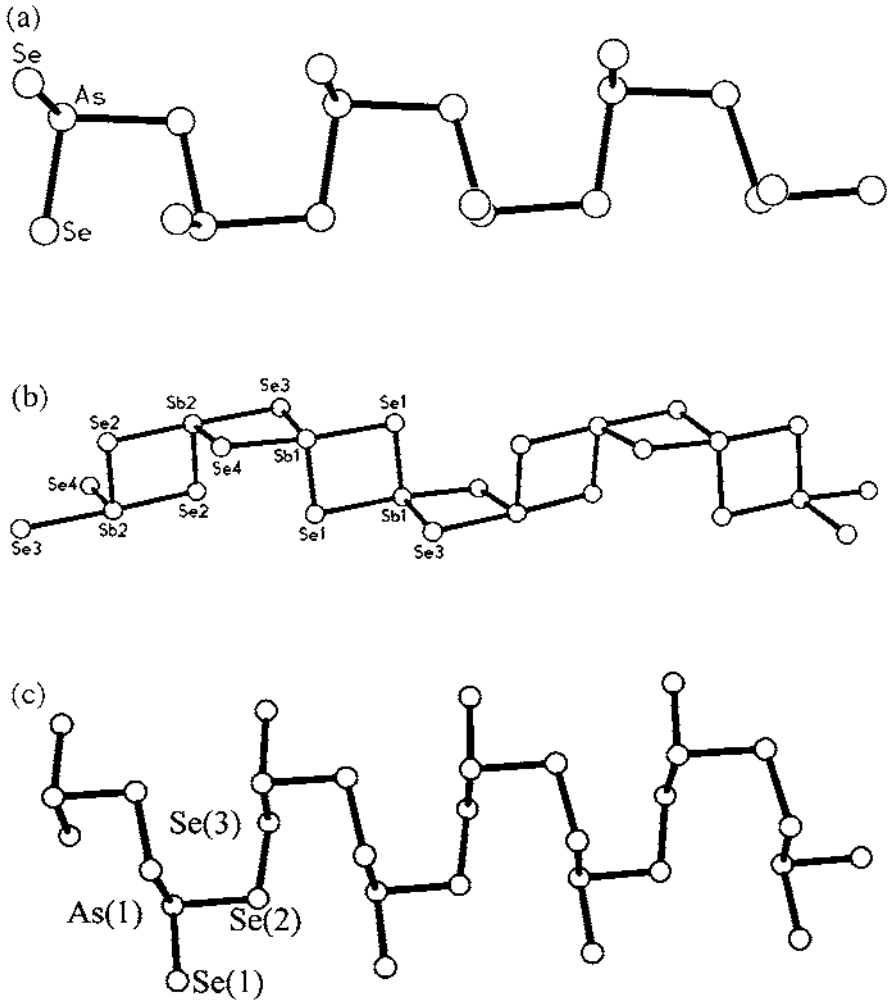

Fig. 43. Polymeric chain-like anions with mononuclear ME_3 or ME_4 building units (M = As, Sb): (a) $^1_\infty[AsSe_2^-]$ chains in $NaAsSe_2$ [261]; (b) $^1_\infty[SbSe_2^-]$ chains in $KSbSe_2$ [283]; (c) $^1_\infty[AsSe_3^-]$ chains in $KAsSe_3 \cdot H_2O$ [263].

second or third ψ-tetrahedral Sb(III) atom (Fig. 44a). This mode of assembly generates double chains with corner-sharing 10-membered Sb_5S_5 rings. Sb–S distances to bridging sulfur atoms lie in the range 2.437–2.491 Å; the lone terminal Sb–S3 bond is somewhat shorter (2.382 Å), as would be predicted in accordance with its increased polarity. When transannular Sb1 ⋯ S3 and Sb2 ⋯ S1 contacts of, respectively, 3.152 and 3.201 Å are included, Sb1 and Sb2 extend their coordination numbers to, respectively, 4 and 5 and typical Sb_3S_3 semicubes can be recognized. Tetranuclear linear repeating units are present in both the single chains of

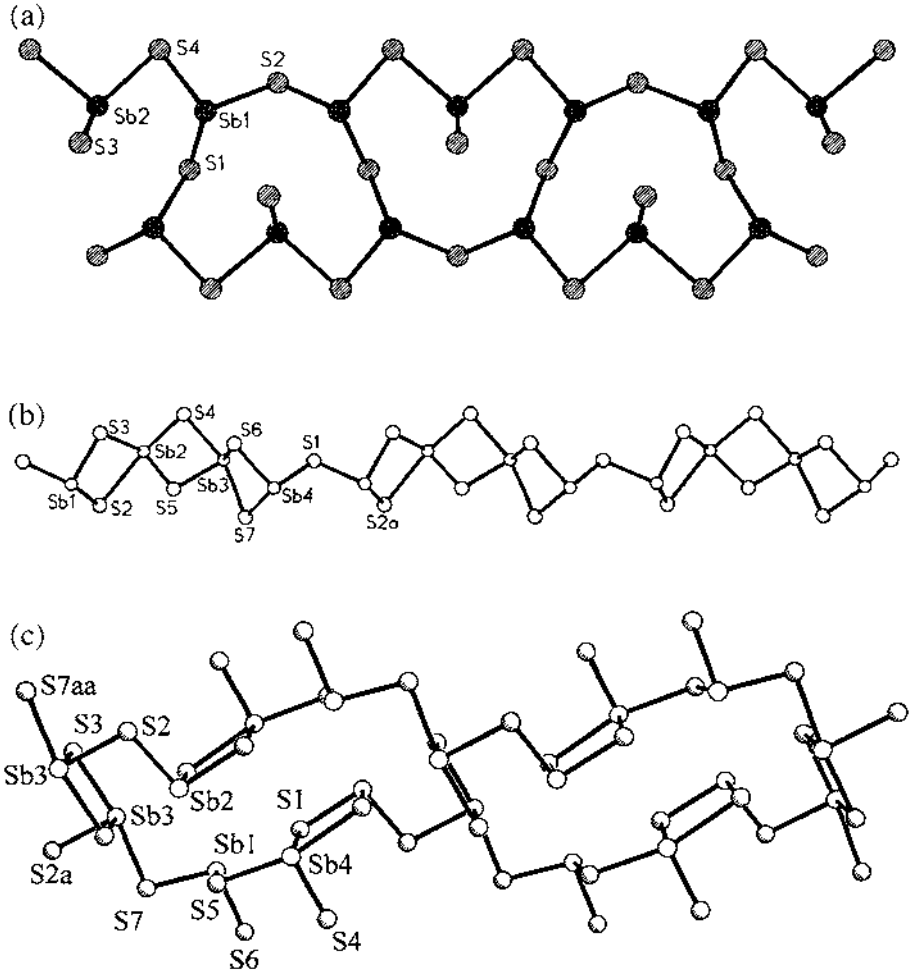

Fig. 44. Polymeric chainlike thioantimonates(III) with linear $[Sb_yE_{2y+1}]^{(2+y)-}$ building blocks: (a) $^1_\infty[Sb_3S_5^-]$ in $(Pr^n_4N)Sb_3S_5$ [286]; (b) $^1_\infty[Sb_4S_7^{2-}]$ in $Cs_2Sb_4S_7$ [289]; (c) $^1_\infty[Sb_2S_4^{2-}]$ in $Ba_2Sb_4S_8$ [294].

$Cs_2Sb_4S_7$ [289] and the double chains of $Ba_2Sb_4E_8$ (E = S [294], Se [295]). The $^1_\infty[Sb_4S_7^{2-}]$ anions of the former compound can be regarded as containing tetranuclear sections of infinite $^1_\infty[SbS_2^-]$ chains with edge-bridged ψ-SbS_4 trigonal bipyramids. Such Sb_4S_6 units are then linked through bridging sulfur atoms into the infinite chains depicted in Fig. 44b with both Sb1 and Sb4 exhibiting ψ-SbS_3 tetrahedral coordination spheres. Whereas the axial Sb3–S distances are similar (2.637, 2.739 Å), Sb2–S2 is much longer (2.997 Å) than Sb2–S4 (2.536 Å).

Although not isotypic, $Ba_2Sb_4S_8$ and $Ba_2Sb_4Se_8$ display similar anionic networks. In contrast to the other solventothermally prepared compounds considered in this section, these barium chalcogenidoantimonates(III) were synthesized by

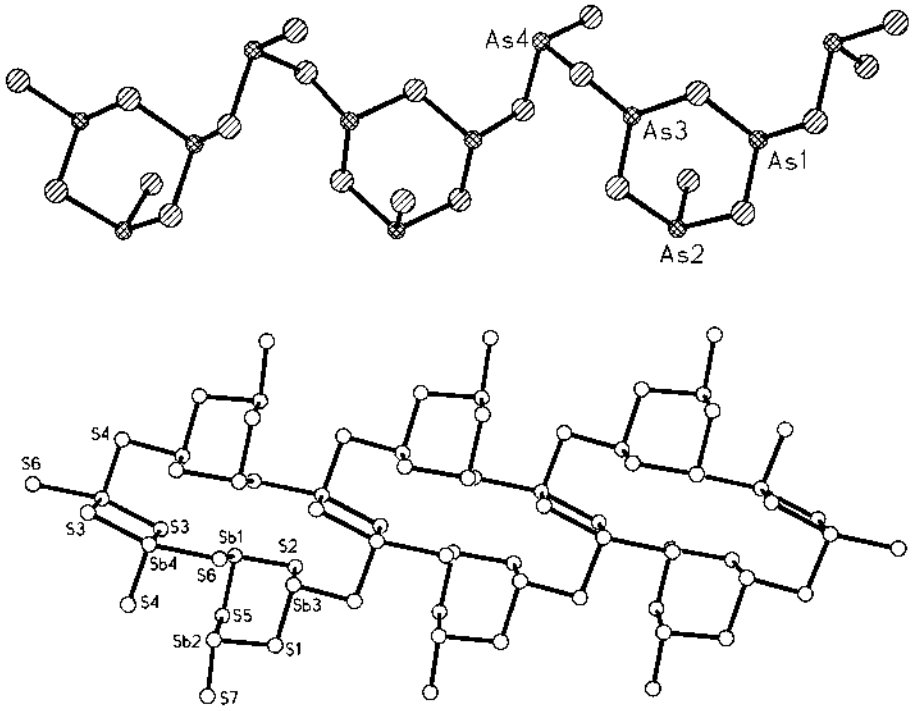

Fig. 45. Cyclic $[M_3S_6]^{3-}$ molecular building units in (a) $(Me_4N)_2As_4S_7$ [51] and (b) $SrSb_4S_7 \cdot 6H_2O$ [290].

high temperature fusion reactions ($Ba_2Sb_4S_8$: Ba + Sb + S at 700°C; $Ba_2Sb_4Se_8$: Ba + Sb_2Se_3 + Se at 980°C). As illustrated for $Ba_2Sb_4S_8$ in Fig. 44c infinite $^1_\infty[SbE_2^-]$ anions are cross-linked through two bridging sulfur atoms at every fifth Sb(III) atom into double chains with large $Sb_{10}E_{10}$ pores. This connectivity mode generates cyclic Sb_2E_2 units with ψ-SbE_4 trigonal bipyramidal antimony atoms and four-membered rings are also constructed by two neighbouring Sb(III) atoms in the linear Sb_4E_4 units.

Simple corner-linkage of cyclic $[M_3E_6]^{3-}$ building units might be expected to afford single chains of the type $^1_\infty[M_3E_5^-]$. Although this connectivity pattern is indeed found in $(Me_4N)_2As_6S_{10}$ [51], individual six-membered rings are further bridged through the remaining terminal sulfur atoms into the unique double chains $[As_6S_{10}^{2-}]$ depicted in Fig. 1. To our knowledge, $(Me_4N)_2As_6S_{10}$ provides the only example of relatively undistorted ψ-AsS_4 trigonal bipyramidal coordination in a chalcogenidoarsenate(III) (distances $As–S_{eq}$ 2.202, 2.288 Å; $As–S_{ax}$ 2.533, 2.648 Å).

Condensation of the characteristic solution anions $[M_3S_6]^{3-}$ and $[MS_3]^{3-}$ generates single chains of the formula type $^1_\infty[M_4S_7^{2-}]$, that have been observed in $(Me_4N)_2As_4S_7$ [51], $(NH_4)_2Sb_4S_7$ [287], $(N_2C_4H_8)Sb_4S_7$ [286] (piperazinium =

$N_2C_4H_8$) and $[Mn(en)_3]Sb_4S_7$ [288], all of which were prepared under mild solventothermal conditions (CH_3CN for M = As; H_2O for M = Sb). As illustrated for $^1_\infty[As_4S_7^{2-}]$ in $(Me_4N)_2As_4S_7$ (Fig. 45a), weaker M ⋯ S contacts to the terminal sulfur atom are characteristic for the cyclic $[M_3S_6]^{3-}$ building units in these chains. The ability of trivalent antimony to extend its coordination number to 4 allows two such $^1_\infty[Sb_4S_7^{2-}]$ single chains to interconnect through Sb_2S_2 rings in $SrSb_4S_7 \cdot 6H_2O$ [19] (Fig. 45b).

The practicability of extending these 'Lego-like' building principles to longer $[M_yS_{2y+1}]^{(2+y)-}$ linear units, by choice of suitable structure-directing cations, has been confirmed through the assembly of the 1-D anionic networks of $A_2As_8S_{13} \cdot H_2O$ (A = K, Rb, NH_4 [53]) $(enH_2)Sb_8S_{13}$ [291] and $(Et_4N)_2As_6S_{10}$ [248]. Corner-bridging of cyclic $[M_3S_6]^{3-}$ and dipyramidal $[M_2S_5]^{4-}$ anions affords the double chains (Fig. 46a) of the type $^1_\infty[M_8S_{13}^{2-}]$ found in the former two compounds and in the mineral Gerstleyite $Na_2[(As, Sb)_8S_{13}] \cdot 2H_2O$ [292]. Alternatively, this connectivity pattern can be regarded as resulting from the corner-linkage of parallel $^1_\infty[M_4S_7^{2-}]$ chains of the type present in $(Me_4N)_2As_4S_7$ (Fig. 45a) or $(NH_4)_2Sb_4S_7$. Indeed, such $^1_\infty[Sb_4S_7^{2-}]$ ribbons occur as a common structural feature in many thioantimonates(III) and may well be assumed to be formed at an early stage of polyanion construction. For instance, they are linked through S–S bonds in the double chains of $(Me_2NH_2)_2Sb_8S_{14}$ [364], which was prepared under hydrothermal conditions from an $Me_2NH/Sb/S$ mixture at 200°C. When Sb ⋯ S contacts longer than 3.0 Å are ignored, $[H_3N(CH_2)_3NH_3]Sb_{10}S_{16}$ (Table 7, $d = 3$) [308] also contains comparable $^1_\infty[Sb_{10}S_{16}]$ double chains, in which $^1_\infty[Sb_4S_7^{2-}]$ ribbons are connected through corner-shared *cis*-$[Sb_2S_4]^{2-}$ units.

A further step in the systematic design of 1-D polyanions is illustrated by $^1_\infty[As_6S_{10}^{2-}]$ in $(Et_4N)_2As_6S_{10}$, in which single chains with alternating cyclic and linear trinuclear building units can be identified as a structural motif (Fig. 46b). These ribbons are linked into double chains through bridging sulfur atoms between linear As_3S_3 units. It will be interesting to see whether further examples of this class of polyanions $^1_\infty[\{As_xS_{3x/2+1}\}^{2-}]$ can be assembled under solventothermal conditions in the presence of large structure-directing cations.

Pentasulfide S_5^{2-} chains join Sb_2S_2 rings into infinite $^1_\infty[Sb_2S_{12}^{2-}]$ double chains in $CsSbS_6$ [369], which was prepared by reacting Sb with a Cs_2S_x flux at 280°C.

Chainlike chalcogenidobismuthates(III) are present in $SrBiSe_3$ [365] (isotypic with $SrSbSe_3$ [366,367]), $BaBiSe_3$ [59] (isotypic with $BaSbTe_3$ [59] and $BaBiTe_3$ [366–368]), $Tl_4Bi_2S_5$ [320] and $Sr_4Bi_6Se_{13}$ [324]. For example, the $^1_\infty[Bi_4S_{10}^{8-}]$ ribbons in $Tl_4Bi_2S_5$ consist of edge-bridged sub-chains, whose individual BiS_6 octahedra are also linked through shared edges. The resulting thiobismuthate(III) rods are depicted in Fig. 47a and can be described as 'fourfold octahedral chains'. Whereas analogous 1-D anions are also found in the isotypic materials $BaSbTe_3$ and $BaBiE_3$ (E = Se, Te), $Sr_4Bi_6Se_{13}$ and $SrBiSe_3$ contain, respectively, six- and eightfold octahedral chains (Fig. 47b,c) with broader cross-sections. $BaBiTe_3$ was recently reinvestigated by Kanatzidis et al. [368], whose EHMO calculations on the nature of the bonding between the $^1_\infty[Bi_4Te_{10}^{8-}]$ rods (Fig. 47a) and linking zig-zag shaped formally neutral $^1_\infty[Te_2]$ chains (Fig. 47a) indicate that the latter motif should not be

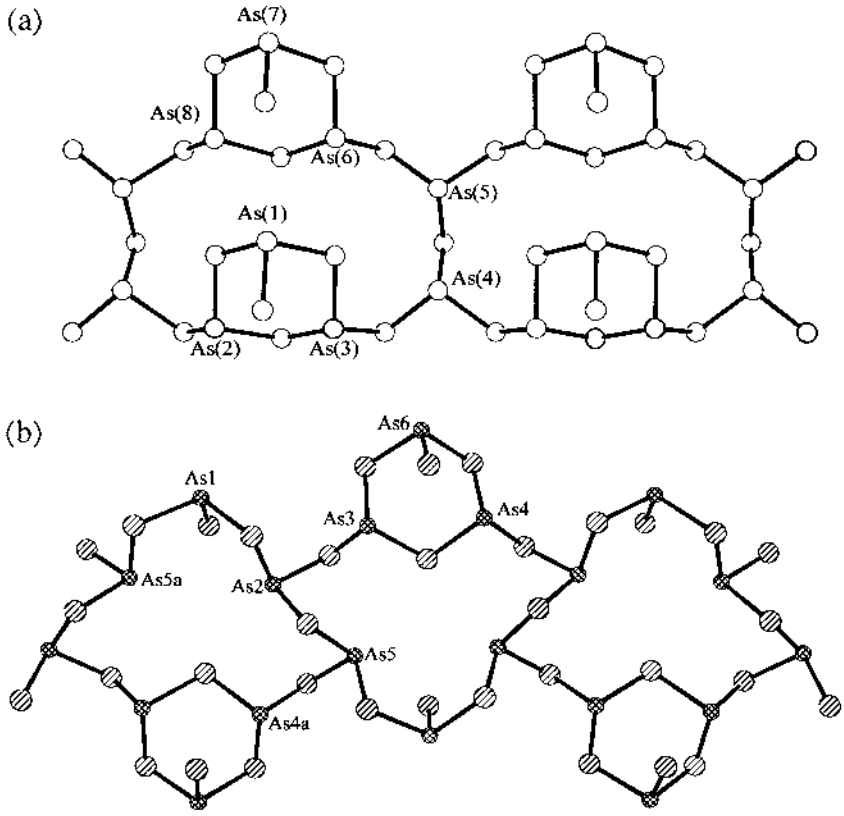

Fig. 46. Double chains with both cyclic $[M_3S_6]^{3-}$ and linear $[M_yS_{2y+1}]^{(2+y)-}$ building blocks: (a) $^1_\infty[As_8S_{13}^{2-}]$ in $Rb_2As_8S_{13} \cdot H_2O$ [53]; and (b) $^1_\infty[As_6S_{10}^{2-}]$ in $(Et_4N)_2As_6S_{10}$ [248].

regarded as an isolated structural feature. Whereas Te–Te contacts [3.098(2) Å] to terminal atoms of the neighbouring $^1_\infty[Bi_4Te_{10}^{8-}]$ rods can be assigned a degree of bonding character, analogous interactions within the $^1_\infty[Te_2]$ motifs themselves [3.170(2) Å] are found to be antibonding. This interpretation leads to a formulation of the infinite ribbons as $^1_\infty[Bi_4Te_{12}^{8-}]$ with *end on* coordinating Te_2^{2-} dumb-bells. An analysis of corresponding distances in the isotypic phases $BaSbTe_3$ and $BaBiSe_3$ suggests that the above description is also apposite for the former telluridoantimonate(III). In contrast, the shorter interchain Se–Se distances in $BaBiSe_3$ [2.862(2) Å], in comparison to those of its $^1_\infty[Sb_4Se_{10}^{8-}]$ rods [3.079(2) Å], indicate that this compound can best be regarded as containing neutral selenium chains.

4.4. Layered structures

A templating role is evident for the Cs^+ cations in the only known lamellar thioarsenate(III), $Cs_2As_8S_{13}$ [52]. The polymeric anion (Fig. 48) is composed of

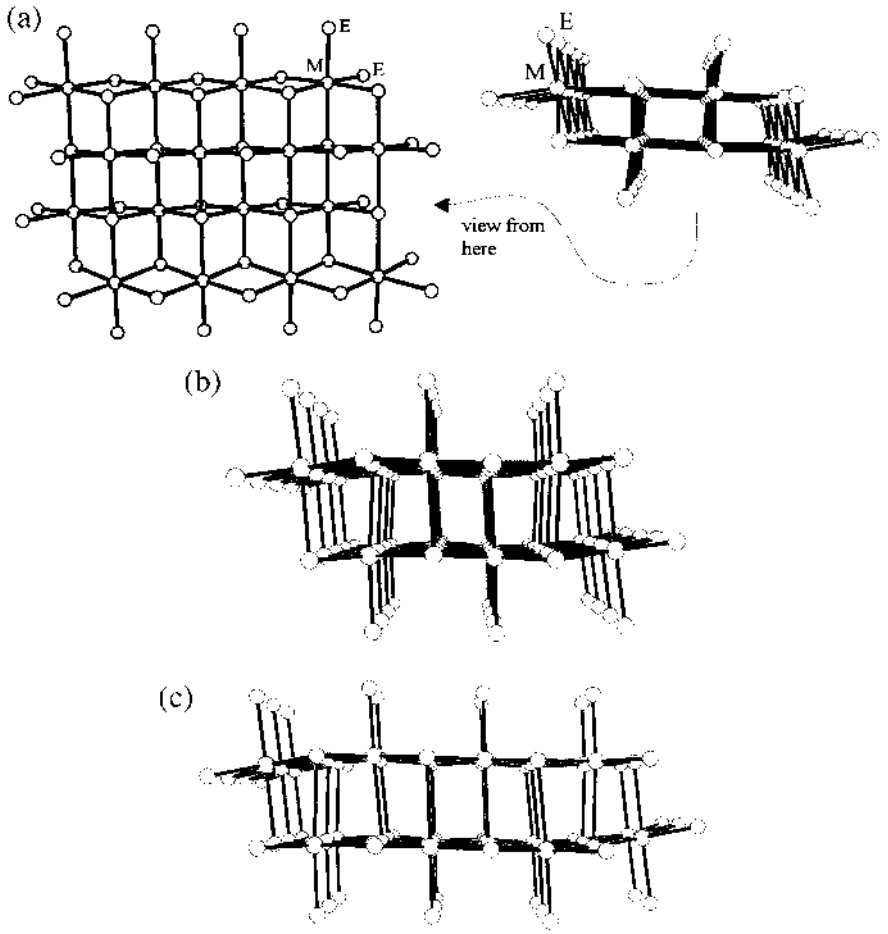

Fig. 47. Chalcogenidoantimonates(III) and -bismuthates(III) with edge-linked Bi(Sb)E_6-octahedra as building units: (a) $[M_4E_{10}]^{8-}$ rods in $Tl_4Bi_2S_5$ [320], $BaBiSe_3$ [59], $BaBiTe_3$ [366–368] and $BaSbTe_3$ [59]; (b) $[Bi_6Se_{14}]^{10-}$ rods in $Sr_4Bi_6Se_{13}$ [324]; and (c) $[Bi_8Se_{18}]^{12-}$ rods in $SrBiSe_3$ [365] and $SrSbSe_3$ [366,367].

individual As_4S_4 rings, that are each connected to three further eight-membered rings through As–S–As bridges, so giving rise to the infinite layer structure.

In contrast to As(III), the ready adoption of higher coordination numbers by trivalent antimony allows the construction of a variety of anionic sheet networks, whose formula types are listed in Table 7. Somewhat surprisingly, only two examples of a 2-D selenidoantimonates(III) appear to be known, namely $RbSb_3Se_5$ [57], whose structure was depicted in Fig. 2, and $Cs_3Sb_5Se_9$ [301]. When only short Sb–Se bonds in the range 2.535–2.756 Å are taken into account and Sb–Se contacts longer than 3.0 Å ignored, the former compound can be regarded as containing discrete $[Sb_6Se_{10}]^{2-}$ anions, in which two typical cyclic $[Sb_3Se_6]^{3-}$

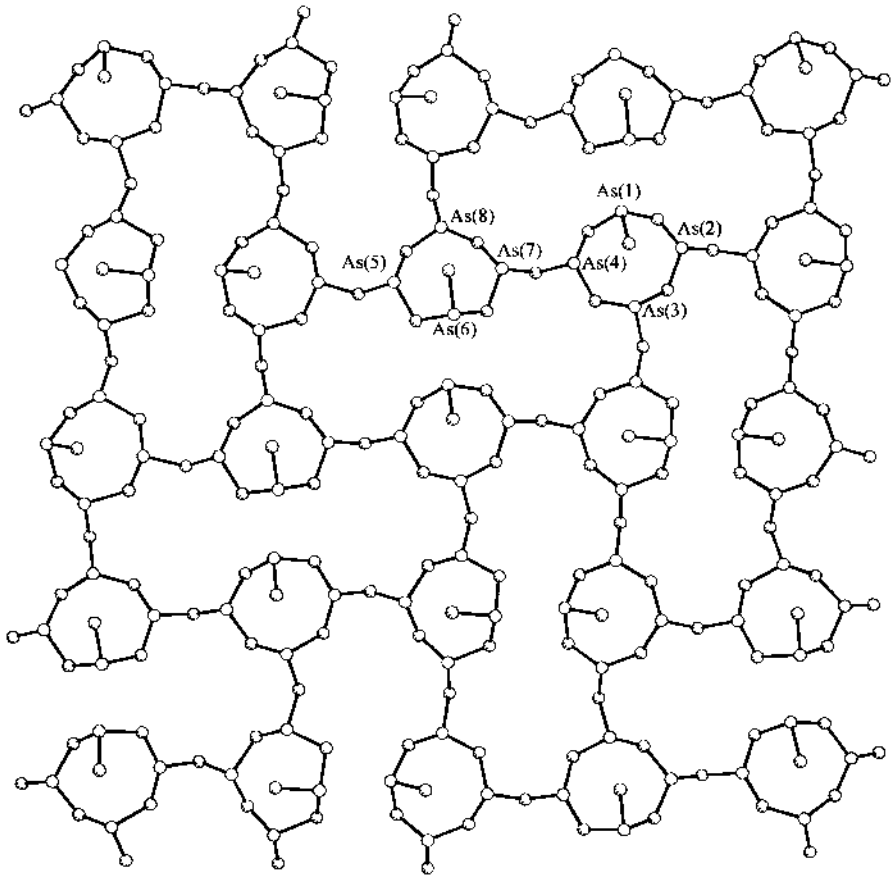

Fig. 48. $^{2}_{\infty}[As_8S^{2-}_{13}]$ layers in $Cs_2As_8S_{13}$ [52].

building blocks are linked through shared Se atoms into a tricyclic unit. Longer Sb–Se_{ax} interactions of 3.055 and 3.103 Å connect these molecular species into infinite layers.

Although the $^{2}_{\infty}[SbS^{-}_{2}]$ sheets of β-$NaSbS_2$ [276,292] are composed of edge-bridged ψ-SbS_5 octahedra, coordination numbers of 3 and 4 are more typical for lamellar thioantimonates(III), many of which exhibit structural features already encountered in 1-D polyanions. For instance, the porous $^{2}_{\infty}[Sb_6S^{2-}_{10}]$ sheets of $RbSb_3S_5 \cdot H_2O$ [296] can be constructed by cross-linking $^{1}_{\infty}[Sb_4S^{4-}_{8}]$ ribbons through cyclic *trans*-$[Sb_2S_4]$ units. The former chains contain tetra-nuclear Sb_4S_6 segments of $^{1}_{\infty}[SbS^{-}_{2}]$ polymers (see Fig. 43b for an example) as do the 1-D anionic networks of $Cs_2Sb_4S_7$ [289]. However, in $RbSb_3S_5 \cdot H_2O$ (Fig. 49a), these tricyclic building blocks are fused together through Sb_2S_2 rings, in which the S and Sb atoms exhibit respective coordination numbers of 3 and 4. $Rb_2Sb_4S_7$ [299] contains $^{2}_{\infty}[SbS^{-}_{2}]$ ribbons, that are connected through common bridging S atoms into $^{2}_{\infty}[Sb_4S^{2-}_{7}]$

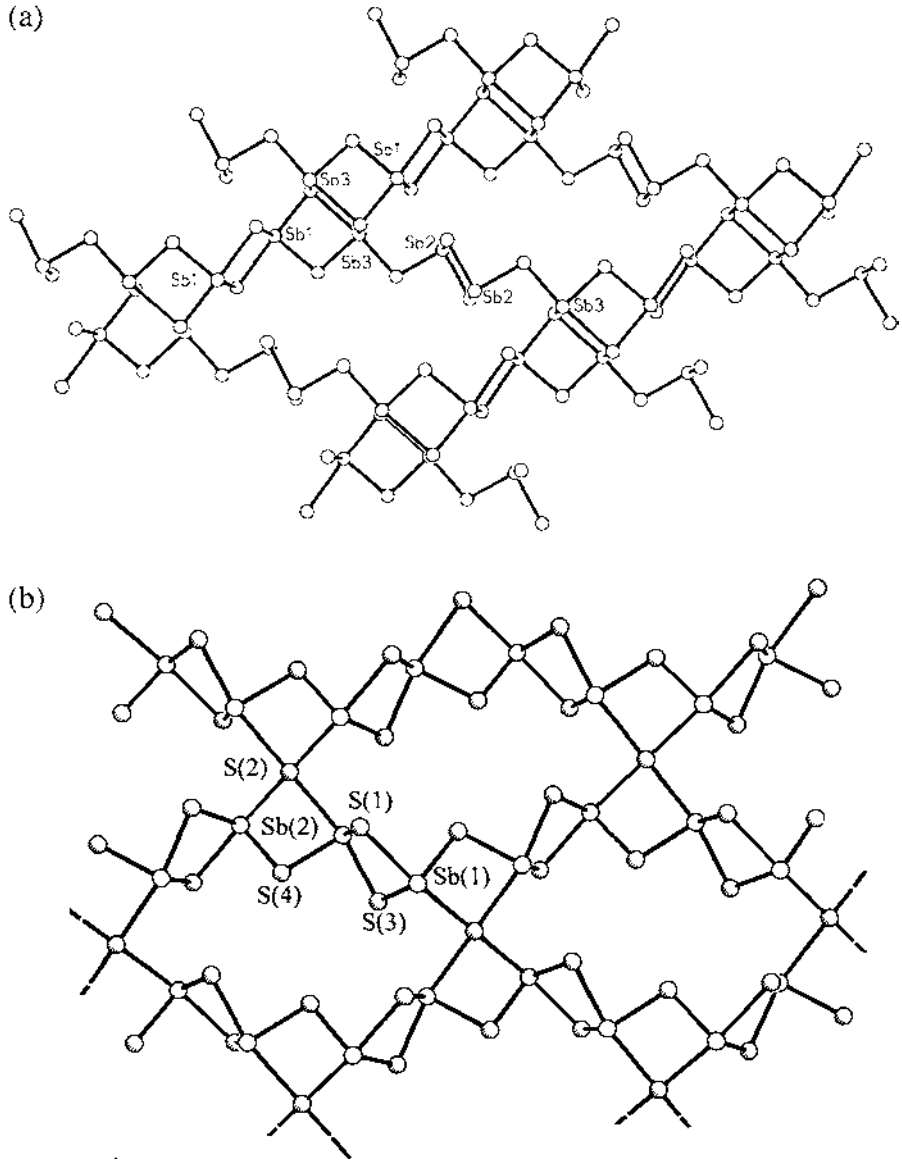

Fig. 49. Ribbons as structural motifs in lamellar thioantimonates: (a) cross-linked $^{1}_{\infty}[Sb_4S_8^{4-}]$ chains in $RbSb_3S_5 \cdot H_2O$ [296]; and (b) $^{1}_{\infty}[SbS_2^{-}]$ chains with bridging μ_4-S atoms in $Rb_2Sb_4S_7$ [296].

sheets with exclusively ψ-SbS_4 trigonal bipyramidal coordination polyhedra (Fig. 49b).

Three other thioantimonates(III) with lamellar $^{2}_{\infty}[Sb_4S_7^{2-}]$ anions have been

prepared hydrothermally, namely the isotypic compounds $A_2Sb_4S_7 \cdot H_2O$ (A = K [297], Rb [298]) and the ethylammonium salt $(C_2H_5NH_3)_2Sb_4S_7$ [300]. In contrast to $Rb_2Sb_4S_7$, the monohydrate $Rb_2Sb_4S_7 \cdot H_2O$ exhibits equal numbers of ψ-SbS_3 tetrahedra and ψ-SbS_4 trigonal bipyramids. Corner linkage of cyclic $[Sb_3S_6]^{3-}$ and monomeric $[SbS_3]^{3-}$ anions in this compound once again affords the structural moiety $[Sb_4S_7]^{2-}$, so typical for chain anions. However, in this case, two such units connect to 12-membered Sb_6S_6 rings, that are then linked into sheets through four-membered Sb_2S_2 rings with ψ-SbS_4 trigonal bipyramidal Sb(III) atoms (Fig. 50a). The structure-directing influence of alkylammonium cations under hydrothermal reaction conditions is particularly apparent for the porous $^2_\infty[Sb_4S_7^{2-}]$ layers in $(C_2H_5NH_3)_2Sb_4S_7$ [300] with their large ellipsoidal 16-membered Sb_8S_8 rings (Fig. 50b). These are joined by chair-shaped Sb_4S_4 rings into ribbons, that are themselves linked together by Sb–S–Sb bridges in such a fashion as to develop suitable channels for the $C_2H_5NH_3^+$ cations. An alterative way of looking at the structure would be to regard it as being composed of $^1_\infty[SbS_2^-]$ chains that are connected through such Sb_4S_4 rings into sheets. N–H ··· S hydrogen bonding appears to be responsible for the assembly of this distinctive anionic network, and, as the authors W. Bensch and M. Schur have pointed out, the deliberate use of such interactions could allow the design of further novel porous thio- and selenidoantimonates(III).

Large Sb_xS_x rings are also characteristic for the highly condensed lammellar thioantimonates(III) of the type $Cs_3Sb_5E_9$ (E = S, Se) [301], $Cs_3Sb_5S_9 \cdot 0.6H_2O$ [302] and $Cs_2Sb_8S_{13}$ [303], that have been assembled solventothermally (CH_3OH, H_2O) in the presence of the large alkali cation Cs^+. For instance, Sb_3E_4 semicubes, composed of two ψ-SbE_5 octahedra and one ψ-SbE_3 tetrahedron, are linked through corner-sharing dipyramidal Sb_2E_5 units into the Sb_6E_6 and $Sb_{10}E_{10}$ rings of the analogous $^2_\infty[Sb_5E_9^{3-}]$ layers in $Cs_3Sb_5E_9$ and $Cs_3Sb_5S_9 \cdot 0.6H_2O$. The $^2_\infty[Sb_8S_{13}^{2-}]$ anionic sheets of $Cs_2Sb_8S_{13}$ and $(C_4H_{10}N)_2Sb_8S_{13} \cdot 0.15H_2O$ [304] contain a striking variety of different ring sizes, namely Sb_2S_2 (in both), Sb_3S_3 (in $Cs_2Sb_8S_{13}$), Sb_4S_4 (in both) Sb_7S_7, Sb_8S_8 (in $Cs_2Sb_8S_{13}$), $Sb_{10}S_{10}$ and $Sb_{18}S_{18}$ [in $(C_4H_{10}N)_2Sb_8S_{13}$].

Both solventothermal and molten salt synthetic techniques have been employed to construct a number of lamellar chalcogenidoantimonates(III) with chainlike E_x^{2-} (E = S, Se) building units. Whereas $Cs_2Sb_4S_8$ [369] was prepared by heating Sb with a Cs_2S_x flux at 280°C, the isostructural selenidoantimonate(III) $Cs_2Sb_4Se_8$ [332] was first isolated by hydrothermal reaction of Cs_2CO_3 with Sb_2Se_3 at 115°C. As depicted in Fig. 51, $^1_\infty[Sb_2Se_4^{2-}]$ ribbons in this compound are joined into infinite sheets through direct Se–Se bonds.

The recently synthesized compounds $K_2Sb_4Se_8$ [370] and $Rb_2Sb_4Se_8$ [371] are isotypic with $Cs_2Sb_4S_8$. Reaction of stoichiometric quantities of Cs_2CO_3, Sb_2S_3 and S_8 in supercritical NH_3 at 160°C leads to the assembly of the unique $^2_\infty[Sb_8S_{18}^{4-}]$ sheets of $Cs_5Sb_8S_{18}(HCO_3)$ [372], in which tricyclic condensed Sb_4S_4 units are joined though Sb–S–Sb bridges into $^1_\infty[Sb_4S_8^{4-}]$ ribbons. These structural motifs are then cross-linked into layers by trisulfide chains S_3^{2-} with shared terminal S atoms; Cs^+ cations and HCO_3^- anions are sited between the anionic networks. β-$CsBiS_2$ [317] crystallizes in the $CsSbS_2$-type. However, in this case, the shortness of the

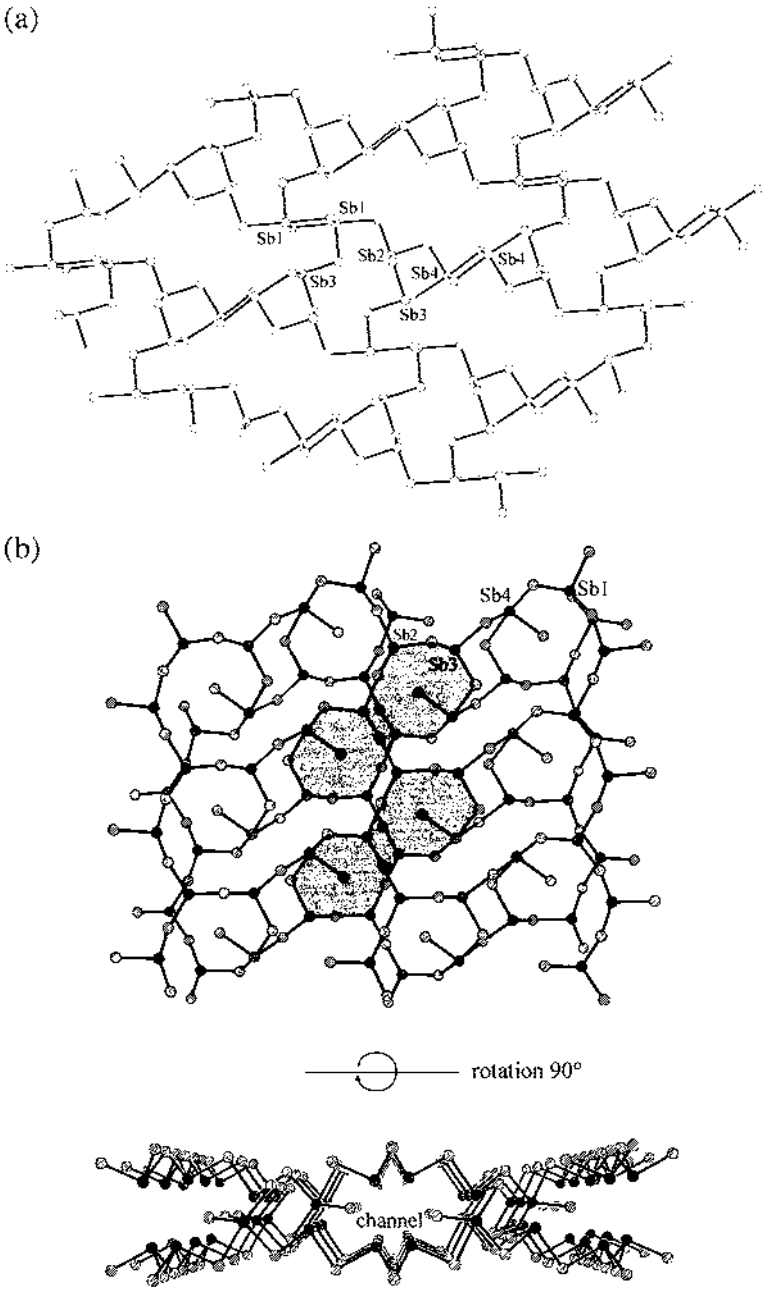

Fig. 50. Sheet structures of $^{2}_{\infty}[Sb_4S_7^{2-}]$ anions: (a) in $A_2Sb_4S_7 \cdot H_2O$ (A = K [297], Rb [298]); and (b) in $(C_2H_5NH_3)_2Sb_4S_7$ [300]; the cavities in (b) are shaded.

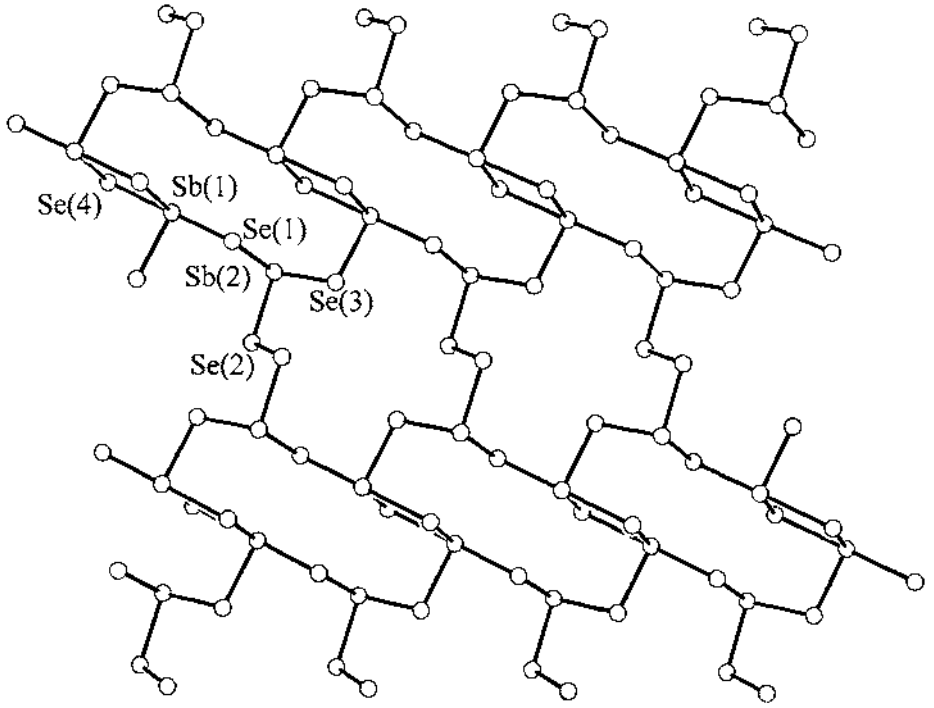

Fig. 51. Structure of the polyanion $^{2}_{\infty}[Sb_4Se_8^{2-}]$ in $A_2Sb_4Se_8$ (A = K [370], Rb [371], Cs [332]).

Bi–S contacts between neighbouring $^{1}_{\infty}[BiS_2^-]$ chains (3.00 vs. 3.125 Å in $CsSbS_2$ [279]) justifies the classification of the polyanions as layers (Fig. 52). As already established for 1-D polymeric anions, other lamellar chalcogenobismuthates(III) are constructed from characteristic BiE_6 octahedra. For instance $SrBiTe_3$ and the isotypic Sb(III) phase, $SrSbTe_3$ [366,367] contain alternating $^{2}_{\infty}[MTe_2^-]$ twofold octahedral sheets and $^{2}_{\infty}[Te^-]$ 4^4 nets in which all tellurium atoms exhibit square-planar coordination (Fig. 53a). The Te–Te distances of 3.279(3) Å in this layer are similar to those of 3.269(2) Å found in the analogous square Te net of $KBa_2[Ag_3Te_3(Te_3)]$ [373,374], whose participating atoms can be assigned a formal charge of 0.667. In contrast to the $^{2}_{\infty}[MTe_2^-]$ sheets of $SrBiTe_3$ and $SrSbTe_3$, that can be regarded as a section of an NaCl-type lattice, Bi_2Te_3- and CdI_2-type fragments are linked together through common edges in the lamellar anionic networks of $Cs_3Bi_7Se_{12}$ [327] (Fig. 53b) and $Sr_4Bi_6Se_{13}$ [324].

4.5. Framework structures

The 3-D thioantimonates(III) listed in Table 7 contain Sb(III) atoms with coordination numbers in the range 3–5. Interestingly, no framework selenidoantimonates(III) appear to have been characterized. Of course, as discussed in Section

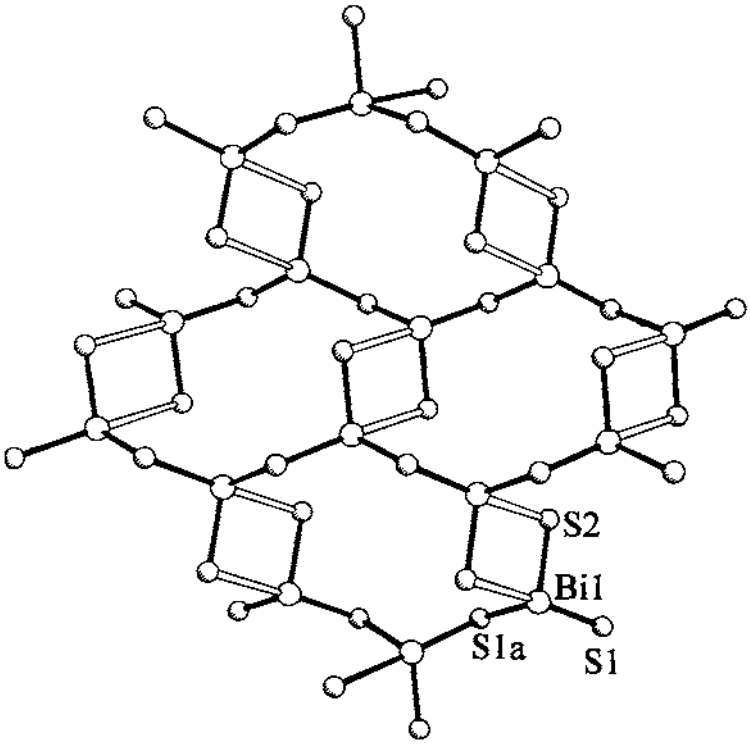

Fig. 52. Layer structure of $^{2}_{\infty}[BiS_2^-]$ in β-$CsBiS_2$ with open bonds for the longer Bi1–S2 distances (3.00 Å) [317].

2.2 and 4.1, any assignment of dimensionality will always be somewhat arbitary in view of the wide range of Sb–E contacts found in such compounds. For instance, on ignoring Sb–S interactions longer than 3.0 Å, it is possible to classify the anionic part of $[H_3N(CH_2)_3NH_3]Sb_{10}S_{16}$ [308] as a double chain $^{1}_{\infty}[Sb_{10}S_{16}^{2-}]$ (Section 4.3). As no new structural motifs are introduced by the 3-D thioantimonates(III) of Table 7, discussion of this class of materials will be restricted to one typical example, $K_2Sb_4S_7$ [306]. In this compound Sb_2S_2-four-membered rings and ψ-SbS_3 tetrahedra link together into chains, that are connected into a framework $^{3}_{\infty}[Sb_4S_7^{2-}]$anion through the terminal sulfur atoms of the latter building blocks (Fig. 54).

Comparison of the structures exhibited by materials with the formula type ABi_3S_5 (A = K [321], Rb [322], Cs [323]) indicates that the void volume in the potassium phase is much larger than for heavier alkali metal cations (Fig. 55a–c). Whereas KBi_3S_5 was synthesized in a Bi/K_2S_x molten flux at 300°C, the other members of this series are products of high temperature fusion reactions. This suggests that the former phase could be metastable and although thermal analysis did not provide any evidence for its conversion to a thermodynamically more stable

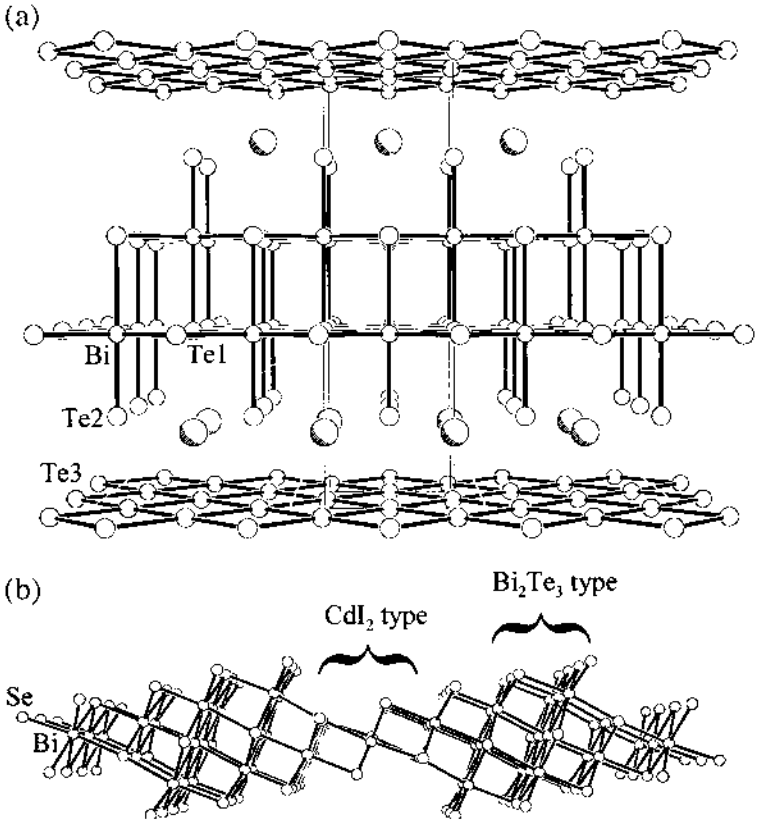

Fig. 53. (a) Structure of $SrBiTe_3$ and isostructural $SrSbTe_3$ [366,367] with alternating $^2_\infty[Bi(Sb)Te_2^-]$ and $^2_\infty(Te_x)^{x-}$ sheets; (b) sheets consisting of Bi_2Te_3- and CdI_2-type fragments in $Cs_3Bi_7Se_{12}$ [327]; similar sheets occur in $Sr_4Bi_6Se_{13}$ [324].

high-temperature modification, it did prove possible to exchange K^+ with Rb^+ cations by solid state reaction with RbCl at temperatures near to 400°C [321]. Metastable β-$RbBi_3S_5$ prepared in this manner undergoes a transformation to the denser α modification discussed above (see Fig. 55).

As for the 1- and 2-D anionic networks in compounds such as $BaBiSe_3$ [59] or $SrBiTe_3$ [366,367] (Section 4.3 and 4.4), typical structural features such as rods or sheets in framework chalcogenobismuthates(III) can generally be related to simple binary solids. For instance, the building blocks in the 3-D $^3_\infty[Bi_8S_{13}^{2-}]$ anions of $K_2Bi_8Se_{13}$ [317] may be regarded as fragments of structures of the CdI_2-, Bi_2Te_3- and Sb_2S_3-types (Fig. 56).

4.6. Quaternary phases

The diversity of Group 15/16 molecular building blocks within the known

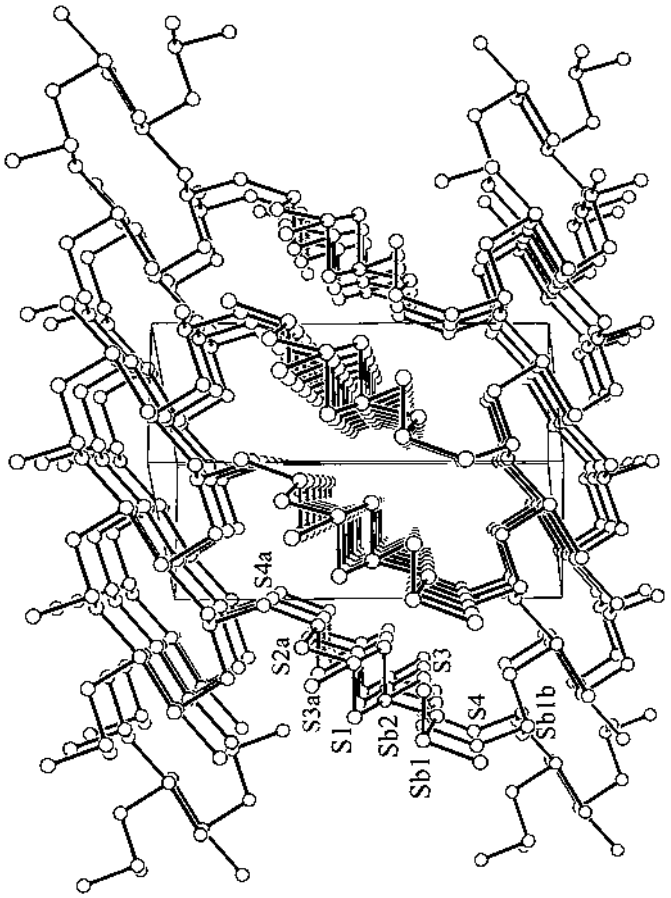

Fig. 54. Framework structure of $K_2Sb_4S_7$ [306].

quaternary phases $A_mM'_xM_yE_z$ contrasts strikingly with the paucity of those formed by Group 14/16 elements in analogous compounds (Section 3.6). Furthermore, a variety of different metals M′ (e.g. Fe, Mn, Cu, Ag, Zn, Hg, Sn, Pb) have been found in Group 15 sulfosalt minerals, which by definition [376] are compounds of the general formula type $M'_xM_yE_z$ with both M′ and M capable of standing for more than one element. Although M′–E interactions are often covalent, as in Stephanite Ag_5SbS_4 [377,378] or Tetrahedrite $Cu_{14}Sb_4S_{13}$ [379,380], M′ can also represent Group 1 or 2 cations for which ionic bonding will predominate. The number of known synthetic quaternary phases $A_mM'_xM_yE_z$ is still surprisingly small in comparison to the numerous examples of ternary compunds $A_mM_yE_z$ considered in the Section 4.2–4.5. However, recent progress in this field has been encouraging and in view of the vast number of known natural sulfosalts and the technological potential of this class of porous materials, it can be expected

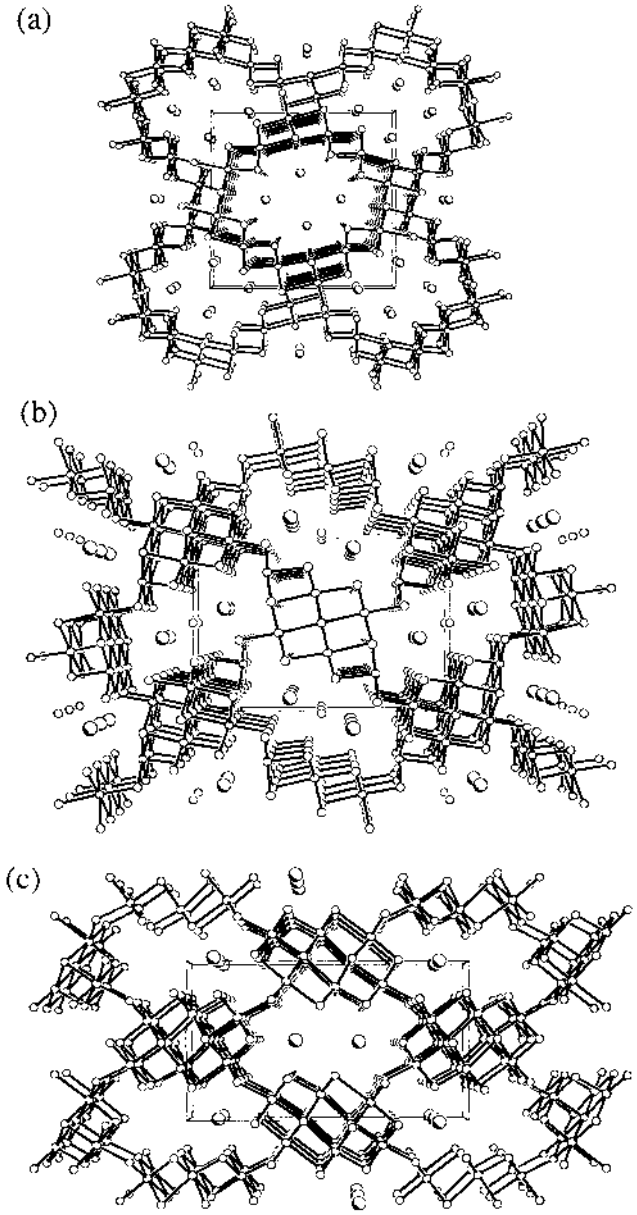

Fig. 55. Comparative view on the structures of thiobismuthates(III) of the same formula type: KBi_3S_5 [321], $RbBi_3S_5$ [322] and $CsBi_3S_5$ [323]. The kinetically stable K-phase possesses much larger channels than the denser Rb- and Cs-phases.

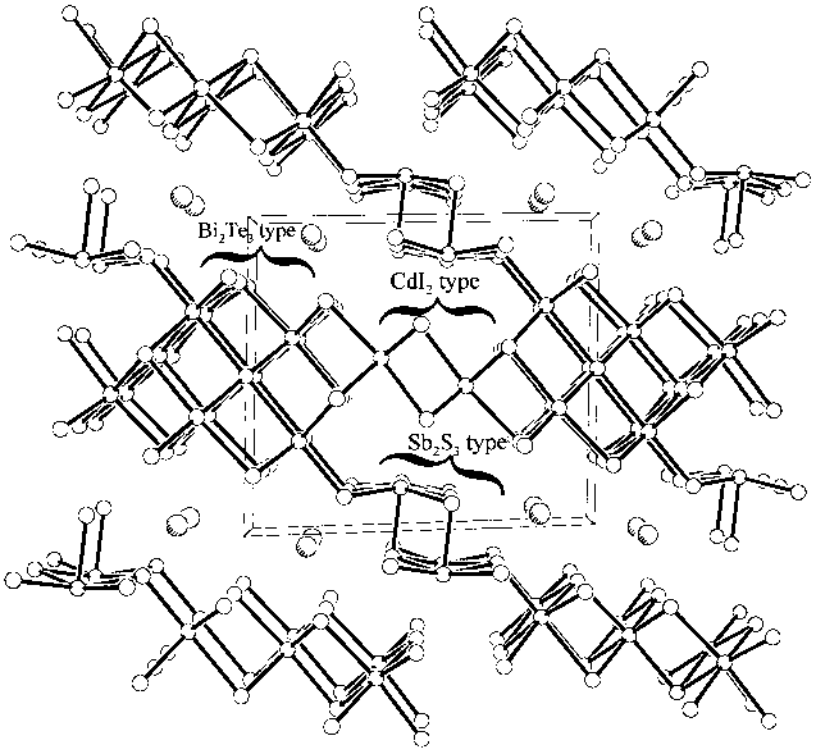

Fig. 56. Schematically presentation of the structural elements of $K_2Bi_8Se_{13}$ [317].

that many new phases will be synthesized in the coming years. As for ternary chalcogenidometalates, quaternary compounds $A_mM'_xM_yE_z$ will be classified in this section according to the nuclearity of their Group 15/16 building units.

4.6.1. Mononuclear building units

Corner bridging of $[ME_3]^{3-}$ pyramids and $M'E_n$ coordination polyhedra is typical for many quaternary phases and allows the construction of a variety 1-, 2- and 3-D anionic networks, examples of which are presented in Table 10. The adoption of a particular structure type and dimensionality will depend on the connectivities of the individual building units. For instance the SbS_3 pyramids in the 2-D anions of $Na_2[CuSbS_3]$ [387] exhibit terminal, μ_2- and μ_3-S atoms (Fig. 57). The average coordination number of the discrete AsS_3 units rises in $K_2[Ag_6(AsS_3)(As_3S_7)]$ [386] to three (μ_2-S, μ_3-S, μ_4-S).

Quaternary chalcogenidoarsenates(V) and -antimonates(V) are unknown in the mineral kingdom and synthetic examples have been found to contain exclusively mononuclear tetrahedral $[ME_4]^{3-}$ units. Solventothermal techniques have been employed for the synthesis of the majority of the compounds listed in Table 11, with supercritical ammonia appearing to be particularly suitable as a reaction

Table 10
Quaternary chalcogenidometalates(III) with the $[ME_3]^{3-}$ pyramidal unit

	d	CN[a] M′/M	N/S[b]
As			
$K[Cu_4(AsS_3)S]$ [384]	3	2, 3, 4	S
$K[Cu_2AsS_3]$ [384]	2	3, 4	S
$TlHgAsS_3$ [382]	2	4	S
$Tl_2Sn(AsS_3)_2$ [383]	2	6	N
$K_2[Ag_6(AsS_3)(As_3S_7)]$ [386]	2	3, 4	S
$(Me_4N)[HgAsSe_3]$ [385]	1	3	S
$(Et_4N)[HgAsSe_3]$ [385]	1	3	S
Sb			
$Na_2[CuSbS_3]$ [387]	2	3	S
$K[HgSbS_3]$ [381]	2	4	S

[a] Coordination number.
[b] Natural/synthetic.

medium. Interestingly some of these phases display connectivity patterns identical to those found in quaternary chalcogenidometalates(IV) of Group 14 elements. For instance, the isotypic compounds $K[Ag_2MS_4]$ (M = As [388], Sb [389]) and $(NH_4)[Ag_2SbS_4]$ [390] all belong to the $Ba[Ag_2GeS_4]$ structure type, with compensation of the higher anion charge in the latter material being achieved by replacement of the monovalent cation through Ba^{2+}. A correlation between cation size and dimensionality of the anion $^{n}_{\infty}[AgSbS_4^{2-}]$ is apparent for the series $A_2[AgSbS_4]$ (Fig. 58). The value of *d* drops from 3 for the smallest cation K^+ over 2 for Rb^+ down to 1 in α-$Cs_2[AgSbS_4]$. This change is accompanied by a reduction in connectivity for the SbS_4 tetrahedra in the latter phase, with one of the participating S atoms no longer bridging to Ag.

The isomeric pyramidal anion $[AsS_4]^{3-}$, in which trivalent arsenic is coordinated by two terminal sulfides and an S_2^{2-} dumb-bell is found in $(Ph_4P)_2K[Pt_3(AsS_4)_3]$ [393]. Respectively, μ_2- and μ_3-bridging modes for these S_x^{2-} ligands enable the construction of chair-shaped Pt_3S_3 rings (Fig. 59a). Analogous $[ME_4]^{3-}$ groups with the same coordination mode are also found in $(Bu^n_4N)_2[Fe_2\{AsTe_2(Te_2)\}_2(CO)_4]$ and $(Ph_4P)_2[Fe_2\{SbSe_2(Se_2)\}_2(CO)_4]$ [394,395], in both of which planar Fe_2E_2 four-membered rings are now formed (Fig. 59b).

The discrete anions in $(Et_4N)[(Cu_7Te)\{AsTe_2(Te_2)\}_3]$ [396] consist of Cu_7Te cubes, whose nine Cu–Cu edges are bridged to As(III) in a μ_3 pattern by each of the nine terminal Te atoms of $[AsTe_2(Te_2)]^{3-}$ pyramids (Fig. 59c).

Whereas a discrete anion of the type $[ME_2(E_2)]^{3-}$ has itself been characterized in the ternary compound $(Bu^n_4N)_3[SbTe_2(Te_2)]$ [224], this is yet to be the case for the next higher member of the pyramidal series, $[ME(E_2)_2]^{3-}$, with its two coordinated E_2^{2-} dumb-bells. However, as illustrated in Fig. 60, such ligands have been stabilized in the quaternary phases $(Et_4N)_3[Cu_4(SbTe_5)(Te_7)]$ [397] (Fig. 60a),

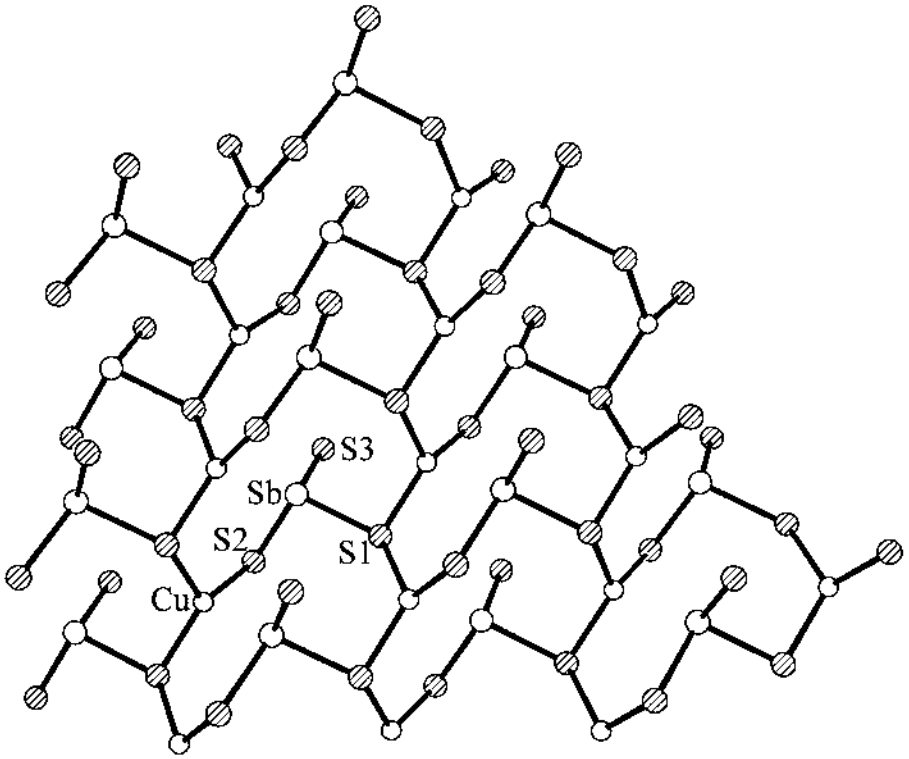

Fig. 57. Sheet structure of Na_2CuSbS_3 [387].

with its bicyclic $CuTe_7$ moiety similar to that in isolated $[MTe_7]^{n-}$ anions [n = 2, M = Zn, Hg [398]; n = 3, M = Ag [399]], $(Bu^n_4N)_2[Mo(AsSe_5)_2]$, $(Bu^n_4N)_2[W(AsSe_5)_2]$ [400,401] (Fig. 60b) and $[W_2(AsSe_5)_2Se_3]$ [401] Fig. 60c).

4.6.2. Dinuclear building units

Corner linkage of two $[ME_3]^{3-}$ pyramids generates the dinuclear $[M_2E_5]^{4-}$ unit, that has been found as a ligand in both isolated and polymeric ternary anions. A series of examples are depicted for $[As_2E_5]^{4-}$ in Fig. 61. All five Se atoms participate in Ag coordination in the hydrothermally synthesized compound $(Me_3NH)[Ag_3As_2Se_5]$ [384] and link, in this fashion, no less than 10 coinage metal atoms through 11 bonds into the sheet anion $^2_\infty[Ag_3As_2Se_5^-]$ shown in Fig. 61a The dipyramidal sulfur analog $[As_2S_5]^{4-}$ is found in $(Ph_4P)_4[Mo_4As_4O_4S_{14}]$ [402], which was prepared by reaction of $(Ph_4P)_2[Mo_2As_4O_2S_{14}]$ (see below) with $(Ph_4P)_2[MoO_2S_2]$ in DMF at room temperature. Two such ligands bridge $Mo_2O_2S_2$ cores to create large $Mo_4As_4S_8$ 16-membered rings in the resulting discrete complex anions. The analogous linkage mode generates wavelike chain anions (Fig. 61b) in the compounds $(R_4N)_2[Mo_2O_2E_2(As_2E_5)]$ (R = Me, E = S; R = Et, E = Se) [403].

Table 11
Quaternary chalcogenidometalates(V) with the tetrahedral $[ME_4]^{3-}$ unit

	d	CN[a] of M′/M
As		
$K[Ag_2AsS_4]$ [388]	3	4/4
$NH_4[Ag_2AsS_4]$ [390]	3	4/4
$(NH_4)_5[Ag_{16}(AsS_4)_7]$ [391]	3	4/4
$K_5[Ag_2(AsSe_4)(As_2Se_5)]$ [386]	2	4/4
$Cs_2[AgAsS_4]$ [392]	1	4/3,4
Sb		
$K[Ag_2SbS_4]$ [389]	3	4/4
$K_2[AgSbS_4]$ [389]	3	4/4
$Rb[Ag_2SbS_4]$ [389]	3	4/4
$Rb_2[AgSbS_4]$ [389]	2	4/4
α-/β-$Cs_2[AgSbS_4]$ [392]	1	4/4
$Cs_3[Ag_2(SbS_2)_2(SbS_4)]$ [392]	1	4/3,4

[a] Coordination number.

Dipyramidal $[Sb_2S_5]^{4-}$ fragments are present in the neutral sheets of both $[Mn_2(Sb_2S_5)(CH_3NH_2)_2]$ and $[Mn_2(Sb_2S_5)\{H_2N(CH_2)_3NH_2\}]$ [404], in which heterocubanes $[Mn_2Sb_2S_4]$ are joined together through bridging sulfur atoms (Fig. 62). Large pores are necessary to accomodate the structure-directing amines, which occupy two sites in the Mn coordination octahedra. The steric requirements of the alkyl groups appear to be responsible for the formation of separated layers, whose structural flexibility is indicated by the successful incorporation of both mono- and bidentate amines. The suitability of $[M_2E_5]^{4-}$ building units for the construction of ternary anionic networks is also documented by their occurence in a number of mineral sulfosalts, e.g. $Tl_2MnAs_2S_5$ [405], Wallisite $TlCuPbAs_2S_5$ [406] or Hatchite, $TlAgPbAs_2S_5$ [407].

A unique structural isomer of $[As_2Se_5]^{4-}$ with a direct As–As bond is present in the methanolothermally synthesized phase $K_5[Ag_2(AsSe_4)(As_2Se_5)]$ [386]. This mixed As(II)/As(IV) dinuclear anion $[As^{II}Se_2As^{IV}Se_3]^{4-}$ connects Ag atoms into infinite chains, that are further linked into sheets by a second building unit, $[As^{V}Se_4]^{3-}$ tetrahedra (Fig. 63).

An unusual $[Sb_2S_6]^{2-}$ ligand has recently been reported by Kolis et al. in the complex cation $[Fe_2(Sb_2S_6)(CO)_6]^{2+}$ [408]. The Sb(III) centers in this dinuclear fragment are bridged in a fourfold manner by two S^{2-} and two S_2^{2-} anions, with the atoms of the latter dumb-bells placed axially in the resulting ψ-SbS_4 trigonal bipyramids. All six sulfur atoms participate in Fe coordination (Fig. 64).

4.6.3. Oligonuclear building units

Further corner condensation of $[ME_3]^{3-}$ pyramids will lead either to cyclic anions $[M_yE_{2y}]^{y-}$ or oligomeric chains $[M_yE_{2y+1}]^{(2+y)-}$. The use of a particular building unit in the construction of ternary polyanions will depend on the subtle

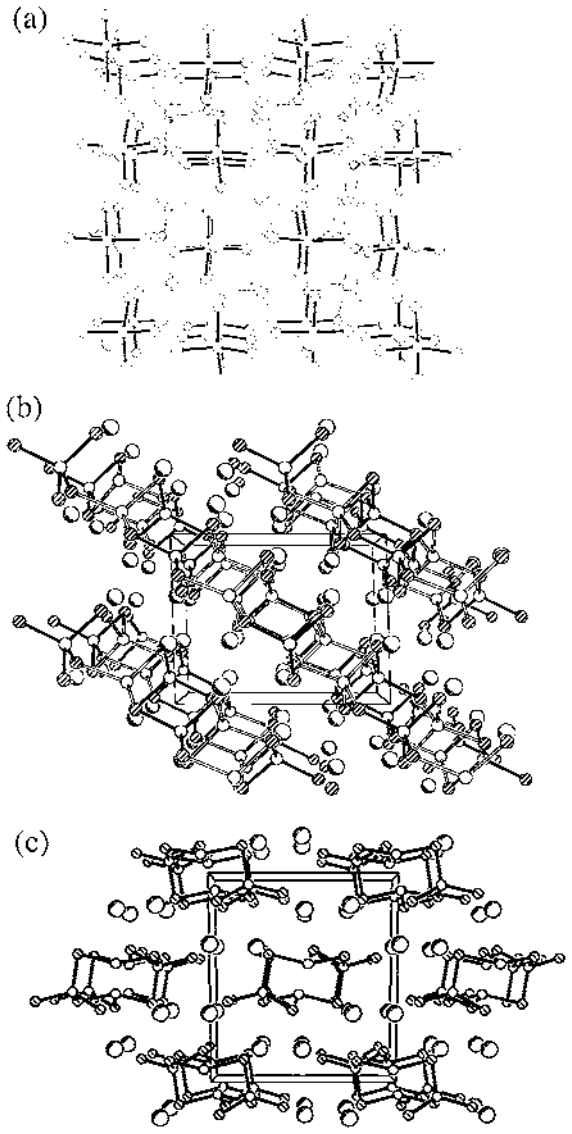

Fig. 58. 3-, 2- and 1-D structures of $A_2[AgSbS_4]$ with A = K, Rb and Cs [388–390].

interplay of reaction parameters such as the size of the structure-directing cation A, the preferred coordination geometry of the second metal M′, temperature, solvent and pH. Although the controlled design of such chalcogenidometalate frameworks still remains an elusive goal, recent exploratory synthetic investigations now provide a solid basis for further work in this field.

Trinuclear $[As_3S_7]^{5-}$ fragments are present in the $^1_\infty[InAs_3S_7^{2-}]$ chains of

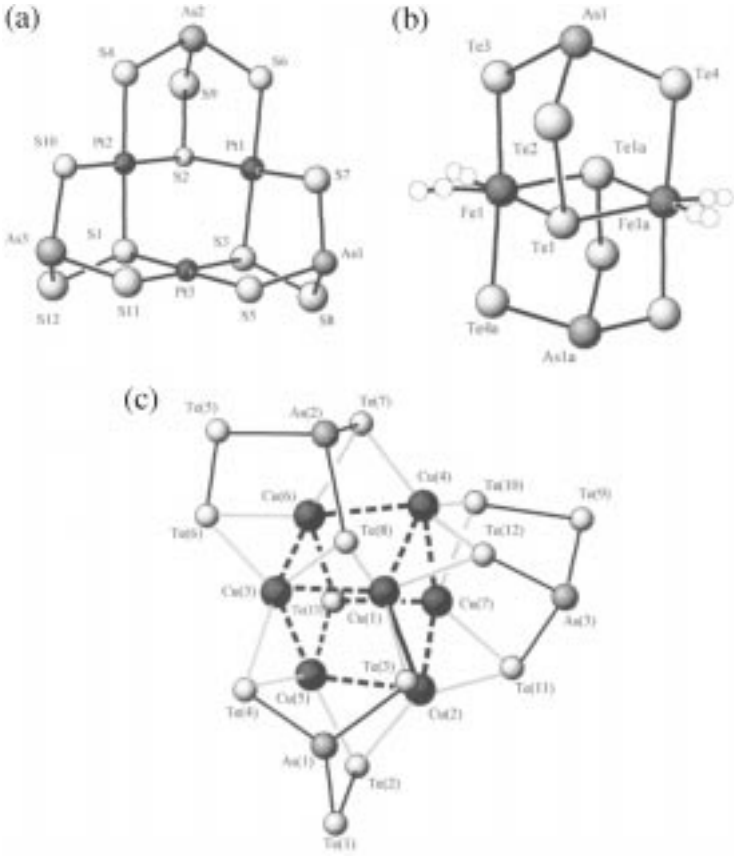

Fig. 59. Different coordination patterns for the $[ME_2(E_2)]^{3-}$ anions in (a) $(Ph_4P)_2K[Pt_3(AsS_4)_3]$ [393], (b) $(Bu^n_4N)_2[Fe_2(CO)_4(AsTe_2(Te_2))_2]$ or $(Ph_4P)_2[Fe_2(CO)_4(SbSe_2(Se_2))_2]$ [394,395] and (c) $(Et_4N)_4[Cu_7Te(AsTe_2(Te_2))_3]$ [396].

$(Ph_4P)_2[InAs_3S_7]$ [409] and the layered anions $^1_\infty[Ag_6(AsS_3)(As_3S_7)]$ of $K_2[Ag_6As_4S_{10}]$ [386], which are depicted in Fig. 65a. The next stage in this condensation process generates the tetrapyramidal building units $[As_4S_9]^{6-}$ of the anion ribbons in $(Ph_4P)_2[Hg_2As_4S_9]$ [410] (Fig. 65b). Related chainlike oligomers have been found in other Group 15 quaternary chalcogenidometalates. For instance, $(Ph_4P)_2[Hg_2As_4Se_{11}]$ [385] contains $[As_4Se_{11}]^{6-}$ fragments, which can be derived from a hypothetical $[As_4Se_9]^{6-}$ anion by substitution of a terminal Se atom on each of the flanking As(III) atoms through Se_2^{2-} dumb-bells (Fig. 65c).

In contrast, the central arsenic atoms of the tetranuclear fragment $[As_4S_8]^{4-}$ in $(Ph_4P)_2[NiAs_4S_8]$ [403] participate in a four-membered As_2S_2 ring with *cis* configuration of the exocyclic substituents (Fig. 66a). All terminal chalcogen atoms are involved in coordination of the metals M′ in these quaternary phases. The suitability of mild solventothermal techniques for the cation-directed assembly of

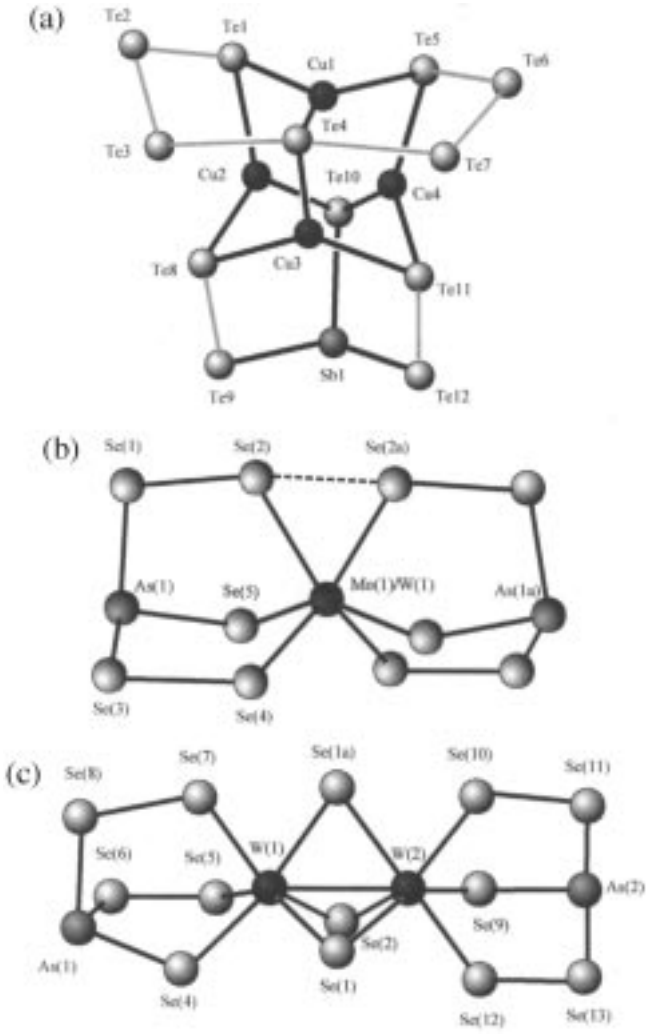

Fig. 60. Coordination patterns for the $[ME(E_2)_2]^{3-}$ anion in (a) $(Et_4N)_3[Cu_4(SbTe_5)(Te_7)]$ [397], (b) $(Bu^n_4N)_2[Mo(AsSe_5)_2]$ or $(Bu^n_4N)_2[W(AsSe_5)_2]$ and (c) $(Ph_4P)_2[W_2(AsSe_5)_2Se_3]$ [401].

such materials is also underlined by the existence of oligomeric building blocks in natural sulfosalts. An interesting example is provided by the mineral Sinnerite, $Cu_{12}As_8S_{18}$, which contains both tri- and pentanuclear linear chains $[As_3S_7]^{5-}$ and $[As_5S_{11}]^{7-}$ (Fig. 65d). The largest known linear oligomeric fragment is present in $Tl_2[Pb_2(As_6S_{12})]$ [411], whose $[As_6S_{12}]^{6-}$ chains contain a central four-membered As_2S_2 ring, which in contrast to $(Ph_4P)_2[NiAs_4S_8]$ adopts the *trans* configuration (Fig. 66b).

In view of their frequent occurence in the ternary Group 15 chalcogenidometa-

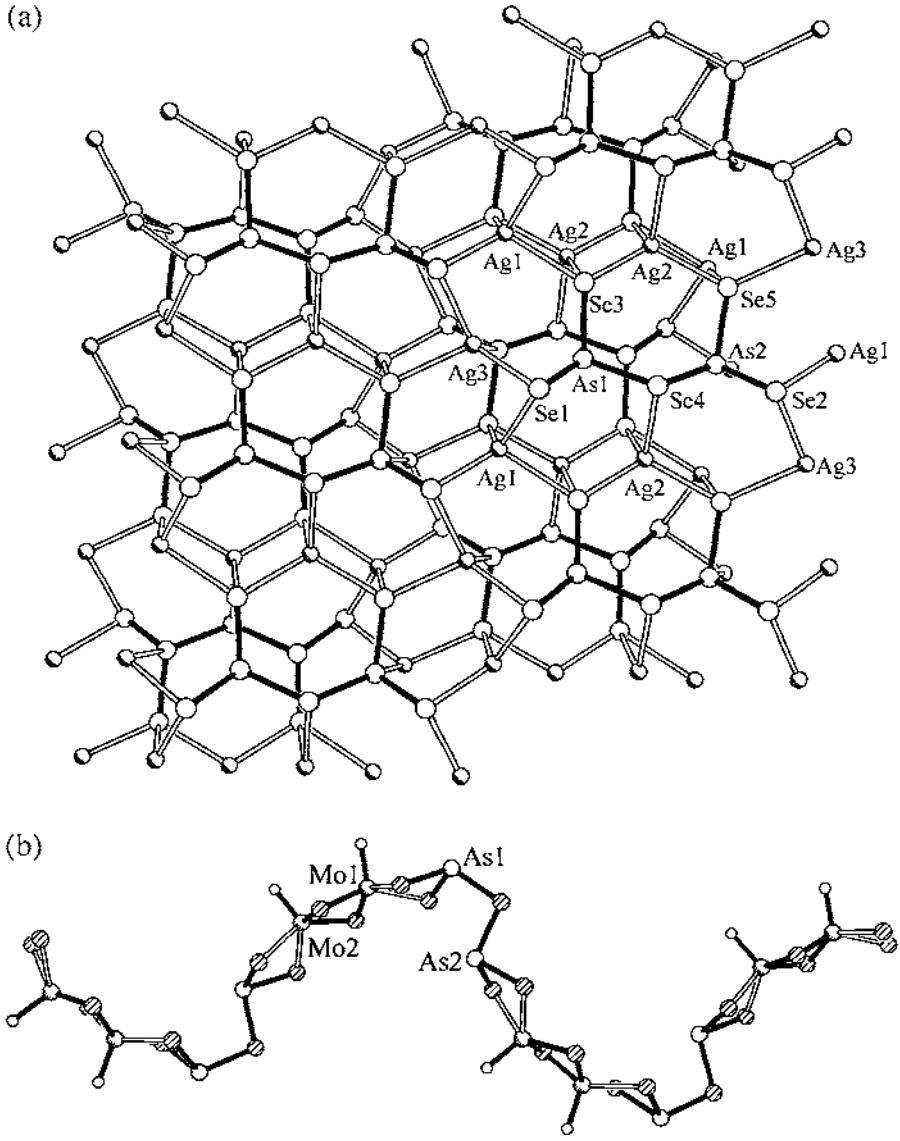

Fig. 61. Examples of the bridging role of the dipyramidal $[M_2E_5]^{4-}$ unit as (a) part of a sheet structure in $(Me_3NH)[Ag_3As_2Se_5]$ [384] and (b) in the linkage of $[Mo_2O_2E_2]$ cores in the chains of $(R_4N)_2[Mo_2O_2E_2(As_2E_5)]$ (R = Me/E = S or R = Et/E = Se) [403].

lates(III) discussed in Section 4.3 and 4.4, it is not surprising that cyclic $[M_3E_6]^{3-}$ anions have also been observed in both synthetic and natural quaternary phases. For instance, the layered $^2_\infty[\{Bi(As_3S_6)_2\}^{3-}]$ anions of $(Me_4N)_2Rb[Bi(As_3S_6)_2]$ [409] display bismuth atoms, that are coordinated in a regular κ^6S octahedral manner

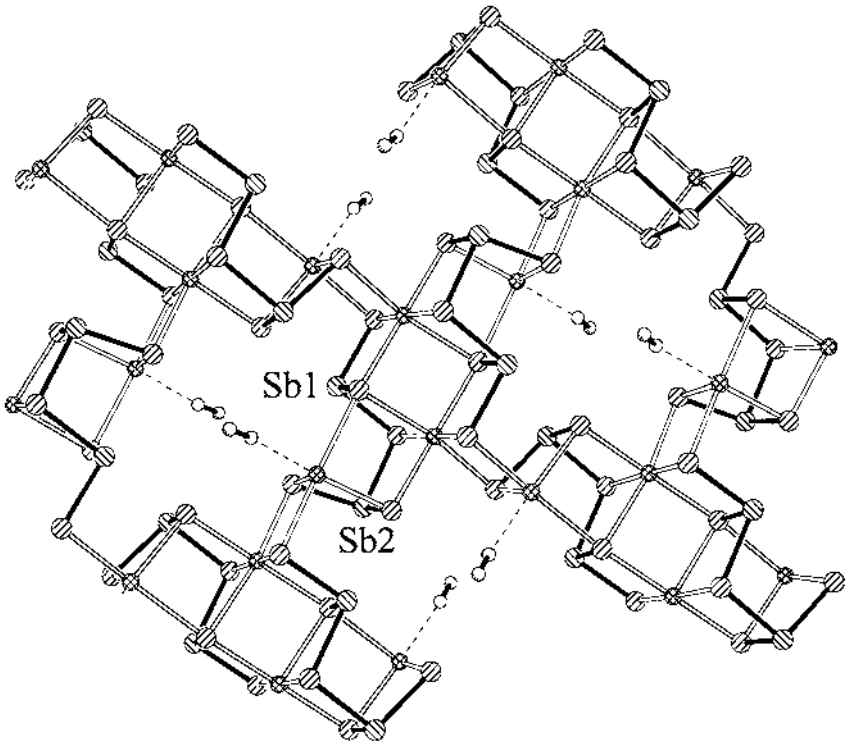

Fig. 62. The neutral sheet structure $^{2}_{\infty}[Mn_2Sb_2S_5]$ in $(CH_3NH_2)_2[Mn_2Sb_2S_5]$ which is similar to that in $(H_2N(CH_2)_3NH_2)[Mn_2Sb_2S_5]$ [404].

(Fig. 66c). Similar chair-shaped $[As_3S_6]^{3-}$ anions join Ag atoms into lamellar $^{2}_{\infty}[Ag_2As_3S_6^-]$ anions in $(NH_4)[Ag_2As_3S_6]$ [391] and this building unit is also present in the mineral Trechmannite, $AgAsS_2$ [413].

An eight-membered As_2S_6 ring has been stabilized in $(Ph_4P)_2[Mo_2O_2S_2(As_4S_{12})]$ [402]. The As atoms occupy the 1,5 positions and share their endocyclic sulfurs with AsS_3 pyramids leading to the formation of $[As_4S_{12}]^{4-}$ fragments, which bridge the dinuclear $[Mo_2O_2S_2]^{2+}$ unit to generate a large 14-membered $Mo_2As_4S_8$ ring (Fig. 66d).

4.6.4. Polymeric chainlike building units

Repeated condensation of $[ME_3]^{3-}$ pyramids will finally result in the assembly of the infinite chains $^{1}_{\infty}[ME_2^-]$, that have been characterized in many ternary chalcogenidometalates(III) (Section 4.3). This structural motif is also present in the quaternary phases $[Co(en)_3][CoSb_4S_8]$ [414] and $Cs_3[Ag_2Sb_3S_8]$ [392]. The first compound was synthesized by reaction of $CoBr_2$ and Na_3SbS_3 in ethylenediamine at 130°C and contains parallel $^{1}_{\infty}[SbS_2^-]$ chains that are linked into $^{2}_{\infty}[\{Co(SbS_2)_4\}^{2-}]$ layers by tetrahedrally coordinated Co(II) atoms (Fig. 67a).

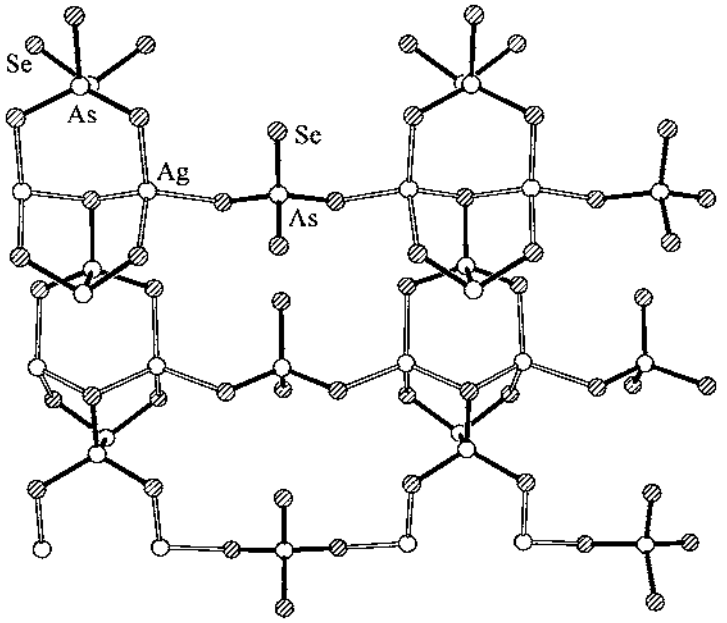

Fig. 63. The mixed As(II)/As(IV) anion $[As_2Se_5]^{4-}$ in $K_5[Ag_2(AsSe_4)(As_2Se_5)]$ [386].

Neighbouring chain sulfur atoms chelate these transition metal atoms to generate small six-membered $CoSb_2S_3$ rings and large 20-membered $Co_2Sb_8S_{10}$ rings, which accomodate the bulky $[Co(en)_3]^{2+}$ countercations. Two such $^1_\infty[SbS_2^-]$ chains are joined by silver atoms in a second compound $Cs_3[Ag_2Sb_3S_8]$ [392], in whose $^1_\infty[Ag_2(SbS_2)_2(SbS_4)]$ chains the coinage metal is also coordinated by $[Sb^VS_4]^{3-}$ tetrahedra. A unique modification of this polymeric structural motif is provided by the branched single chains $[As_3S_6^{3-}]$ of $(Me_4N)[HgAs_3S_6]$ [410], in which every second ribbon As atom shares its terminal sulfur with that of an additional side-chain AsS_3 unit (Fig. 67b).

4.7. Lower oxidation states

4.7.1. Chalcogen-rich anions ($z \geq y$)

Group 15 chalcogenidometalates with direct M–M-bonding can be generated either by controlled oxidation of elemental M or by reduction of a suitable binary M(III) chalcogenide, e.g. As_2Te_3 or Sb_2Te_3. Phases synthesized by the first method include the telluridoarsenates(II) $Na_4As_2Te_4$ and $K_4As_2Te_4$ [415,416], whose dinuclear anions $[As_2Te_4]^{4-}$ are isosteric to the dithionite anion $[S_2O_4]^{2-}$. While $[S_2O_4]^{2-}$ displays a *cis* conformation with a rather long S–S bond, the tellurido anions adopt, respectively, *gauche* and *trans* conformations in their Na^+ and K^+-salts salts (Fig. 68a,b). There are now no repulsive terminal Te ⋯ Te contacts and the central As–As distances lie in the typical range for such bonds [2.481(2)

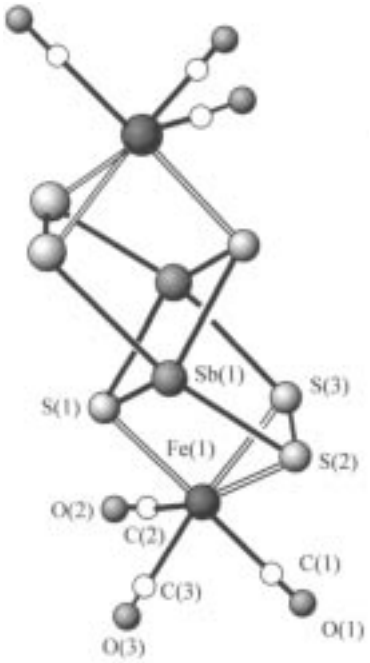

Fig. 64. The $[Sb_2S_6]^{2-}$ anion, acting as a bridging ligand in the cationic cluster $[Fe_2(CO)_6(Sb_2S_6)]^{2+}$ [408].

and 2.475(2) Å, respectively]. The conformational change from *gauche* to *trans* generates larger cavities for the more voluminous K^+ cations of $K_2As_2Te_4$. Dark red crystals of $Rb_4As_2Te_4 \cdot en$ were synthesized by extraction of an alloy of the same nominal composition with ethylenediamine [417] and also contain discrete *trans*-$[As_2Te_4]^{4-}$ anions (Fig. 68b) without significant intermolecular $Te \cdots Te$ contacts between one another.

A derivative of this anion has also been found in the novel compound $Cs_4As_2Te_6$ [418], which can be synthesized by methanolothermal reaction of Cs_2CO_3 with As_2Te_3 at 145°C. The larger Cs^+ cation appears to be responsible for the substitution of a terminal Te^{2-} by a Te_2^{2-} dumb-bell on each of the As atoms (Fig. 68c), which leads to the presence of two significantly different As–Te bonds [2.691(2) to Te_2^{2-} ligands vs. 2.554(2) to terminal tellurium]. Interestingly, these larger $[As_2Te_6]^{4-}$ anions once again adopt a *trans* conformation and are connected through intermolecular secondary $Te \cdots Te$ contacts of 3.489(2) Å into sheets separated by the voluminous Cs^+ ions. The unique dinuclear selenidoarsenate fragment $[As_2Se_5]^{4-}$ participates in the phase $K_5[Ag_2As_3Se_9]$ [386], already discussed in Section 4.6. This mixed As(II)/As(IV) anion $[As^{II}Se_2As^{IV}Se_3]^{4-}$ contains direct As–As bonding between a pyramidally coordinated As(II) and a tetrahedrally coordinated As(IV) center (Fig. 68d).

Many other lower oxidation state phases can be related to this basic $[M_2E_4]^{4-}$

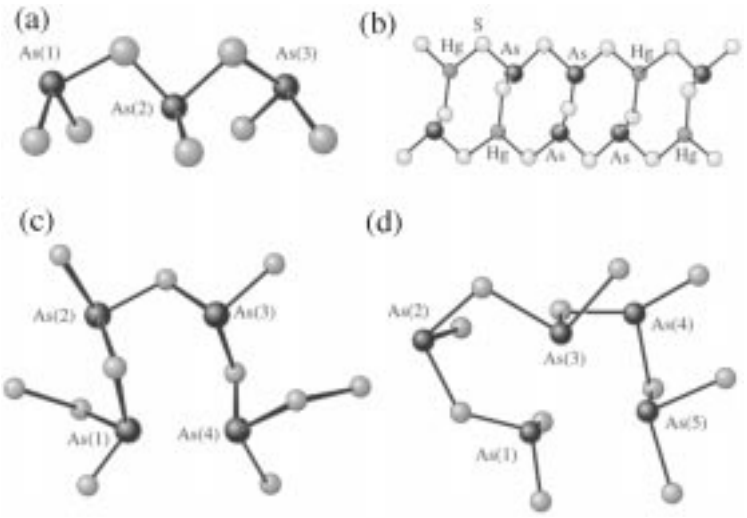

Fig. 65. Examples for oligomeric thio- or selenidoarsenates(III): (a) $[As_3S_7]^{5-}$ anions in $(Ph_4P)_2[InAs_3S_7]$ [409] and $K_2[Ag_6(AsS_3)(As_3S_7)]$ [386]; (b) $[As_4S_9]^{6-}$ anions in $(Ph_4P)_2[Hg_2As_4S_9]$ [410]; (c) $[As_4Se_{11}]^{6-}$ with Se_2^{2-} dumb-bells in $(Ph_4P)_2[Hg_2As_4Se_{11}]$ [385]; and (d) $[As_5S_{11}]^{7-}$ (as well as $[As_3S_7]^{5-}$) in the sulfosalt $Cu_{12}As_8S_{18}$ [412].

building block. For instance, $[Ba(en)_4]_2[As_4Te_6]$ [419], contains two $[As_2Te_4]^{4-}$ anions linked together in an 'head to head'/'tail to tail' fashion through two common Te atoms to create a $[As_4Te_6]^{4-}$ six-membered ring (Fig. 69a). This cyclic system exhibits a chair conformation with the four terminal Te atoms all sited in equatorial positions. The same anion is also present in $(Me_4N)_4As_4Te_6 \cdot 2en$ [37], which was prepared by eletrochemical reduction of an As_2Te_3 electrode in an ethylenediamine solution of $(Et_4N)I$. Contrastingly, a polymeric anion results under similar reaction conditions when the cation source is changed to $(Me_4N)I$. The chain anion $^1_\infty[As_2Te_5^{2-}]$ of the isolated telluridoarsenate $(Me_4N)_2As_2Te_5$ [37] can be regarded as the infinite condensation product of *trans*-$[As_2Te_4]^{4-}$ fragments and square-planar $[TeTe_4]^{6-}$ anions (Fig. 69b) and represents the only known polymeric Group 15/16 compound with M in an oxidation state lower than +III. Such $[TeTe_4]^{6-}$ cross-shaped moieties have often been observed as a characteristic building unit in tellurium-rich tellurides and telluridometalates, e.g. Rb_2Te_5 [422], Cs_2Te_5 [420], Cs_2Te_8 [421], K_2SnTe_5 [135] or Rb_2SnTe_5 [158]. The average Te–Te bond length of 3.05 ± 0.05 Å in such compounds is characteristically lengthened in comparison to the typical distances observed for two-coordinate Te, e.g. 2.78 Å in elemental tellurium [423].

Contrasting conformations have also been observed for discrete anions of the type $[M_4E_6]^{2-}$ (M = As, Sb; E = S, Se) that can be described as the condensation product of two $[ME_3]^{3-}$ ψ-tetrahedra with a central *cis*-$[M_2E_4]^{2-}$ unit. The resulting bicyclic species contain two envelope-like M_3E_2 rings with a common central M–M bond. As the remaining M atoms can take up either an *endo* or an

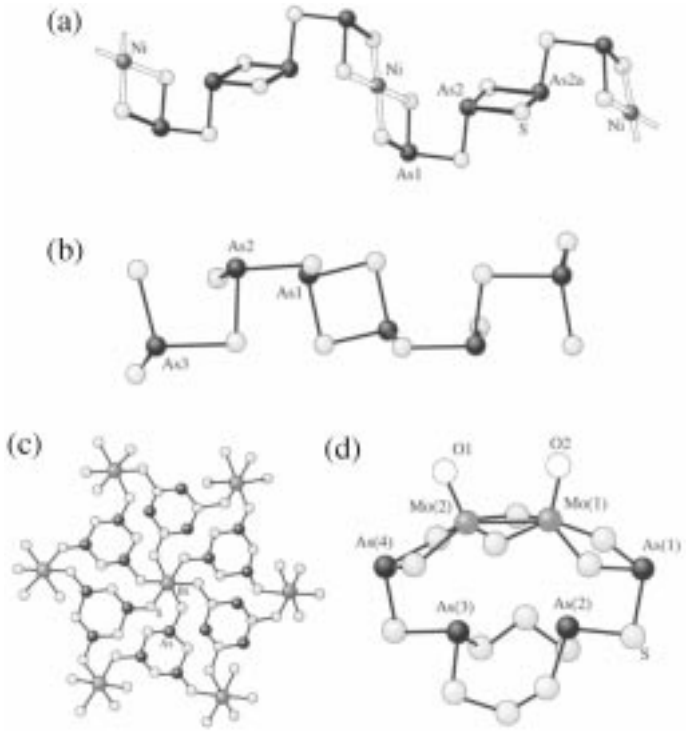

Fig. 66. Cyclic AsS building units in quaternary compounds: (a) $[As_4S_8]^{4-}$ fragments with a central *trans*-As_2S_4 ring in $(Ph_4P)[NiAs_4S_8]$ [403]; (b) a *cis*-As_2S_4 ring in the chain anions $[As_6S_{12}]^{6-}$ of $Tl_2[Pb_2(As_6S_{12})]$ [411]; (c) six-membered $[As_3S_6]^{3-}$ anions in $(Me_4N)_2Rb[BiAs_3S_6]$ [409]; and (d) the eight-membered As_2S_6-ring in $(Ph_4P)_2[Mo_2O_2As_4S_{14}]$ [402], with As atoms occupying the 1,5 positions.

exo-position relative to the central $[M_2E_4]^{2-}$ units, the three conformations shown in Fig. 70a–c are possible. Examples are listed in Table 12.

The *endo–endo* structure can be regarded as being derived from that of α- or β-As_4S_4. Cleavage of an As–As bond in such cage-like molecules by nucleophilic attack of E^{2-} ions at the participating As atoms leads to formation of the basket-like anion depicted in Fig. 70a. It is not clear why this *endo–endo* conformation is only present in As containing anions, whereas corresponding Sb-phases have been found to exhibit the opposite *exo–exo* (Fig. 70b) arrangement. EHMO calculations do, in fact, favor an idealized *endo–endo* conformation for $[Sb_4Se_6]^{2-}$, while no significant energy difference is found for the corresponding selenidoarsenates. The two isomers cannot easily be converted into each other, so it has been suggested that their actual geometries may be directed by the respective synthesis conditions [427]. A mixed *endo–exo* variant (Fig. 70c) has been found in $[K(2,2,2\text{-crypt})]_2As_4Se_6$ [249], which was synthesized by reduction of As_4Se_4 with K in DMF in a manner similar to the corresponding *endo–endo* species $(Ph_4P)_2As_4Se_6$ [424],

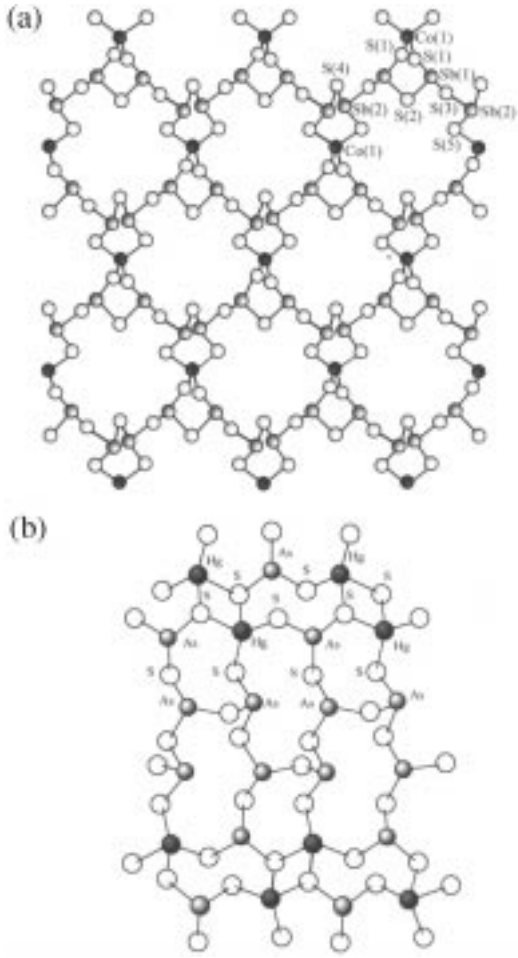

Fig. 67. (a) $^{1}_{\infty}[SbS_2^-]$-chains in $[Co(en)_3][CoSb_4S_8]$ [414] and (b) the unique $[\{AsS_2AsS(AsS_3)\}^{2-}]$ chain in $(Me_4N)[HgAs_3S_6]$ [410].

which was crystallized from NH_3. It is therefore possible that packing effects could in fact be responsible for the adoption of a particular conformation.

When five-membered M_3E_2 rings no longer possess a common M–M edge as in $[M_4E_6]^{2-}$, but are connected through additional M–M bonds, then an $[M_6E_6]^{2-}$ anion with a central M_4 ring will result, as has indeed been found in the thioantimonate $(Ph_4P)_2Sb_6S_6$ [426]. The terminal S atoms are sited above the central ring in this tricyclic species and exhibit short Sb ··· S contacts of 2.934(5) Å, depicted as dashed lines in Fig. 70d. An Sb_4-ring with a distinctly non-planar conformation is present in the electrochemically synthesized phase $(Pr^n_4N)_4Sb_4Te_4$ [39], whose Te atoms adopt equatorial positions (Fig. 70e). The unique isolated

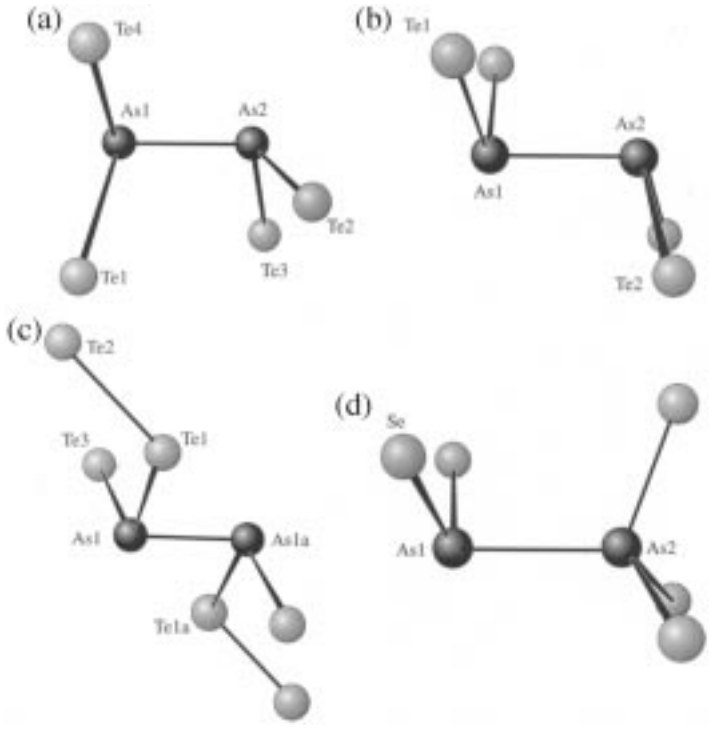

Fig. 68. The building block $[M_2E_4]^{2-}$ as (a) *gauche*-$[As_2Te_4]^{4-}$ in $Na_4As_2Te_4$ [415], (b) *trans*-$[As_2Te_4]^{4-}$ in $K_4As_2Te_4$ [416] or $Rb_4As_2Te_4 \cdot en$ [417], (c) in a derivative *trans*-$[As_2Te_6]^{4-}$ with one Te_2^{2-} dumb-bell on each As atom in $Cs_4As_2Te_6$ [418] and (d) in the mixed As(II)/As(IV) fragment $[As_2Se_5]^{4-}$ of $K_5[Ag_2(AsSe_4)(As_2Se_5)]$ [386].

anion $[Sb_6Te_8]^{2-}$ of $(Et_4N)_4Sb_6Te_9 \cdot 0.5en$ [428] can be derived from the $[Sb_6E_6]^{2-}$ structure (Fig. 70d) by insertion of two Te atoms in the central Sb_4-square so as to construct a Sb_4Te_2 ring with a boat conformation (Fig. 70f). As for $[Sb_6S_6]^{2-}$, weak interactions are present between the terminal chalcogen and central Sb atoms and an additional Te^{2-} ion adopts a remarkable position above the central six-membered ring that is stabilized by four Te ⋯ Sb contacts in the range 3.133–3.229 Å (dashed lines in Fig. 70f). Such an unusual 'presented on a tray' coordination has also been found in $K_4Cu_8Te_{11}$ [429].

4.7.2. Chalcogen-poor anions ($z < y$)

Chalcogenidoarsenates and -antimonates with $z < y$ always contain more than one direct M–M bond. Belin et al. have synthesized red crystals of $(Ph_4P)As_7Se_4$ [430,431] by reduction of As_4Se_4 with Na in ethylenediamine, filtration of the precipitated yellow Na_2Se and subsequent treatment of the filtrate with a $(Ph_4P)Br$ solution. The singly charged cage anion $[As_7Se_4]^-$ consists of a central slightly waved As_5 ring coordinated on both sides by $AsSe_2$ fragments (Fig. 71a). Three of

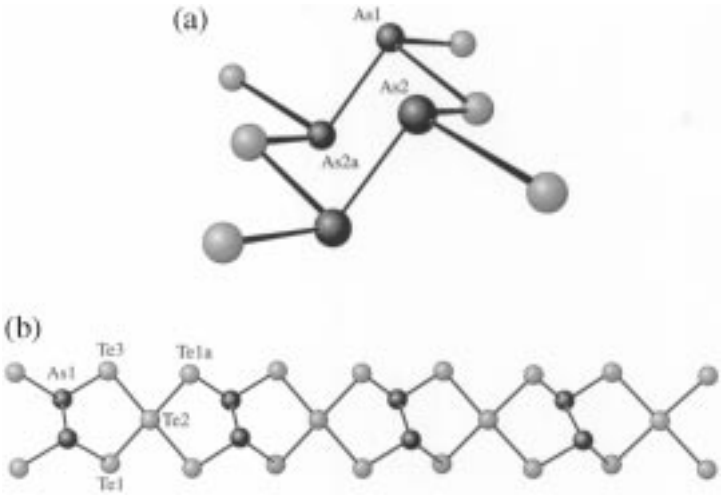

Fig. 69. (a) The oligomeric $[As_4Te_6]^{4-}$ anion in $[Ba(en)_4]_2[As_4Te_6]$ [419] or $(Me_4N)_4[As_4Te_6]\cdot 2en$ [37] and (b) the $^1_\infty[As_2Te_5]^{2-}$ chain in $(Et_4N)_2[As_2Te_5]$ [37] with its characteristic square planar anion $[TeTe_4]^{6-}$.

the five As ring atoms [As(2), As(6), As(7)] display ψ-trigonal bipyramidal coordination spheres with equatorial As–As bonds. Whereas this polyhedron is strongly distorted with strikingly different axial As–Se distances [3.158(3)/3.127(3) Å vs. 2.378(3)/2.383(3) Å] in the first two cases, the corresponding distances of 2.639(3) and 2.734(3) Å in the third ψ-trigonal bipyramid [As(7)] are rather similar. As commented for $(Me_4N)_2As_6S_{10}$ [51] (Section 4.3), a regular coordination sphere of this type is highly unusual for arsenic.

The anion $[Sb_9Te_6]^{3-}$ of the electrochemically synthesized phase $(Pr^n_4N)_3Sb_9Te_6$ [39] can be regarded as a condensation product of two Sb_6Te_3 groups through a common Sb_3 face (Fig. 71b).

Anions of the type $[As_{10}E_3]^{2-}$ seems to represent a rather stable cluster type (Fig. 71c) and are known for all chalcogenides E = S–Te. They have been synthesized by reduction of As_4E_4 (E = S, Se) or As_2Te_3 with elemental K in NH_3 or ethlyenediamine in the presence of Ph_4P^+ (E = Se [432], Te [37,38]) or [K(2,2,2-crypt)]$^+$ [249] (E = S) as the precipitating counterion. As depicted in Fig. 71c–e the cage structures of these species are closely related to that of As_{11}^{3-}. Finally, the

Table 12
The three possible conformations for $[M_4E_6]^{2-}$ anions (M = As, Sb; E = S, Se) (see Fig. 70)

Endo–endo	*Exo–exo*	*Endo–exo*
$(C_5H_{12}N)_2[As_4S_6]$ [425]	$(Ph_4P)_2[As_4Se_6]$ [426]	$[K(2,2,2\text{-crypt})]_2[As_4Se_6]$ [249]
$(Ph_4P)_2[Sb_4S_6]$ [424]	$(Ph_4P)_2[Sb_4Se_6]$ [427,394,395]	

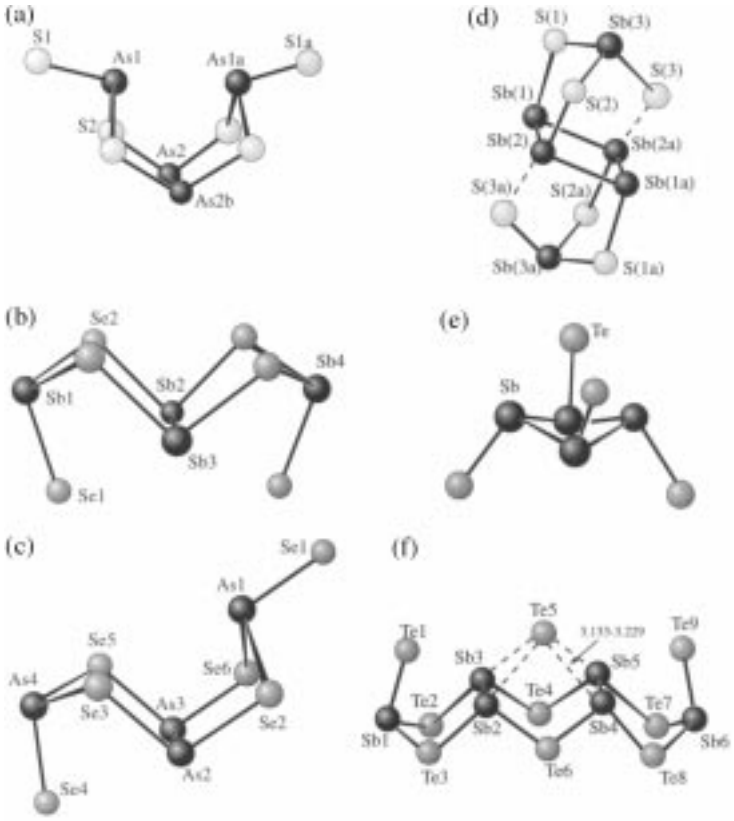

Fig. 70. The three conformations, (a) endo–endo, (b) exo–exo and (c) endo–exo, for the $[M_4E_6]^{2-}$ anion [250,424–426]; (d) the $[Sb_6S_6]^{2-}$ anion in $(Ph_4P)_2[Sb_6S_6]$ [426] with a central square Sb_4 ring; (e) the non-planar Sb_4 ring in the electrochemically synthesized compound $(Pr^n_4N)_4Sb_4Te_4$ [39]; and (f) the $[Sb_6Te_8]^{2-}$ anion in $(Et_4N)_4Sb_6Te_9 \cdot 0.5en$ [428] with its additional Te^{2-} anion sited above the four Sb atoms of the central Sb_4Te_2 ring.

chalcogen-poorest known anion, $[As_{11}Te]^{3-}$ in $[K(2,2,2\text{-crypt})]_3[As_{11}Te] \cdot en$ [434], was synthesized in an analogous fashion by ethylenediamine extraction of a nominal alloy $K_8As_8Te_5$ in the presence of the sequestering agent 2,2,2-crypt. The As–As bonds in the As-rich clusters of $[As_{10}E_3]^{2-}$ and $[As_{11}Te]^{3-}$ range from 2.388 to 2.479 Å and are therefore markedly shorter than in elemental gray arsenic (2.517 Å) [435].

5. Summary and outlook

As reviewed in the current article, a series of guidelines for the use of molecular building blocks in the design of lamellar and framework chalcogenidometalates are

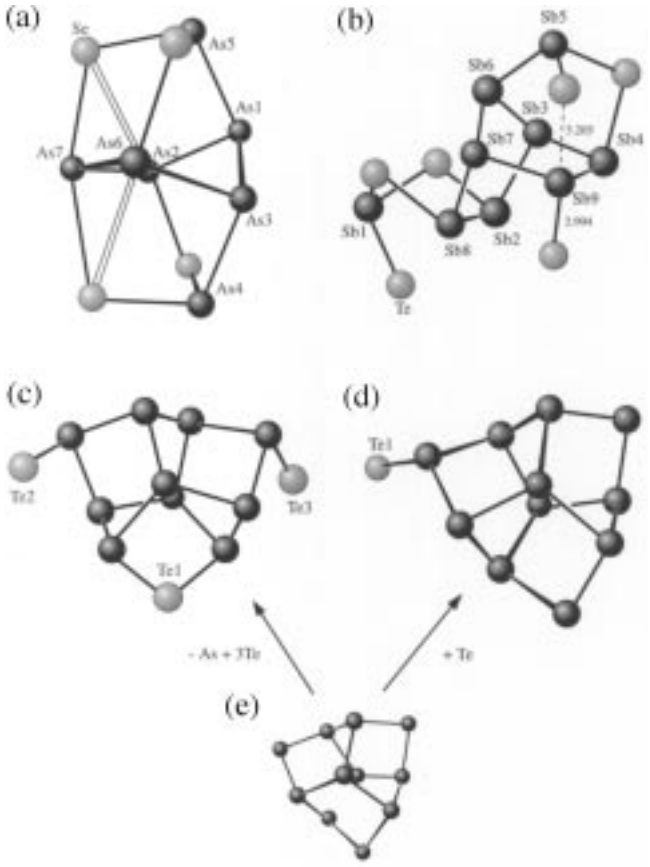

Fig. 71. The anions of the chalcogenide-poor phases (a) $[As_7Se_4]^-$ in $(Ph_4P)As_7Se_4$ [430,431], (b) $[Sb_9Te_6]^{3-}$ in $(Pr^n_4N)_3Sb_9Te_6$ [39], (c) $[As_{10}E_3]^{2-}$ in $(Ph_4P)_2As_{10}Se_3$ [432], $(Ph_4P)_2As_{10}Te_3$ [37,38] and [K(2,2,2-crypt)]$As_{10}S_3$ [249] and (d) $[K(2,2,2\text{-crypt})]_3As_{11}Te \cdot en$ [434]. The anions of (c) and (d) can be derived from (e) As_{11}^{3-} [433].

now beginning to emerge. Mild solventothermal conditions (T = 110–200°C) are particularly suitable for the assembly of such anion networks, in which the dimensions of the resulting channels or cavities are often found to reflect the geometry and size of structure-directing alkali metal or alkylammonium cations. Although underlying correlations between cation volume and the condensation grade c ($c = y/z$), dimensionality d and average M coordination number n of the resulting chalcogenidometalate have been commented upon throughout this review, it is still not generally possible to predict which particular formula or structure type will result even result under carefully controlled reaction conditions.

An increased emphasis on materials with potentially useful ion exchange, molecular recognition, optoelectronic or catalytic properties has become apparent in the

past few years and it is therefore fitting at the end of this review, to once again highlight some of the most promising developments.

5.1. Lamellar thio- and Selenidostannates(IV)

Compounds of the type $A_2Sn_3S_7$ and $A_2Sn_4S_9$ have been shown to exhibit both remarkable network flexibility and stacking variability of their porous sheets. Their structure-property relationships (e.g. optical absorption edge) are sensitive to the identity and adsorption mode of small molecules such as H_2O or CO_2 [124], thereby indicating a potential application of such materials in molecular recognition. Furthermore, as Ozin and co-workers have demonstrated for the series $(Me_4N)_2[Sn_3(S_xS_{1-x})_7]$ [176], the compositional tunability of their electronic band structures could open attractive perspectives for their integration into transistor and diode array-type devices [436,437]. In an extension of this work, the first mesoporous forms of lamellar thiostannates were recently isolated in the presence of a surfactant template [436]. An interlayer spacing of 48.6 Å is indicated by the first most intense reflection in the X-ray powder diffraction diagram of one of these novel phases. Following the original submission of this article, we have been successful in synthesising three further novel porous lamellar selenidostannates(IV) [444], all of which exhibit the formula type $A_4Sn_4Se_{10} \cdot xH_2O$. Whereas the structure of $Cs_4Sn_4Se_{10} \cdot 3.2H_2O$ (Fig. 72) can be derived from that of $Cs_2Sn_2Se_6$ by replacement of the bridging Se_2^{2-} units in Fig. 18 by ditetrahedral $[Sn_2Se_6]^{4-}$ anions, those of $K_4Sn_4Se_{10} \cdot 4.5H_2O$ (Fig. 73) and the isotypic compound $Rb_4Sn_4Se_{10} \cdot 1.5H_20$ are unique for layered selenidostannates(IV) in containing only tetracoordinated Sn atoms. $[SnSe_4]^{4-}$ tetrahedra and $[Sn_2Se_6]^{4-}$ ditetrahedra corner-bridge to construct 36-membered rings of nanometer dimensions (1.29 × 1.41 nm for A = Rb), which thereby represent the largest known pores for this class of compounds.

5.2. Quaternary transition metal / main group chalcogenidometalates

Following up on R.L. Bedard's original patents of 1989 [12,20], the recent synthesis of a variety of 3-D anions $^3_\infty[M'_xM_yE_z]$ (M′ = Transition metal, M = Group 14/15 metal) has once again spotlighted the potential of such zeotype sulfide- and selenide-based networks in ion exchange and molecular recognition. Particular interest has been aroused by the burgeoning family of quaternary chalcogenidogermanates(IV) $A_2[M'Ge_4E_{10}]$ (M′ = Mn, Fe, Cd) and $A_3[AgGe_4S_{10}]$ [189–192], whose zinc blende-like frameworks exhibit a remarkable capacity to accomodate cations of different sizes. The framework $^2_\infty[FeGe_4S_{10}^{2-}]$ in $Cs_2[FeGe_4S_{10}] \cdot xH_2O$ [191] loses physi- and chemisorbed water at, respectively, 116 and 188°C, but remains intact up to 630°C in vacuum, thereby providing encouragement for the technological application of such advanced materials. The research teams of Kanatzidis [4–7] and Kolis [14] have reported considerable recent progress in the neighboring field of quaternary Group 15 chalcogenidometalates (Section 4.6).

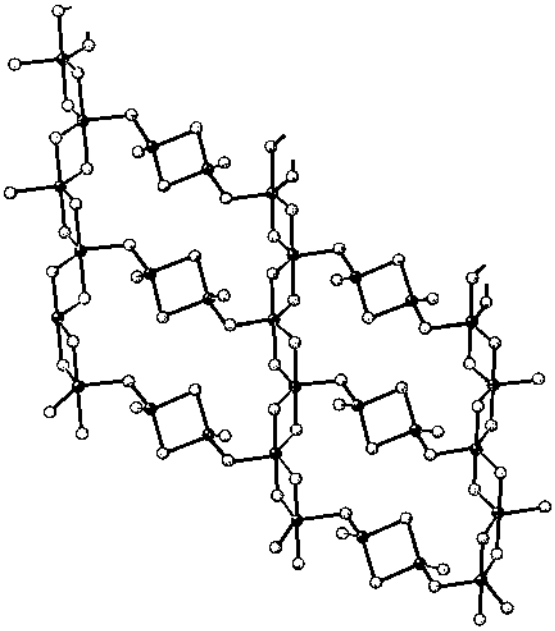

Fig. 72. The sheet structure of $^{2}_{\infty}[Sn_4Se_{10}^{4-}]$ in $Cs_4Sn_4Se_{10} \cdot 3.2H_2O$ [444].

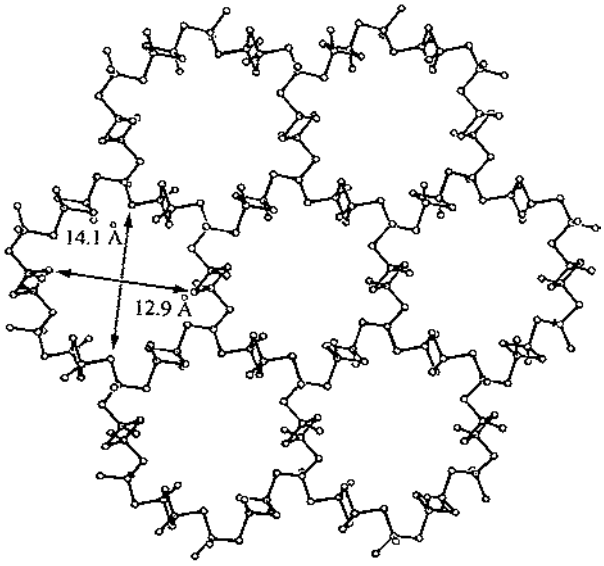

Fig. 73. The open lamellar structure of $^{2}_{\infty}[Sn_4Se_{10}^{4-}]$ in $K_4Sn_4Se_{10} \cdot 4.5H_2O$ and $Rb_4Sn_4Se_{10} \cdot 1.5H_2O$ [444] with its large nanometer-sized 36-membered pores.

5.3. Tellurium-containing phases

In comparison to the lighter congeners S and Se, only relatively few Group 14/15 telluridometalates have been studied. However, the potential of tellurium-rich phases as low-dimensional metals has led to increased interest in such compounds in recent years [185,374]. On the basis of bond structure calculations both the tellurium-rich cesium telluride Cs_3Te_{22} [45,438–440] and the novel telluridostannate(IV) $Rb_{4+x}Sn_4Te_{17}$ ($0 \leq x \leq 1$) [185] are expected to display metallic conductivity. The latter phase (Figs. 20 and 21) represents the first example of a potentially multifunctional porous zeotype framework for this class of materials. Another interesting example of a non-classical Zintl anion is provided by the quaternary chains of $(Et_4N)_4[Au(Ag_{1-x}Au_x)_2Sn_2Te_9]$ ($x = 0.32$) [225] with their Te_3^{3-} fragments as part of a one-dimensional semiconductor.

5.4. Note added in proof

Articles on the following chalcogenidometalates appeared in 1997–98 after completion of this article or were not included in the original version: $(Ph_4P)[Se_5AsSe]$, $(Ph_4P)_2As_2Se_6 \cdot 2CH_3CN$, $(Ph_4P)_2[Se_6SbSe]_2$ [446], $Na_8[Pb_2(Ge_2S_6)_2]$, $Na_8[Sn_2(Ge_2S_6)_2]$ and $Na_8[Pb_2(Si_2Se_6)_2]$ [447]; $K_2[K(2,2,2\text{-crypt})]_2Sn_2Te_6$ and $[K(2,2,2\text{-crypt})]_2Sn_2Te_3$ [448], $K[In(en)_2SnTe_4]$ [449], $[M(NH_3)_6][Cu_8Sb_3S_{13}]$ (M = Mn, Fe, Ni) and $[Fe(NH_3)_6][AgMS_4]$ (M = As, Sb) [450]; $(Et_4N)BiSe_2$ and $[Ge(en)_3](enH)SbSe_4$ [451], $(Ph_4P)_4Sn_6Se_{21}$, $(Ph_4P)_4[Sn_3Se_{11}]_2$, $(Ph_4P)_2[Sn(Se)_4(Se_6)_2]$ [452], $(Ph_4P)_3Sb_3S_{25}$, $(Ph_4P)_2Sb_2S_{15} \cdot 2C_3N_2H_6$ [453], Li_4GeS_4 [454], $(Et_4N)_2As_2Se_6$, $(enH)AsSe_6 \cdot 2,2,2\text{-crypt}$, $(Et_4N)AsSe_8$, $[In(en)_2\{SeAs(Se)Se_2\}] \cdot en$ [455], $Cs_2Sn_2Se_6$ [456] and $RbCuSb_2Se_4 \cdot H_2O$ [457].

Acknowledgements

We would like to thank all co-workers directly involved in our own research efforts in this field over the period 1985–1998, in particular Dr Jürgen Kaub, Dr Hans-Joachim Häusler, Dr Hans Georg Braunbeck, Dr Bernhard Schaaf, Dipl.-Chem. Anja Loose and Dipl.-Chem. Viola Vater. We are also indebted to Professors W. Bensch, M.G. Kanatzidis, F. Liebau and G.A. Ozin for providing us with their unpublished results.

References

[1] D.W. Breck, Zeolite Molecular Sieves, Wiley, New York, 1984.
[2] H. van Bekkum, E.M. Flanigen, J.C. Jansen (Eds.), Introduction to Zeolite Science and Practice, Elsevier, Amsterdam, 1991.
[3] M.E. Davis, R.F. Lobo, Chem. Mater. 4 (1992) 756.
[4] M.G. Kanatzidis, Chem. Mater. 2 (1990) 353.

[5] Y. Park, J.-H. Liao, K.-W. Kim, M.G. Kanatzidis, in: J.F. Harrod, R.M. Laine (Eds.), Inorganic and Organometallic Oligomers and Polymers, Kluwer, Dordrecht, 1991, p. 263.
[6] M.G. Kanatzidis, Phosphorus, Sulfur, Silicon Relat. Elem. 93 (1994) 159.
[7] M.G. Kanatzidis, A.C. Sutorik, Prog. Inorg. Chem. 43 (1995) 151.
[8] A. Rabenau, Angew. Chem. Int. Ed. Engl. 24 (1985) 1026.
[9] H. Schäfer, Annu. Rev. Mater. Sci. 15 (1985) 1.
[10] W.S. Sheldrick, M. Wachhold, Angew. Chem. Int. Ed. Engl. 36 (1997) 206.
[11] B. Krebs, Angew. Chem. Int. Ed. Engl. 22 (1983) 113.
[12] R.L. Bedard, S.T. Wilson, L.D. Vail, J.M. Bennett, E.M. Flanigen, in: P.A. Jacobs, R.A. van Santen (Eds.), Zeolites: Facts, Figures, Future, Elsevier, Amsterdam, 1989, p. 375.
[13] C.L. Bowes, G.A. Ozin, Adv. Mater. 8 (1996) 13.
[14] G.W. Drake, J.W. Kolis, Coord. Chem. Rev. 137 (1994) 131.
[15] M.G. Kanatzidis, S.-P. Huang, Coord. Chem. Rev. 130 (1994) 509.
[16] W. Mark, O. Lindqvist, J.C. Jumas, E. Philippot, Acta Crystallogr., Sect. B 30 (1974) 2620.
[17] W. Schiwy, C. Blutau, D. Gäthje, B. Krebs, Z. Anorg. Allg. Chem. 412 (1975) 1.
[18] O.M. Yaghi, Z. Sun, D.A. Richardson, T.L. Groy, J. Am. Chem. Soc. 116 (1994) 807.
[19] H. Schäfer, K. Volk, B. Eisenmann, Fifth European Crystallographic Meeting, Copenhagen, Colected Abstracts, (1979) 0–52.
[20] J.D. Corbett, Chem. Rev. 85 (1985) 383.
[21] C.J. Warren, R.C. Haushalter, A.B. Bocarsly, J. Alloys Compd. 229 (1995) 175.
[22] S.A. Sunshine, J.A. Ibers, J. Am. Chem. Soc. 109 (1987) 6202.
[23] B. Eisenmann, E. Kieselbach, H. Schäfer, H. Schrod, Z. Anorg. Allg. Chem. 516 (1984) 49.
[24] B. Eisenmann, J. Hansa, H. Schäfer, Mater. Res. Bull. 20 (1985) 1339.
[25] G. Dittmar, Z. Anorg. Allg. Chem. 453 (1978) 68.
[26] C. Brinkmann, B. Eisenmann, H. Schäfer, Z. Anorg. Allg. Chem. 517 (1984) 143.
[27] B. Eisenmann, H. Schwerer, H. Schäfer, Mater. Res. Bull. 18 (1983) 1189.
[28] G. Eulenberger, J. Less-Common Met. 108 (1985) 65.
[29] K.O. Klepp, F. Fabian, Z. Naturforsch. Teil B 47 (1992) 406.
[30] K.O. Klepp, F. Fabian, Z. Kristallogr. Suppl. 8 (1994) 626.
[31] M. Björgvinsson, H.P.A. Mercier, K.M. Mitchell, G.J. Schrobilgen, G. Strobe, Inorg. Chem. 32 (1993) 6046.
[32] M. Björgvinsson, J.F. Sawyer, G.J. Schroilgen, Inorg. Chem. 26 (1987) 741.
[33] M. Björgvinsson, J.F. Sawyer, G.J. Schrobilgen, Inorg. Chem. 30 (1991) 2231.
[34] C.-W. Park, R.J. Salm, J.A. Ibers, Can. J. Chem. 73 (1995) 1148.
[35] J.E. Iglesias, H. Steinfink, Acta Crystallogr., Sect. B 29 (1973) 1480.
[36] S. del Bucchia, J.C. Jumas, M. Maurin, Acta Crystallogr., Sect. B 36 (1980) 2935.
[37] C.J. Warren, R.C. Haushalter, A.B. Bocarsly, Chem. Mater. 6 (1994) 780.
[38] R.C. Haushalter, J. Chem. Soc., Chem. Commun., (1987) 196.
[39] C.J. Warren, D.M. Ho, R.C. Haushalter, A.B. Bocarsly, Angew. Chem. Int. Ed. Engl. 32 (1993) 1646.
[40] H. Gerl, B. Eisenmann, P. Roth, H. Schäfer, Z. Anorg. Allg. Chem. 407 (1974) 135.
[41] G. Dittmar, H. Schäfer, Z. Anorg. Allg. Chem. 439 (1978) 212.
[42] R. Zagler, B. Eisenmann, Z. Kristallogr. 183 (1988) 193.
[43] P. Böttcher, Angew. Chem. Int. Ed. Engl. 27 (1988) 759.
[44] W.S. Sheldrick, B. Schaaf, Z. Naturforsch., Teil B 49 (1994) 993.
[45] W.S. Sheldrick, M. Wachhold, Angew. Chem. Int. Ed. Engl. 34 (1995) 450.
[46] B. Schreiner, K. Dehnicke, K. Maczek, D. Fenske, Z. Anorg. Allg. Chem. 619 (1993) 1414.
[47] D. Fenske, G. Kräuter, K. Dehnicke, Angew. Chem. Int. Ed. Eng. 29 (1990) 390.
[48] B. Krebs, E. Lührs, L. Stork, R. Willmer, Abstr. Pap. Congr. Int. Union Crystallogr., Perth, Australia, 1987, pp. 08.2–5.
[49] M.G. Kanatzidis, S.-P. Huang, Inorg. Chem. 28 (1989) 4667.
[50] B. Krebs, E. Lührs, R. Willmer, F.-P. Ahlers, Z. Anorg. Allg. Chem. 592 (1991) 17.
[51] V. Vater, W.S. Sheldrick, Z. Naturforsch., Teil B 52 (1997) 1119.
[52] W.S. Sheldrick, J. Kaub, Z. Naturforsch., Teil B 40 (1985) 571.

[53] W.S. Sheldrick, J. Kaub, Z. Naturforsch., Teil B 40 (1985) 1130.
[54] W.S. Sheldrick, Z. Anorg. Allg. Chem. 562 (1988) 23.
[55] W.S. Sheldrick, H.G. Braunbeck, Z. Naturforsch., Teil B 45 (1990) 1643.
[56] W.S. Sheldrick, B. Schaaf, Z. Naturforsch., Teil B 49 (1994) 57.
[57] W.S. Sheldrick, H.-J. Häusler, Z. Anorg. Allg. Chem. 557 (1988) 98.
[58] A. Bondi, J. Phys. Chem. 68 (1964) 441.
[59] K. Volk, G. Cordier, R. Cook, H. Schäfer, Z. Naturforsch., Teil B 35 (1980) 136.
[60] F. Liebau, Structural Chemistry of Silicates, Structure, Bonding and Classification, Springer, Heidelberg, 1985.
[61] R.D. Shannon, C.T. Prewitt, Acta Crystallogr., Sect. B 25 (1969) 925.
[62] S. Pohl, W. Schiwy, N. Weinstock, B. Krebs, Z. Naturforsch., Teil B 28 (1973) 565.
[63] J. Olivier-Fourcade, J.C. Jumas, M. Ribes, E. Philippot, M. Maurin, J. Solid State Chem. 23 (1978) 155.
[64] G. Eulenberger, Z. Kristallogr. 145 (1977) 427.
[65] B. Krebs, H.J. Jacobsen, Z. Anorg. Allg. Chem. 421 (1976) 97.
[66] K.O. Klepp, Z. Naturforsch, Teil B 40 (1985) 878.
[67] B. Krebs, S. Pohl, W. Schiwy, Z. Anorg. Allg. Chem. 393 (1972) 241.
[68] G. Eulenberger, Acta Crystallogr., Sect. B 34 (1978) 2614.
[69] C.-W. Park, M.A. Pell, J.A. Ibers, Inorg. Chem. 35 (1996) 4555.
[70] B. Krebs, H. Müller, Z. Anorg. Allg. Chem. 496 (1983) 47.
[71] B. Eisenmann, J. Hansa, Z. Kristallogr. 203 (1993) 301.
[72] G. Eulenberger, Monatsh. Chem. 113 (1982) 859.
[73] J.C. Jumas, J. Olivier-Fourcade, F. Vermot-Gaud-Daniel, M. Ribes, E. Philippot, M. Maurin, Rev. Chim. Minér. 11 (1974) 13.
[74] B. Eisenmann, J. Hansa, H. Schäfer, Rev. Chim. Minér. 23 (1986) 8.
[75] E. Philippot, M. Ribes, O. Lindqvist, Rev. Chim. Minér. 8 (1971) 477.
[76] M. Ribes, J. Olivier-Fourcade, E. Philippot, M. Maurin, J. Solid State Chem. 8 (1973) 195.
[77] S. Pohl, B. Krebs, Z. Anorg. Allg. Chem. 424 (1976) 265.
[78] B. Krebs, S. Pohl, Z. Naturforsch., Teil B 26 (1971) 853.
[79] G. Eulenberger, Acta Crystallogr., Sect. B 32 (1976) 3059.
[80] J.Y. Pivan, O. Achak, M. Louër, D. Louër, Chem. Mater. 6 (1994) 827.
[81] B. Eisenmann, J. Hansa, Z. Kristallogr. 205 (1993) 325.
[82] B. Eisenmann, J. Hansa, Z. Kristallogr. 206 (1993) 101.
[83] W.S. Sheldrick, B. Schaaf, Z. Naturforsch., Teil B 50 (1995) 1469.
[84] W.S. Sheldrick, B. Schaaf, Z. Naturforsch., Teil B 49 (1994) 655.
[85] G. Eulenberger, Z. Naturforsch., Teil B 36 (1981) 523.
[86] H.-J. Wallstab, Dissertation, Universität Bielefeld, 1979.
[87] J. Olivier-Fourcade, E. Philippot, M. Ribes, M. Maurin, Rev. Chim. Minér. 9 (1972) 757.
[88] B. Eisenmann, J. Hansa, H. Schäfer, Z. Naturforsch., Teil B 40 (1985) 450.
[89] D.M. Nellis, Y. Ko, K. Tan, S. Koch, J.B. Parise, J. Chem. Soc., Chem. Commun., (1995) 541.
[90] B. Eisenmann, J. Hansa, H. Schäfer, Rev. Chim. Minér. 21 (1984) 817.
[91] W. Schiwy, S. Pohl, B. Krebs, Z. Anorg. Allg. Chem. 402 (1973) 77.
[92] J.C. Jumas, F. Vermot-Gaud-Daniel, E. Philippot, Cryst. Struct. Commun. 2 (1973) 157.
[93] J.C. Jumas, E. Philippot, F. Vermot-Gaud-Daniel, M. Ribes, M. Maurin, J. Solid State Chem. 14 (1975) 319.
[94] K.O. Klepp, F. Fabian, Z. Kristallogr., Suppl. 9 (1995) 189.
[95] K.O. Klepp, Z. Naturforsch., Teil B 39 (1984) 705.
[96] Y. Piffard, M. Tournoux, A.-L. Ajavon, R. Eholie, Rev. Chim. Minér. 21 (1984) 21.
[97] B. Krebs, H.-U. Hürter, Z. Anorg. Allg. Chem. 462 (1980) 143.
[98] B. Krebs, H. Uhlen, Z. Anorg. Allg. Chem. 549 (1987) 35.
[99] K.O. Klepp, Z. Naturforsch., Teil B 47 (1992) 411.
[100] G. Akinocho, P. Houenou, S. Oyetola, et al., J. Solid State Chem. 93 (1991) 336.
[101] J. Campbell, L.A. Devereux, M. Gerken, H.P.A. Mercier, A.M. Pirani, G.J. Schrobilgen, Inorg. Chem. 35 (1996) 2945.

[102] H. Borrmann, A.M. Pirani, G.J. Schrobilgen, Acta Crystallogr., Sect. C 53 (1997) 1004.
[103] B. Eisenmann, J. Hansa, Z. Kristallogr. 203 (1993) 299.
[104] W.S. Sheldrick, B. Schaaf, Z. Anorg. Allg. Chem. 620 (1994) 1041.
[105] W.S. Sheldrick, H.G. Braunbeck, Z. Naturforsch., Teil B 44 (1989) 851.
[106] S. Jaulmes, P. Houenou, Mater. Res. Bull. 15 (1980) 911.
[107] B. Krebs, W. Schiwy, Z. Anorg. Allg. Chem. 398 (1973) 63.
[108] J.C. Jumas, J. Olivier-Fourcade, F. Vermot-Gaud-Daniel, M. Ribes, E. Philippot, M. Maurin, Rev. Chim. Minér. 11 (1974) 13.
[109] B. Eisenmann, J. Hansa, Z. Kristallogr. 203 (1993) 297.
[110] B. Eisenmann, J. Hansa, Z. Kristallogr. 203 (1993) 303.
[111] W.S. Sheldrick, Z. Naturforsch., Teil B 43 (1988) 249.
[112] J. Campbell, D.P. DiCiommo, H.P.A. Mercién, A.M. Pirani, G.J. Schrobilgen, M. Willuhn, Inorg. Chem. 34 (1995) 6265.
[113] A. Loose, W.S. Sheldrick, unpublished results.
[114] A. Loose, W. S. Sheldrick, Z. Naturforsch., Teil B 53 (1998) 349.
[115] K.O. Klepp, Monatsh. Chem. 115 (1984) 1133.
[116] B. Eisenmann, J. Hansa, Z. Kristallogr. 203 (1993) 291.
[117] B. Eisenmann, J. Hansa, Z. Kristallogr. 203 (1993) 293.
[118] K.O. Klepp, J. Solid State Chem. 117 (1995) 365.
[119] J.C. Jumas, M. Ribes, E. Philippot, M. Maurin, C.R. Acad. Sci., Ser. C 272 (1971) 1811.
[120] S. Yamaoka, B. Okai, Mater. Res. Bull. 5 (1970) 789.
[121] B. Schaaf, Dissertation, Bochum, 1994.
[122] J.B. Parise, Y. Ko, J. Rijssenbeck, D.M. Nellis, K. Tan, S. Koch, J. Chem. Soc., Chem. Commun., (1994) 527.
[123] Y. Ko, K. Tan, J.B. Parise, Acta Crystallogr., Sect. C 51 (1995) 398.
[124] H. Ahari, C.L. Bowes, T. Jiang, et al., Adv. Mater. 7 (1995) 375.
[125] G.A. Marking, M.G. Kanatzidis, Chem. Mater. 7 (1995) 1915.
[126] H.G. Braunbeck, Dissertation, Kaiserslautern, 1991.
[127] T. Jiang, A.J. Lough, G.A. Ozin, D. Young, Chem. Mater. 7 (1995) 245.
[128] Y. Ko, K. Tan, D.M. Nellis, S. Koch, J.B. Parise, J. Solid State Chem. 114 (1995) 506.
[129] K.O. Klepp, Z. Naturforsch., Teil B 47 (1992) 197.
[130] G. Eulenberger, Z. Naturforsch., Teil B 36 (1981) 687.
[131] W.S. Sheldrick, H.G. Braunbeck, Z. Naturforsch., Teil B 47 (1992) 151.
[132] J.C. Jumas, E. Philippot, M. Maurin, J. Solid State Chem. 14 (1975) 152.
[133] Y. Piffard, M. Tournoux, A.L. Ajavon, R. Eholie, Rev. Chim. Minér. 21 (1984) 56.
[134] J.-H. Liao, Ph.D. Thesis, Michigan State University, East Lansing, MI, 1993.
[135] B. Eisenmann, H. Schwerer, H. Schäfer, Mater. Res. Bull. 18 (1983) 383.
[136] G. Rocktäschel, W. Ritter, A. Weiss, Z. Naturforsch., Teil B 19 (1964) 958.
[137] H. Vincent, G. Perrault, Bull Soc. Fr. Minéral Cristallogr. 94 (1971) 551.
[138] M. Ribes, E. Philippot, M. Maurin, C.R. Acad. Sci. Paris, Ser. C 270 (1970) 716.
[139] E. Philippot, M. Ribes, M. Maurin, Rev. Chim. Miner. 8 (1971) 99.
[140] M. Ribes, M. Maurin, Rev. Chim. Minér. 7 (1970) 75.
[141] K. Susa, H. Steinfink, J. Solid State Chem. 3 (1971) 75.
[142] B. Eisenmann, H. Schäfer, H. Schrod, Z. Naturforsch., Teil B 38 (1983) 921.
[143] R.G. Teller, L.J. Krause, R.C. Haushalter, Inorg. Chem. 22 (1983) 1809.
[144] J. Li, H.-Y. Guo, D.M. Proserpio, A. Sironi, J. Solid State Chem. 117 (1995) 247.
[145] J. Olivier-Fourcade, J.C. Jumas, M. Ribes, E. Philippot, M. Maurin, J. Solid State Chem. 23 (1978) 155.
[146] C. Brinkmann, B. Eisenmann, H. Schäfer, Mater. Res. Bull. 20 (1985) 1207.
[147] W. Bubenheim, U. Müller, Z. Naturforsch., Teil B 50 (1995) 1135.
[148] R.M.H. Hearth, J. Cusick, M.C. Scudder, D.C. Craig, I.G. Dance, Polyhedron 8 (1989) 1999.
[149] S.P. Huang, S. Dhingra, M.G. Kanatzidis, Inorg. Chem. 28 (1989) 2024.
[150] A. Müller, J. Schimanski, M. Römer, et al., Chimia 39 (1985) 25.
[151] J.-H. Liao, C. Varotsis, M.G. Kanatzidis, Inorg. Chem. 32 (1993) 2453.

[152] K.O. Klepp, P. Ecker, J. Solid State Chem. 117 (1995) 351.
[153] J.C. Huffmann, J.P. Haushalter, A.M. Umarji, G.K. Shenoy, R.C. Haushalter, Inorg. Chem. 23 (1984) 2312.
[154] M.A. Ansari, J.C. Bollinger, J.A. Ibers, Inorg. Chem. 32 (1993) 231.
[155] J.L. Shreeve-Keyer, C.J. Warren, S.S. Dhingra, R.C. Haushalter, Polyhedron 16 (1997) 1199.
[156] V. Agafonov, B. Legendre, N. Rodier, J.M. Cense, E. Dichi, G. Kra, Acta Crystallogr., Sect. C 47 (1991) 1300.
[157] W.S. Sheldrick, A. Loose, unpublished results.
[158] C. Brinkmann, B. Eisenmann, H. Schäfer, Mater. Res. Bull. 20 (1985) 299.
[159] J.C. Jumas, J. Olivier-Fourcade, F. Vermot-Gaud-Daniel, M. Ribes, E. Philippot, M. Maurin, Rev. Chim. Minér. 11 (1974) 13.
[160] B. Eisenmann, J. Hansa, H. Schäfer, Z. Anorg. Allg. Chem. 526 (1985) 55.
[161] S.S. Dhingra, R.C. Haushalter, Polyhedron 13 (1994) 2775.
[162] W. Schiwy, B. Krebs, Angew. Chem. 87 (1975) 451.
[163] J. Li, Y.Y. Liszewski, L.A. MacAdams, F. Chen, S. Mulley, D.M. Proserpio, Chem. Mater. 8 (1996) 598.
[164] B. Eisenmann, H. Schrod, H. Schäfer, Mater. Res. Bull. 19 (1984) 293.
[165] C. Brinkmann, B. Eisenmann, J. Hansa, H. Schäfer, Ninth European Crystallography Meeting, Turin, Italy, 1985.
[166] A.A. Touré, G. Kra, R. Eholié, J. Olivier-Fourcade, J.-C. Jumas, M. Maurin, J. Solid State Chem. 84 (1990) 245.
[167] V. Agafonov, B. Legendre, N. Rodier, J.M. Cense, E. Dichi, G. Kra, Acta Crystallogr., Sect. C 47 (1991) 850.
[168] J. Bernstein, R. Hoffmann, Inorg. Chem. 24 (1985) 4100.
[169] P. Böttcher, Angew. Chem. Int. Ed. Engl. 27 (1988) 759.
[170] G. Busch, G. Frohlich, C. Mullinger, E. Steigmeier, Helv. Phys. Acta 34 (1961) 359.
[171] Y. Ko, C.L. Cahill, J.B. Parise, J. Chem. Soc., Chem. Common., (1994) 69.
[172] R.L. Bedard, L.D. Vail, S.T. Wilson, E.M. Flanigen, U.S. Patent 4, (1989) 880, 761.
[173] R.L. Bedard, L.D. Vail, S.T. Wilson, E.M. Flanigen, U.S. Patent 4, (1990) 933, 068.
[174] W.S. Sheldrick, H.G. Braunbeck, Z. Anorg. Allg. Chem. 619 (1993) 1300.
[175] J.B. Parise, Y. Ko, K. Tan, D.M. Nellis, S. Koch, J. Solid State Chem. 117 (1995) 219.
[176] H. Ahari, G.A. Ozin, R.L. Bedard, S. Petrov, D. Young, Adv. Mater. 7 (1995) 370.
[177] T. Jiang, G.A. Ozin, R.L. Bedard, Adv. Mater. 7 (1995) 166.
[178] W. Hoffmann, Z. Kristallogr. 92 (1935) 161.
[179] R. Kniep, D. Mootz, U. Severin, H. Wunderlich, Acta Crystallogr., Sect. B 38 (1982) 2022.
[180] G.A. Ozin, P. Enzel, G.S. Henderson, R.L. Bedard, Adv. Mater. 7 (1995) 64.
[181] T. Jiang, G.A. Ozin, R.L. Bedard, Adv. Mater. 6 (1994) 860.
[182] R.J. Francis, S.J. Price, J.S.O. Evans, S. O'Brien, D. O'Hare, S.M. Clark, Chem. Mater. 8 (1996) 2102.
[183] H. Ahari, R.L. Badard, C.L. Bowes, et al., Nature 388 (1997) 857.
[184] J.B. Parise, Y. Ko, Chem. Mater. 6 (1994) 718.
[185] W.S. Sheldrick, M. Wachhold, S. Jobic, R. Brec, E. Canadell, Adv. Mater. 9 (1997) 669.
[186] S.M. Kauzlarich, Chemistry, Structure, and Bonding of Zintl Phases and Ions, VCH Publisher, Inc, New York, 1996.
[187] M. Ribes, J. Olivier-Fourcade, E. Philippot, M. Maurin, Acta Crystallogr., Sect. B 30 (1974) 1391.
[188] J. Fenner, D. Mootz, Naturwissenschaften 61 (1974) 127.
[189] O. Achak, J.Y. Pivan, M. Maunage, M. Louër, D. Louër, J. All. Compd. 219 (1995) 111.
[190] O. Achak, J.Y. Pivan, M. Maunage, M. Louër, D. Louër, J. All. Compd. 221 (1996) 473.
[191] C.L. Bowes, A.J. Lough, A. Malek, G.A. Ozin, S. Petrov, D. Young, Chem. Ber. 129 (1996) 283.
[192] A. Loose, W.S. Sheldrick, Z. Naturforsch., Teil B 52 (1997) 687.
[193] C.L. Bowes, W.U. Huynh, S.J. Kirkby, et al., Chem. Mater. 8 (1996) 2147.
[194] K. Tan, A. Darovsky, J.B. Parise, J. Am. Chem. Soc. 117 (1995) 7039.
[195] K. Tan, Y. Ko, J.B. Parise, A. Darovsky, Chem. Mater. 8 (1996) 448.
[196] J.B. Parise, K. Tan, J. Chem. Soc., Chem. Commun., (1996) 1687.

[197] C.L. Cahill, J.B. Parise, Chem. Mater. 9 (1997) 807.
[198] W.M. Meier, D.H. Olsen, C. Baerlocher, Atlas of Zeolite Structure Types, 4th revised ed., Butterworth, London, 1996.
[199] C.L. Teske, Z. Naturforsch., Teil B 35 (1980) 7.
[200] C.L. Teske, Z. Anorg. Allg. Chem. 468 (1980) 27.
[201] C.L. Teske, Z. Anorg. Allg. Chem. 460 (1980) 163.
[202] C.L. Teske, Z. Naturforsch., Teil B 35 (1980) 509.
[203] W. Klee, H. Schäfer, Rev. Chim. Minér. 16 (1979) 465.
[204] J.A.A. Ketelaar, W.H. T'Hart, D. Polder, Z. Kristallogr. 101 (1939) 396.
[205] C.L. Teske, Z. Naturforsch., Teil B 34 (1979) 544.
[206] C.L. Teske, Z. Naturforsch., Teil B 34 (1979) 386.
[207] C.L. Teske, Z. Anorg. Allg. Chem. 419 (1976) 67.
[208] C.L. Teske, O. Vetter, Z. Anorg. Allg. Chem. 427 (1976) 200.
[209] C.L. Teske, O. Vetter, Z. Anorg. Allg. Chem. 426 (1976) 281.
[210] C.L. Teske, Z. Anorg. Allg. Chem. 522 (1985) 122.
[211] C.L. Teske, Z.Anorg. Allg. Chem. 531 (1985) 52.
[212] C.L. Teske, Z. Naturforsch., Teil B 35 (1980) 672.
[213] J.-H. Liao, M.G. Kanatzidis, Chem. Mater. 5 (1993) 1561.
[214] E. Zintl, K. Loosen, Z. Phys. Chem. 174A (1935) 301.
[215] J. Peters, B. Krebs, Acta Crystallogr., Sect. B 38 (1982) 1270.
[216] J. Olivier-Fourcade, J.C. Jumas, M. Ribes, E. Philippot, M. Maurin, J. Solid State Chem. 23 (1978) 155.
[217] C.L. Teske, Z. Anorg. Allg. Chem. 445 (1978) 193.
[218] G. Eulenberger, Z. Naturforsch., Teil B 35 (1980) 335.
[219] P. Wu, Y.-J. Lu, J.A. Ibers, J. Solid State Chem. 97 (1992) 383.
[220] M.A. Pell, J.A. Ibers, Chem. Ber. 130 (1997) 1.
[221] Y. Nakamura, A. Aruga, I. Nakai, K. Nagashima, Bull. Chem. Soc. Jpn. 57 (1984) 1718.
[222] E.R. deGil, C.D. Gomez, A.V. Rivera, A. Lopez-Rivera, Progr. Crys. Growth Characteriz. 10 (1985) 217.
[223] S.S. Dhingra, R.C. Haushalter, Chem. Mater. 6 (1994) 2376.
[224] J. Shreeve-Keyer, R.C. Haushalter, Polyhedron 15 (1996) 1213.
[225] S.S. Dhingra, D.-K. Seo, G.R. Kowach, et al., Angew. Chem. Int. Ed. Engl. 36 (1995) 1087.
[226] S. delBucchia, J.C. Jumas, E. Philippot, M. Maurin, Z. Anorg. Allg. Chem. 487 (1982) 199.
[227] K. Ploog, W. Stetter, A. Nowitzki, E. Schönherr, Mater. Res. Bull. 11 (1976) 1147.
[228] B. Eisenmann, H. Schwerer, H. Schäfer, Z. Naturforsch., Teil B 36 (1981) 1538.
[229] G. Dittmar, Angew. Chem. Int. Ed. Engl. 16 (1977) 554.
[230] G. Dittmar, Acta Crystallogr., Sect. B 34 (1978) 2390.
[231] C. Brinkmann, Dissertation, TH Darmstadt, 1986.
[232] G. Eulenberger, J. Solid State Chem. 55 (1984) 306.
[233] A. Feltz, G. Pfaff, Z. Anorg. Allg. Chem. 442 (1978) 41.
[234] B. Eisenmann, H. Schäfer, H. Schwerer, Rev. Chim. Minér. 20 (1983) 78.
[235] B. Eisenmann, J. Hansa, H. Schäfer, Z. Naturforsch., Teil B 40 (1985) 450.
[236] B. Eisenmann, H. Schäfer, H. Schwerer, Z. Naturforsch., Teil B 38 (1983) 924.
[237] C. Brinkmann, B. Eisenmann, H. Schäfer, III. European Conference on Solid State Chemistry, Regensburg, (1986) 29.–31.05.
[238] H. Sommer, R. Hoppe, Z. Anorg. Allg. Chem. 430 (1997) 199.
[239] M. Palazzi, Anal. Chim. Fr. 3 (1978) 47.
[240] M. Palazzi, Acta Crystallogr., Sect. B 32 (1976) 3175.
[241] Z.-M. Yang, F. Pertlik, J. All. Compd. 216 (1994) 155.
[242] M. Gostojic, Z. Kristallogr. 151 (1980) 249.
[243] G. Cordier, C. Schwidetzky, H. Schäfer, Rev. Chim. Minér. 20 (1983) 877.
[244] H.Y.P. Hong, J.C. Mikkelsen, Jr., G.W. Roland, Mater. Res. Bull. 9 (1974) 365.
[245] G. Cordier, C. Schwidetzky, H. Schäfer, Rev. Chim. Minér. 22 (1985) 93.
[246] B. Siewert, U. Müller, Z. Anorg. Allg. Chem. 609 (1992) 82.

[247] B. Siewert, U. Müller, Z. Anorg. Allg. Chem. 595 (1991) 211.
[248] V. Vater, W.S. Sheldrick, unpublished results.
[249] D.M. Smith, C.-W. Park, J.A. Ibers, Inorg. Chem. 35 (1996) 6682.
[250] D.M. Smith, C.-W. Park, J.A. Ibers, Inorg. Chem. 36 (1997) 3798.
[251] K. Wendel, U. Müller, Z. Anorg. Allg. Chem. 621 (1995) 979.
[252] M.A. Ansari, J.A. Ibers, S.C. O'Neal, W.T. Pennington, J.W. Kolis, Polyhedron 11 (1992) 1877.
[253] C.H.E. Belin, M.M. Charbonnel, Inorg. Chem. 21 (1982) 2504.
[254] C.R. Belin, Acad. Sci. Paris, Série II 298 (1984) 691.
[255] W.S. Sheldrick, J. Kaub, Z. Naturforsch., Teil B 40 (1985) 19.
[256] J. Kaub, Dissertation, Kaiserslautern, 1986.
[257] W.S. Sheldrick, J. Kaub, Z. Naturforsch., Teil B 40 (1985) 1020.
[258] M. Palazzi, S. Jaulmes, Acta Crystallogr., Sect. B 33 (1977) 908.
[259] J.E. Iglesias, F.J. Zuniga, W. Nowacki, Z. Kristallogr. 146 (1977) 43.
[260] H.-J. Häusler, Dissertation, Kaiserslautern, 1987.
[261] B. Eisenmann, H. Schäfer, Z. Anorg. Allg. Chem. 456 (1979) 87.
[262] W.S. Sheldrick, H.-J. Häusler, Z. Anorg. Allg. Chem. 561 (1988) 139.
[263] W.S. Sheldrick, J. Kaub, Z. Anorg. Allg. Chem. 535 (1986) 179.
[264] N. Rey, J.C. Jumas, J. Olivier-Fourcade, E. Philippot, Acta Crystallogr., Sect. C 40 (1984) 1655.
[265] H.A. Graf, H. Schäfer, Z. Anorg. Allg. Chem. 44 (1975) 220.
[266] G. Cordier, H. Schäfer, Rev. Chim. Minér. 18 (1981) 218.
[267] W. Dörrscheidt, H. Schäfer, Z. Naturforsch., Teil B 36 (1981) 410.
[268] A. Olsen, P. Goodman, H.J. Whitfield, J. Solid State Chem. 60 (1985) 305.
[269] J. Lin, G.J. Miller, J. Solid State Chem. 113 (1994) 296.
[270] B. Eisenmann, R. Zagler, Z. Kristallogr. 197 (1991) 255.
[271] J.-S. Jung, B. Wu, E.D. Stevens, C.J. O'Connor, J. Solid State Chem. 94 (1991) 362.
[272] F. Kluger, F. Pertlik, Monatsh. Chem. 116 (1985) 149.
[273] G. Cordier, R. Cook, H. Schäfer, Angew. Chem. Int. Ed. Engl. 92 (1980) 310.
[274] G. Cordier, H. Schäfer, C. Schwidetzky, Rev. Chim. Minér. 22 (1985) 722.
[275] T.M. Martin, P.T. Wood, J.W. Kolis, Inorg. Chem. 33 (1994) 1587.
[276] J. Olivier-Fourcade, E. Philippot, M. Maurin, Z. Anorg. Allg. Chem. 446 (1978) 159.
[277] H.A. Graf, H. Schäfer, Z. Anorg. Allg. Chem. 414 (1975) 211.
[278] A.S. Kanishcheva, V.G. Kuznetsov, V.B. Lazarev, T.G. Tarsova, Zhurnal Strukturnoi Khimii 18 (1977) 1069.
[279] A.S. Kanishcheva, Y.N. Milchailov, V.G. Kuznetsov, V.M. Batoy, Dokl. Akad. Nauk SSSR 251 (1980) 603.
[280] N. Rey, J.C. Jumas, J. Olivier-Fourcade, E. Philippot, Acta Crystallogr., Sect. C 39 (1983) 971.
[281] A.K. Volk, P. Bickert, R. Kolmer, H. Schäfer, Z. Naturforsch., Teil B 34 (1979) 380.
[282] G. Cordier, C. Schwidetzky, H. Schäfer, Rev. Chim. Minér. 19 (1982) 179.
[283] G. Dittmar, H. Schäfer, Z. Naturforsch., Teil B 32 (1977) 1346.
[284] A.S. Kanishcheva, Y.N. Milchailov, V.B. Lazarev, N.A. Moshchalkova, Dokl. Akad. Nauk SSSR 252 (1980) 872.
[285] T. König, B. Eisenmann, H. Schäfer, Z. Anorg. Allg. Chem. 488 (1982) 126.
[286] J.B. Parise, Y. Ko, Chem. Mater. 4 (1992) 1446.
[287] G. Dittmar, H. Schäfer, Z. Anorg. Allg. Chem. 437 (1977) 183.
[288] W. Bensch, M. Schur, Z. Naturforsch., Teil B 52 (1997) 405.
[289] G. Dittmar, H. Schäfer, Z. Anorg. Allg. Chem. 441 (1978) 98.
[290] G. Cordier, H. Schäfer, C. Schwidetzky, Z. Naturforsch., Teil B 39 (1984) 131.
[291] K. Tan, Y. Ko, J.B. Parise, Acta Crystallogr., Sect. C 50 (1994) 1439.
[292] I. Nakai, D.E. Appleman, Chem. Lett., (1981) 1327.
[293] K. Volk, H. Schäfer, Z. Naturforsch., Teil B 33 (1978) 827.
[294] G. Cordier, C. Schwidetzky, H. Schäfer, J. Solid State Chem. 54 (1984) 84.
[295] G. Cordier, H. Schäfer, Z. Naturforsch., Teil B 34 (1979) 1053.
[296] K. Volk, H. Schäfer, Z. Naturforsch., Teil B 34 (1979) 172.
[297] B. Eisenmann, H. Schäfer, Z. Naturforsch., Teil B 34 (1979) 383.

[298] G. Dittmar, H. Schäfer, Z. Anorg. Allg. Chem. 441 (1978) 93.
[299] W.S. Sheldrick, H.-J. Häusler, Z. Anorg. Allg. Chem. 557 (1988) 105.
[300] W. Bensch, M. Schur, Eur. J. Solid State Ínorg. Chem., (1997) in press.
[301] W.S. Sheldrick, H.-J. Häusler, Z. Anorg. Allg. Chem. 561 (1988) 149.
[302] J.B. Parise, J. Chem. Soc., Chem. Commun., (1990) 1553.
[303] K. Volk, H. Schäfer, Z. Naturforsch., Teil B 34 (1979) 1637.
[304] Y. Ko, K. Tan, J.B. Parise, A. Darovsky, Chem. Mater. 8 (1996) 493.
[305] J.B. Parise, Science 251 (1991) 293.
[306] H.A. Graf, H. Schäfer, Z. Naturforsch., Teil B 37 (1972) 735.
[307] X. Wang, F. Liebau, J. Solid State Chem. 111 (1994) 385.
[308] X. Wang, Eur. J. Solid State Inorg. Chem. 32 (1995) 303.
[309] A.S. Kanishcheva, V.G. Kuznetsov, Y.N. Mikhailov, V.N. Batog, V.M. Skorikov, Zhurnal Strukturnoi Khimii 21 (1980) 136.
[310] W. Bronger, A. Donike, D. Schmitz, Z. Anorg. Allg. Chem. 622 (1996) 1003.
[311] B. Eisenmann, R. Zagler, Z. Kristallogr. 197 (1991) 257.
[312] O. Glemser, M. Filcek, Z. Anorg. Allg. Chem. 279 (1955) 321.
[313] G. Gattow, T. Zeman, Z. Anorg. Allg. Chem. 279 (1955) 324.
[314] J.W. Boon, Recl. Trav. Chim. Pays-Bas. 63 (1944) 32.
[315] Y.V. Voroshilov, E.Y. Peresh, M.I. Golovei, Inorg. Mater. 8 (1972) 677.
[316] V.B. Lazarev, A.F. Trippel, S.I. Berul, Russ. J. Inorg. Chem. 25 (1980) 1694.
[317] T.J. McCarthy, S.-P. Ngeyi, J.-H. Liao, et al., Chem. Mater. 5 (1993) 331.
[318] E.F. Hockings, J.G. White, Acta Crystallogr. 14 (1961) 328.
[319] B. Aurivillius, Acta Chem. Scand, Sect. A 37 (1983) 399.
[320] M. Julien-Pouzol, S. Jaulmes, P. Laruelle, Acta Crystallogr., Sect. B 35 (1979) 1313.
[321] T.J. McCarthy, T.A. Tanzer, M.G. Kanatzidis, J. Am. Chem. Soc. 117 (1995) 1294.
[322] D. Schmitz, W. Bronger, Z. Naturforsch., Teil B 29 (1974) 438.
[323] A.S. Kanishcheva, J.N. Milchailov, V.B. Lazarev, A. Trippel, Dokl. Akad. Nauk SSSR (Kryst.) 252 (1980) 96.
[324] G. Cordier, H. Schäfer, C. Schwidetzky, Rev. Chim. Miner. 22 (1985) 631.
[325] M.G. Kanatzidis, T.J. McCarthy, T.A. Tanzer, et al., Chem. Mater. 8 (1996) 1465.
[326] B. Chen, C. Uher, L. Iordanidis, M.G. Kanatzidis, Chem. Mater. 9 (1997) 1655.
[327] G. Cordier, H. Schäfer, C. Schwidetzky, Rev. Chim. Minér. 22 (1985) 676.
[328] S.V. Vorob'eva, A.A. Ivakin, A.M. Gorelov, E.M. Gertman, Russ. J. Inorg. Chem. 22 (1977) 1479.
[329] P.K. Dorhout, personal communication.
[330] P. Bayliss, W. Nowacki, Z. Kristallogr. 135 (1972) 308.
[331] G.P. Voutsas, A.G. Papazoglou, P.J. Rentzeperis, D. Siapkas, Z. Kristallogr. 171 (1985) 261.
[332] W.S. Sheldrick, J. Kaub, Z. Anorg. Allg. Chem. 536 (1986) 114.
[333] L. Pauling, J. Am. Chem. Soc. 51 (1929) 1010.
[334] L. Pauling, J. Am. Chem. Soc. 69 (1947) 542.
[335] L. Pauling, Die Natur der chemischen Bindung, Verlag Chemie, Weinheim, 1962.
[336] I.D. Brown, R.D. Shannon, Acta Crystallogr., Sect. A 29 (1973) 266.
[337] I.D. Brown, D. Attermatt, Acta Crystallogr., Sect. B 41 (1985) 244.
[338] N.E. Brese, M. O'Keeffe, Acta Crystallogr., Sect. B 47 (1991) 192.
[339] M. O'Keeffe, N.E. Brese, Acta Crystallogr., Sect. B 48 (1992) 152.
[340] X. Wang, F. Liebau, Acta Crystallogr., Sect. B 52 (1996) 7.
[341] X. Wang, F. Liebau, Z. Kristallogr. 211 (1996) 437.
[342] W.S. Sheldrick, C. Horn, Z. Naturforsch., Teil B 44 (1989) 405.
[343] W.S. Sheldrick, C. Martin, Z. Naturforsch., Teil B 46 (1991) 639.
[344] W.S. Sheldrick, J. Kiefer, Z. Naturforsch., Teil B 47 (1992) 1079.
[345] S.A. Semiletov, Z.G. Pinsker, Dokl. Akad. Nauk SSSR 100 (1955) 1079.
[346] S. Nakjima, J. Phys. Chem. Solids 24 (1963) 479.
[347] G. Dittmar, H. Schäfer, Z. Naturforsch., Teil B 33 (1978) 678.
[348] G. Cordier, C. Schwidetzky, H. Schäfer, Z. Naturforsch., Teil B 40 (1985) 1.
[349] J. Kaub, Z. Naturforsch., Teil B 41 (1986) 436.

[350] B. Krebs, H.-U. Hürter, J. Enax, R. Fröhlich, Z. Anorg. Allg. Chem. 581 (1990) 141.
[351] K. Mereiter, A. Preisinger, H. Gruth, Acta Crystallogr., Sect. B 35 (1979) 19.
[352] H. Mayer, K. Mereiter, Monatsh. Chem. 123 (1992) 515.
[353] M. Palazzi, S. Jaulmes, P. Laruelle, Acta Crystallogr., Sect. B 30 (1974) 2378.
[354] M. Wachhold, W.S. Sheldrick, Z. Naturforsch., Teil B 51 (1996) 32.
[355] H. Schäfer, G. Schäfer, A. Weiss, Z. Naturforsch., Teil B 18 (1963) 665.
[356] H.A. Graf, H. Schäfer, Z. Anorg. Allg. Chem. 425 (1976) 67.
[357] R.W. Alkire, P.J. Vergamini, A.C. Larson, B. Morosin, Acta Crystallogr., Sect. C 40 (1984) 1502.
[358] W. Bensch, P. Dürichen, Z. Kristallogr., 212 (1997) in press.
[359] W. Bensch, P. Dürichen, Z. Kristallogr.. 211 (1996) 636.
[360] B. Eisenmann, R. Zagler, Z. Naturforsch., Teil B 44 (1989) 249.
[361] P.P. Paul, T.B. Rauchfuss, S.R. Wilson, J. Am. Chem. Soc. 115 (1993) 3316.
[362] A. Müller, M. Zimmermann, H. Bögge, Angew. Chem. 98 (1986) 259.
[363] M. Evain, F. Boucher, R. Brec, J. Rouxel, J.-S. Jung, C.J. O'Conner, Eur. J. Solid State Inorg. Chem. 29 (1992) 1055.
[364] K. Tan, Y. Ko, J.B. Parise, J.-H. Park, A. Darovsky, Chem. Mater. 8 (1996) 2510.
[365] R. Cook, H. Schäfer, Rev. Chim. Miner. 19 (1982) 19.
[366] R. Cook, H. Schäfer, Studies Inorg. Chem. 3 (1983) 757.
[367] R. Cook, Dissertation, Darmstadt, 1984.
[368] D.-Y. Chung, S. Jobic, T. Hogan, et al., J. Am. Chem. Soc. 119 (1997) 2505.
[369] T.J. McCarthy, M.G. Kanatzidis, Inorg. Chem. 33 (1994) 1205.
[370] M. Wachhold, W.S. Sheldrick, Z. Kristallogr., New Structures, 213 (1998) 25.
[371] ibid, 213 (1998) 24.
[372] G.L. Schimek, J.W. Kolis, Inorg. Chem. 36 (1997) 1689.
[373] X. Zhang, J. Li, B. Foran, et al., J. Am. Chem. Soc. 117 (1995) 10513.
[374] M.G. Kanatzidis, Angew. Chem. Int. Ed. Engl. 34 (1995) 2109.
[375] T. Doert, P. Böttcher, Z. Kristallogr. 209 (1994) 95.
[376] Gmelin Handbook of Inorganic and Organometallic Chemistry, 8th Edition: TYPIX-Standardized Date and Crystal Chemical Characterization of Inorganic Structure Types, Vol. 1, Springer-Verlag, Berlin, 1993.
[377] B. Ribar, W. Nowacki, Schweizerische Mineralogische und Petrologische Mitteilungen 49 (1969) 379.
[378] B. Ribar, W. Nowacki, Acta Crystallogr., Sect. B 26 (1970) 201.
[379] L.T. Bryndzia, A.M. Davis, Am. Mineral. 74 (1989) 236.
[380] K. Tatsuka, N. Morimoto, Am. Mineral. 58 (1973) 425.
[381] M. Imafuku, I. Nakai, K. Nagashima, Mater. Res. Bull. 21 (1986) 493.
[382] K.L. Brown, F.W. Dickson, Z. Kristallogr. 144 (1976) 367.
[383] S. Graeser, R. Wulf, A. Edenharter, Schweizerische Mineralogische und Petrologische Mitteilungen 72 (1992) 293.
[384] J.E. Jerome, P.T. Wood, W.T. Pennington, J.W. Kolis, Inorg. Chem. 33 (1994) 1733.
[385] J.-H. Chou, M.G. Kanatzidis, J. Solid State Chem. 123 (1996) 115.
[386] M.G. Kanatzidis, J.-H. Chou, J. Solid State Chem. 127 (1996) 186.
[387] J.E. Jerome, G.L. Schimek, G.W. Drake, J.W. Kolis, Eur. J. Solid State Inorg. Chem. 33 (1996) 765.
[388] G.L. Schimek, J.W. Kolis, Acta Crystallogr., Sect. C 53 (1997) 991.
[389] G.L. Schimek, W.T. Pennington, P.T. Wood, J.W. Kolis, J. Solid State Chem. 123 (1996) 277.
[390] M. Auernhammer, H. Effenberger, E. Irran, F. Pertlik, J. Rosenstingl, J. Solid State Chem. 106 (1993) 421.
[391] F. Pertlik, Monatsh. Chem. 125 (1994) 1311.
[392] P.T. Wood, G.L. Schimek, J.W. Kolis, Chem. Mater. 8 (1996) 721.
[393] J.-H. Chou, M.G. Kanatzidis, Inorg. Chem. 33 (1994) 5372.
[394] T.M. Martin, P.T. Wood, G.L. Schimek, W.T. Pennington, J.W. Kolis, Inorg. Chem. 34 (1995) 4385.

[395] T.M. Martin, G.L. Schimek, D.A. Mlsna, J.W. Kolis, Phosphorus, Sulfur, Silicon Relat. Elem. 93-94 (1994) 93.
[396] C. Wang, R.C. Haushalter, Chem. Commun. (1997) 1457.
[397] S.S. Dhingra, R.C. Haushalter, J. Am. Chem. Soc. 116 (1994) 3651.
[398] U. Müller, C. Grebe, B. Neumüller, B. Schreiner, K. Dehnicke, Z. Anorg. Allg. Chem. 619 (1993) 500.
[399] J.M. McConnachie, M.A. Ansari, J.C. Bollinger, R.J. Salm, J.A. Ibers, Inorg. Chem. 32 (1993) 3201.
[400] S.C. O'Neal, W.T. Pennington, J.W. Kolis, Inorg. Chem. 31 (1992) 888.
[401] S.C. O'Neal, W.T. Pennington, J.W. Kolis, J. Am. Chem. Soc. 113 (1991) 710.
[402] G.A. Zank, T.B. Rauchfuss, S.R. Wilson, A.L. Rheingold, J. Am. Chem. Soc. 106 (1984) 7621.
[403] J.-H. Chou, J.A. Hanko, M.G. Kanatzidis, Inorg. Chem. 36 (1997) 4.
[404] W. Bensch, M. Schur, Eur. J. Solid State Inorg. Chem. 33 (1996) 1149.
[405] M. Gostojic, A. Edenharter, W. Nowacki, P. Engel, Z. Kristallogr. 158 (1982) 43.
[406] Y. Takeuchi, M. Ohmasa, W. Nowacki, Z. Kristallogr. 127 (1968) 349.
[407] E. Marumo, W. Nowacki, Z. Kristallogr. 125 (1967) 249.
[408] G.W. Drake, G.L. Schimek, J.W. Kolis, Inorg. Chem. 35 (1996) 4534.
[409] J.-H. Chou, M.G. Kanatzidis, Inorg. Chem. 33 (1994) 1001.
[410] J.-H. Chou, M.G. Kanatzidis, Chem. Mater. 7 (1995) 5.
[411] T. Balic-Zunic, P. Engel, Z. Kristallogr. 165 (1983) 261.
[412] E. Makovicky, B.J. Skinner, Am. Mineral. 60 (1975) 998.
[413] T. Matsumoto, W. Nowacki, Z. Kristallogr. 129 (1969) 163.
[414] H.-O. Stephan, M.G. Kanatzidis, J. Am. Chem. Soc. 118 (1996) 12226.
[415] B. Eisenmann, R. Zagler, Z. Kristallogr. 197 (1991) 261.
[416] B. Eisenmann, J. Jäger, R. Zagler, Z. Kristallogr. 197 (1991) 259.
[417] S.S. Dhingra, C.J. Warren, R.C. Haushalter, Polyhedron 16 (1997) 3055.
[418] M. Wachhold, W.S. Sheldrick, Z. Naturforsch., Teil B, 51 (1996).
[419] B. Eisenmann, R. Zagler, Z. Naturforsch., Teil B 42 (1987) 1079.
[420] P. Böttcher, U. Kretschmann, J. Less-Common Met. 95 (1983) 81.
[421] P. Böttcher, U. Kretschmann, Z. Anorg. Allg. Chem. 491 (1982) 39.
[422] P. Böttcher, U. Kretschmann, Z. Anorg. Allg. Chem. 523 (1985) 145.
[423] C. Adenis, V. Langer, O. Lindqvist, Acta Crystallogr., Sect. C 45 (1989) 941.
[424] M.A. Ansari, J.A. Ibers, S.C. O'Neal, W.T. Pennington, J.W. Kolis, Polyhedron 11 (1992) 1877.
[425] E.J. Porter, G.M. Sheldrick, J. Chem. Soc., Sect. A, (1971) 3130.
[426] T.M. Martin, G.L. Schimek, W.T. Pennington, J.W. Kolis, J. Chem. Soc. Dalton. Trans., (1995) 501.
[427] S. Sportouch, J. Thumin, M. Tillard-Charbonnel, C. Belin, New. J. Chem. 19 (1995) 133.
[428] C.J. Warren, S.S. Dhingra, D.M. Ho, R.C. Haushalter, A.B. Bocarsly, Inorg. Chem. 33 (1994) 2709.
[429] Y. Park, M.G. Kanatzidis, Chem. Mater. 3 (1991) 781.
[430] V. Angilella, H. Mercier, C. Belin, J. Chem. Soc. Chem. Commun., (1989) 1654.
[431] H.P. Mercier, V.E. Angilella, C.H. Belin, New J. Chem. 14 (1990) 121.
[432] C. Belin, V. Angilella, H. Mercier, Acta Crystallogr., Sect. C 47 (1991) 61.
[433] C.H.E. Belin, J. Am. Chem. Soc. 102 (1980) 6036.
[434] C. Belin, H. Mercier, J. Chem. Soc. Chem. Commun., (1987) 190.
[435] D. Schiferl, C.S. Barret, J. Appl. Cryst. 2 (1969) 30.
[436] G.A. Ozin, Supramol. Chem. 6 (1995) 125.
[437] G.A. Ozin, Materials Chemistry: An Emerging Discipline, L.V. Interrante, L.A. Casper, A.B. Ellis (Eds.), ACS Advances in Chemistry Series 245 (1995) 335.
[438] Q. Liu, N. Goldberg, R. Hoffmann, Chem. Eur. J. 2 (1996) 390.
[439] S. Jobic, W.S. Sheldrick, E. Canadell, R. Brec, Bull. Soc. Chim. Fr. 133 (1996) 221.
[440] R. Hoffmann, Am. J. Sci. 84 (1996) 327.
[441] Ö. Dag, H. Ahari, N. Coombs, et al., Adv. Mater. 9 (1997) 1133.
[442] J. Li, B. Marler, H. Kessler, M. Soulard, S. Kallus, Inorg. Chem. 36 (1997) 4697.
[443] T. Jiang, A. Lough, G.A. Ozin, Adv. Mater. 10 (1998) 42.

[444] A. Loose, W. S. Sheldrick, unpublished results.
[445] H.-O. Stephan, M.G. Kanatzidis, Inorg. Chem. 36 (1997) 6050.
[446] W. Czado, U. Müller, Z. Anorg. Allg. Chem., 624 (1998) 239.
[447] G.A. Marking, M.G. Kanatzidis, J. All. Compd. 259 (1997) 122.
[448] T.F. Fässler, U. Schütz, J. Organomet. Chem. 541 (1997) 269.
[449] C. Wang, R.C. Haushalter, J. Chem. Soc., Chem. Common. 1997, 1719.
[450] G.L. Schimek, J.W. Kolis, G.J. Long, Chem. Mater. 9 (1997) 2776.
[451] M.A. Pell, J.A. Ibers, Inorg. Chem. 35 (1996) 4559.
[452] S.E. Lehman, Jr., G.L. Schimek, J.M. Cusick, J.W. Kolis, Inorg. Chim. Acta. 260 (1997) 173.
[453] M. Schur, W. Bensch, Z. Anorg. Allg. Chem. 624 (1998) 310.
[454] Y. Matsushita, M.G. Kanatzidis, Z. Naturforsch. Teil B 53 (1998) 23.
[455] D.M. Smith, M.A. Pell, J.A. Ibers, Inorg. Chem. 37 (1998) 2340.
[456] K.O. Klepp, F. Fabian, Z. Kristallogr., New Structures 213 (1998) 17.
[457] J.A. Hanko, M.G. Kanatzidis, Angew. Chem. Int. Ed. Engl. 37 (1998) 342.